

UNCONVENTIONAL HIGH-THROUGHPUT SCREENING TECHNIQUES FOR
THE DISCOVERY OF CELL WALL ANTIBIOTICS

By: TOMASZ L. CZARNY, B.Sc.

A Thesis Submitted to the School of Graduate Studies In Partial Fulfillment of the
Requirements for the Degree of Doctor of Philosophy

McMaster University © Tomasz L. Czarny, February 2016

Ph.D. Thesis - T. Czarny; McMaster University - Biochemistry & Biomedical Sciences

DOCTOR OF PHILOSOPHY (2016), McMaster University,
(Biochemistry and Biomedical Sciences) Hamilton, Ontario

TITLE: Unconventional High-Throughput Screening Techniques for The
Discovery of Cell Wall Antibiotics

AUTHOR: Tomasz L. Czarny, B.Sc. (McMaster University)

SUPERVISOR: Dr. Eric D. Brown

NUMBER OF PAGES: xi, 172

Abstract

The emergence of antibiotic resistance in recent years has radically reduced the clinical efficacy of many antibacterial treatments and now poses a significant threat to human health. One of the earliest studied and well validated targets for antimicrobial discovery is the bacterial cell wall. The essential nature of this pathway, its conservation among bacterial pathogens, and absence in human biology have made cell wall synthesis an attractive pathway for new antibiotic drug discovery. Indeed, nearly all cell wall active agents have been discovered using screens for growth inhibition, followed by cumbersome secondary screens to identify the cell wall target. What is lacking are selective primary screening assays for the sensitive detection of cell wall active compounds while avoiding off-target and nuisance compounds. The overarching objective of this work is to explore new and unconventional screening techniques for the discovery of new cell wall antibiotics. These approaches take an integrative approach merging the positive aspects of whole-cell phenotypic and target based screening while obviating many of their individual pitfalls. Two main approaches are taken herein. First we explore the validity of using the recently developed P_{ywaC} reporter based system in *B. subtilis* 168 to enrich for cell wall inhibitors. A pilot screen of 26,000 small molecules led to the discovery of 9 cell wall actives of which one had its direct target identified. Secondly we harness the powerful and complex dispensability pattern found within wall teichoic acid (WTA) in Gram-positives. Developed is a powerful antagonism screen to search for early step and

substrate producing WTA inhibitors. This approach led to prolific enrichment for inhibitors of undecaprenyl-pyrophosphate synthase (UppS) through the interrogation of a small molecule library of 140,000 compounds. Overall, this thesis outlines effective and innovative approaches toward the identification of novel cell wall active compounds.

Acknowledgments

Firstly, I would like to thank Dr. Eric Brown, my supervisor and mentor who has helped foster my research and personal development over the past 5 years. It has been an absolute pleasure being part of the Brown lab; certainly a life changing experience which I will forever cherish.

Thanks to my committee members Dr. Nathan Magarvey, Dr. Lori Burrows, and Dr. Justin Nodwell. I have learned a great deal from all of you through meetings and our various collaborations. Without you my graduate experience certainly would have been diminished.

To my mother and father. Thank you for all your life-long sacrifices, unwavering support and love. Without your perseverance, and longing for a better life for your children I would certainly not be the person I am today. I love the two of you very much.

A special thanks to Georgina Cox, who has spent many hours listening to my scientific ramblings, guided my ideas, and transferred much of her knowledge onto me. I love you.

Lastly a thank you to the entire Brown Lab, especially all the members of the Wall Teichoic Acid group who have shared their knowledge and expertise.

Table of Contents

Abstract	ii
Acknowledgments	iii
Table of Contents	v
List of Figures	viii
List of Tables	x
List of Abbreviations	xi
CHAPTER ONE – Introduction	1
- Antibiotic Discovery and Effectiveness	2
- Components & Synthesis of the Gram-positive Cell Wall	4
- Peptidoglycan	6
- Wall Teichoic Acid	8
- Undecaprenyl-phosphate Synthesis	10
- Peptidoglycan and Wall Teichoic Acid Synthesis is Intricately Linked	11
- High Throughput Techniques in Antibacterial Drug Discovery	12
- A Promoter-reporter system for the detection of lesions in cell wall synthesis	14
- Unique Dispensability Pattern Found in the WTA Biosynthetic Pathway Leads to a Platform for Drug Discovery	16
- Objectives and Outline of This Thesis	18
- References	21
CHAPTER TWO – P _{ywaC} , a sensitive reporter of cell wall stress	26
- PREFACE	27
- SUMMARY	28
- INTRODUCTION	29
- RESULTS	35
- Amenability of the P _{ywaC} reporter system to high-throughput screening	35
- Kinetic screening of a 26K member small molecule library for P _{ywaC} activation	37
- EC ₅₀ and membrane permeabilization studies	41
- P _{ywaC} transcriptional activity of cell wall active antibiotics can be suppressed by osmoprotectants	42
- P _{ywaC} actives show morphological affects against <i>B. subtilis</i> 168 at sub-MIC concentrations	46
- Sensitization of the <i>B. subtilis</i> 168 CRISPRi essential knockdown library identifies the target of MAC-0170636	47
- Over-expression and knockdown of UppS results in suppression and sensitization to MAC-0170636 respectively	50
- Intrinsic resistance of <i>S. aureus</i> provides further validation of UppS as the target of MAC-0170636	51
- MAC-0170636 inhibits recombinant UppS <i>in vitro</i>	52
- DISCUSSION	55
- METHODS	63
- SUPPLEMENTAL DATA	69

- REFERENCES	75
CHAPTER THREE – A small molecule screening platform for the discovery of inhibitors of undecaprenyl diphosphate synthase	79
- PREFACE	80
- SUMMARY	81
- INTRODUCTION	82
- RESULTS	88
- High throughput screen of 142,000 compounds for <i>B. subtilis</i> 168 growth inhibition	88
- High throughput screen of 3,705 <i>B. subtilis</i> 168 actives for antagonists of targocil	90
- Potency assessment of 181 targocil antagonists on solid media	93
- Spontaneously generated mutant to MAC-0547630 contains a SNP in <i>uppS</i>	94
- Overexpression and establishment of kinetic parameters for UppS isolated from <i>B. subtilis</i> 168, <i>S. aureus</i> , and <i>E. coli</i>	94
- <i>In vitro</i> enzyme based screen for UppS inhibition	96
- Dose dependent <i>in vitro</i> inhibition of UppS cloned from <i>B. subtilis</i> 168, <i>S. aureus</i> , and <i>E. coli</i>	98
- Growth inhibition studies against <i>B. subtilis</i> 168, <i>S. aureus</i> and <i>E. coli</i>	99
- Generation of mutants against MAC-0547630 & MAC-0588238 reveal binding sites in UppS	101
- Assessing cross resistance of MAC-0547630 and MAC-0588238 mutants	103
- Evaluating the affects of the 5 novel UppS inhibitors on membrane potential	104
- Evaluation of 5 novel UppS inhibitors as potential adjuvants of cefuroxime in CA-MRSA USA300	106
- DISCUSSION	107
- METHODS	113
- SUPPLEMENTAL DATA	123
- REFERENCES	128
CHAPTER FOUR – Exploring the antagonism of bepridil with targocil	132
- PREFACE	133
- SUMMARY	134
- INTRODUCTION	135
- RESULTS	136
- A screen of 1,600 previously approved drugs for targocil antagonism coupled with <i>S. aureus</i> growth inhibition led to 12 priority active molecules	136
- Bepridil shows strong antagonistic and synergistic interactions with targocil and β -lactams respectively	138
- Bepridil has no activity on UppS <i>in vitro</i>	139
- Sensitization of <i>B. subtilis</i> 168 CRISPRi essential knockdown library to the presence of bepridil at sub-MIC	140
- Attempts in generating spontaneous mutants to bepridil	142
- Assessing bepridils affect on membrane potential	142
- Inhibitors of membrane potential do not have antagonistic interactions with targocil	144
- Assessing the bepridil spectrum of activity	146

- Bepridil interacts with the first lipid-linked steps of peptidoglycan and wall teichoic acid synthesis 147
- Interactions of bepridil with Und-P 149
- Affects of osmo-protectants on bepridil in *B. subtilis* 168 151
- DISCUSSION 153
- METHODS 158
- REFERENCES 164

CHAPTER FIVE – Future Directions 166

- A brief summary and a look into the future 167
- REFERENCES 172

List of Figures

CHAPTER ONE

- Figure 1-1: Cell wall biosynthesis in *B. subtilis* 168 5
- Figure 1-2: PG, WTA and the lipid carrier Und-P 6
- Figure 1-3: Dispensability pattern of Wall Teichoic Acid (WTA) biosynthesis in *B. subtilis* 168 17

CHAPTER TWO

- Figure 2-1. Screening workflow 31
- Figure 2-2: Mechanism of gene inactivation using the CRISPRi system in *B. subtilis* 168 34
- Figure 2-3: Assessing the robustness of the P_{ywaC} reporter HTS assay 39
- Figure 2-4. Replica plot and hit selection for the primary 26,000 small molecule P_{ywaC} kinetic screen 40
- Figure 2-5. Correlation of potency and P_{ywaC} activity 41
- Figure 2-6. P_{ywaC} promoter-reporter response to a panel of antibiotics in presence and absence of osmoprotective medium 43
- Figure 2-7. Dose response of the P_{ywaC} promoter-reporter in the absence and presence of osmoprotectants leads to 9 novel, cell wall-active inhibitors 44
- Figure 2-8. Morphological studies of *B. subtilis* 168 in the presence of 9 novel cell wall actives 47
- Figure 2-9: Sensitization of the *B. subtilis* 168 CRISPRi essential knockdown library to the presence of MAC-0170636 49
- Figure 2-10: Susceptibility of wild type and engineered *B. subtilis* 168 strains to MAC-0170636 51
- Figure 2-11: UppS from *S. aureus* as the sole source of UppS in *B. subtilis* 168 confers resistance to MAC-0170636 52
- Figure 2-12: Monitoring *in vitro* activity of UppS using a coupled pyrophosphate detection assay 53
- Figure 2-13: Assessing inhibitory activity of MAC-0170636 *in vitro* 54

CHAPTER THREE

- Figure 3-1: Dispensability pattern of Wall Teichoic Acid (WTA) biosynthesis in *B. subtilis* 168 84
- Figure 3-2. Screening workflow for identifying inhibitors of UppS 87
- Figure 3-3: Optimized conditions for *B. subtilis* 168 growth inhibition screen 89
- Figure 3-4: Replica plot of primary *B. subtilis* 168 growth inhibition screen 90
- Figure 3-5: Optimization of the targocil antagonism screen 91
- Figure 3-6: Replica plot depicting data from secondary targocil antagonism screen 93
- Figure 3-7. Establishing parameters for *in vitro* assessment of UPPS cloned from *B. subtilis*, *E. coli*, and *S. aureus* 96
- Figure 3-8: Replica plot depicting the results from the *in vitro* UppS screen of 35 priority antagonists 97
- Figure 3-9. Dose dependent inhibition of *B. subtilis* 168, *S. aureus*, and *E. coli* 100

- Figure 3-10: Mapping of spontaneously generated mutants developed in the presence of MAC-0547630 and MAC-0588238 102
- Figure 3-11: Assessment of the affects of UppS inhibitors on membrane potential 105
- Figure 3-12. Interaction of 5 novel UppS inhibitors with cefuroxime in in methicillin resistant *S. aureus* (MRSA) 106

CHAPTER FOUR

- Figure 4-1: Screen for targocil antagonists and growth inhibition led to the study of bepridil 137
- Figure 4-2: Assessment of bepridils interaction with targocil and cefuroxime in *S. aureus* CA-MRSA USA300 138
- Figure 4-3: Bepridil does not inhibit UppS^{BS} activity *in vitro* 139
- Figure 4-4: Sensitization of *B. subtilis* 168 CRISPRi knockdowns to bepridil . 141
- Figure 4-5: Dose dependent assessment of bepridils affect on the proton motive force 143
- Figure 4-6: General PMF perturbing compounds do not interact with targocil in *S. aureus* CA-MRAS USA300 145
- Figure 4-7: Bepridil antibacterial spectrum 147
- Figure 4-8: Bepridil displays interactions with the first lipid linked step of wall teichoic acid and peptidoglycan 148
- Figure 4-9: Assessing bepridils interaction with undecaprenyl-phosphate . . 150
- Figure 4-10: Affects of osmo-protectants on Bepridil's activity in *B. subtilis* . 152

List of Tables

CHAPTER TWO

- Table 2-1. Evaluation of the sensitivity of the HTS optimized P_{ywaC} reporter system against select cell wall associated and membrane perturbing compounds. 37
- Table 2-2: Nine cell wall-active lead compounds 45

CHAPTER THREE

- Table 3-1: Assessment of *in vitro* inhibition of 5 novel inhibitors against UppS isolated from *B. subtilis*, *S. aureus*, and *E. coli* 99
- Table 3-2. Cross resistance of spontaneous mutants generated in the presence of MAC-0547630 and MAC-0588238 104

List of Abbreviations

DNA – deoxyribonucleic acid
RNA – ribonucleic acid
MDR – multi drug resistance
GAIN – generating antibiotics incentive now
MRSA – methicillin resistant *S. aureus*
CDC – center for disease control and prevention
PG – peptidoglycan
WTA – wall teichoic acid
Und-P – undecaprenyl phosphate
Und-PP – undecaprenyl pyrophosphate
MurNAc - *N*-acetylmuramic acid
GlcNAc - *N*-acetylglucosamine
UDP – uridine diphosphate
ManNAc *N*-acetyl-mannosamine
DAP - diaminopimelic acid
GroP - glycerol-3-phosphate
DOXP - 1-deoxy-D-xylulose-5-diphosphate
IPP - isopentenyl pyrophosphate
FPP - fransyl pyrophosphate
PBPs – penicillin binding proteins
MOA – mode of action
GTP – guanosine triphosphate
CRISPR - Clustered Regularly Interspaced Short Palindromic Repeats
sgRNA – single guide RNA
RNAP – RNA polymerase
HTS – high throughput screening
LB – lysogeny broth
MHB – Mueller hinton broth
MAC - minimum activation concentration
MIC - minimum inhibitory concentration
DMSO – dimethyl sulfoxide
MSM – Magnesium Chloride, Sucrose, Maleic acid
LC/MS - liquid chromatography mass spectrometry
IQM – Inter quartile method
TEV - Tobacco Etch Virus
MESG - 2-amino-6-mercapto-7-methyl-purine ribonucleoside
SNP – single nucleotide polymorphism
PMF – proton motive force
PADs – previously approved drugs
CFU – colony forming units

CHAPTER ONE – Introduction

Antibiotic Discovery and Effectiveness

There is no doubt that the discovery of penicillin in 1929, is one of the most significant discoveries in modern medicine. In addition to being one of the first clinically used antibiotics, the discovery of the drug jumpstarted the golden age of antibiotic discovery (Lewis, 2013). In the span of 20-years, between 1940 and 1960, more than 11 different classes of antibiotics were discovered. Most of which target macromolecular biosynthetic processes including cell wall, DNA, RNA and protein synthesis (Clatworthy et al., 2007). Indeed, half of the drugs commonly used today were discovered between 1950 and 1970 (Davies, 2006). Although this golden age ended quite abruptly, the rapid development of antimicrobial therapies, resulted in a rapid decline in morbidity and mortality rates. Indeed, this caused the United States surgeon general to deem that the battle against infectious disease was over – “the time has come to close the book on infectious disease” (1967). With the proverbial low-hanging fruit gone, coupled with this mentality, the emergence of multi-drug resistance came at a time of steep decline in the search and development of novel antibacterial agents (Davies, 2006; Wright, 2007). Alexander Fleming warned against the emergence of resistance in 1946 when he proclaimed “There is probably no chemotherapeutic drug to which in suitable circumstances the bacteria cannot react by in some way acquiring ‘fastness’ [resistance].”

In current times the emergence of multidrug-resistant (MDR) bacterial pathogens is quickly becoming the main challenge facing modern medicine (Boucher et al., 2009; Nathan, 2015). Though MDR is receiving increased amounts of coverage in the media and acknowledgment from governments through implementation of legislation such as the Generating Antibiotics Incentives Now (GAIN) act (Spellberg, 2014); the importance of combating resistance cannot be overstated. Since the golden age of discovery, resistance has prevailed in all known classes of antibiotics (Wright, 2007), severely diminishing their effectiveness. A recent report titled 'Antibiotic Resistance Threats in the United States', published by the center for disease control and prevention (CDC) has expanded on the well recognized list of 'ESKAPE' pathogens (*Enterobacter*, *Staphylococcus aureus*, *Klebsiella pneumoniae*, *Acinetobacter baumannii*, *Pseudomonas aeruginosa* and *Enterococcus faecium*) (Boucher et al., 2009) and classified 18 threats into three categories: urgent, serious, and concerning threats. Though the field has taken great interest in combating Gram-negative resistance (Livermore, 2012; Silver, 2011) due to the difficulty of drug penetration and active efflux, methicillin-resistant *Staphylococcus aureus* (MRSA) still remains a major threat to human health. The CDC classified it as a 'serious threat' causing 80,461 severe infections per year, ultimately resulting in 11,285 deaths. Indeed, MRSA is one of the leading causes of healthcare associated infections and should not be forgotten in the fight against bacterial resistance.

One of the earliest studied and well validated targets for antimicrobial discovery is the bacterial cell wall. Although well explored, the cell wall has many underutilized targets that could be leveraged (Bugg et al., 2011; Silver, 2006). The attractiveness of this target stems from the fact that most of its biosynthetic pathway is essential for survival. In addition, genes involved in cell wall biosynthesis are well conserved among various bacterial species and are absent in mammalian systems. Modern-day researchers are once again turning to this target and developing new techniques and methodologies to aid discoveries (Ling et al., 2015; Sewell and Brown, 2013; Zhu et al., 2013).

Components & Synthesis of the Gram-positive Cell Wall

The Gram-positive bacterial cell wall is an essential macro-molecular structure, mainly comprised of a thick murein layer with covalently bound anionic polymers that play key roles in numerous cellular functions including maintenance of cell shape, growth and division (Hancock, 1997). The Gram-positive cell wall is comprised of three main components; proteins, peptidoglycan (PG) and wall teichoic acid (WTA), where the latter two make up the bulk of the cell wall in almost equal quantities and are synthesized on the lipid carrier undecaprenyl phosphate (Bhavsar and Brown, 2006). Below, is an overview of the synthesis of PG, WTA and the pivotal lipid carrier undecaprenyl-phosphate (Und-P) (Figure 1-1, Figure 1-2).

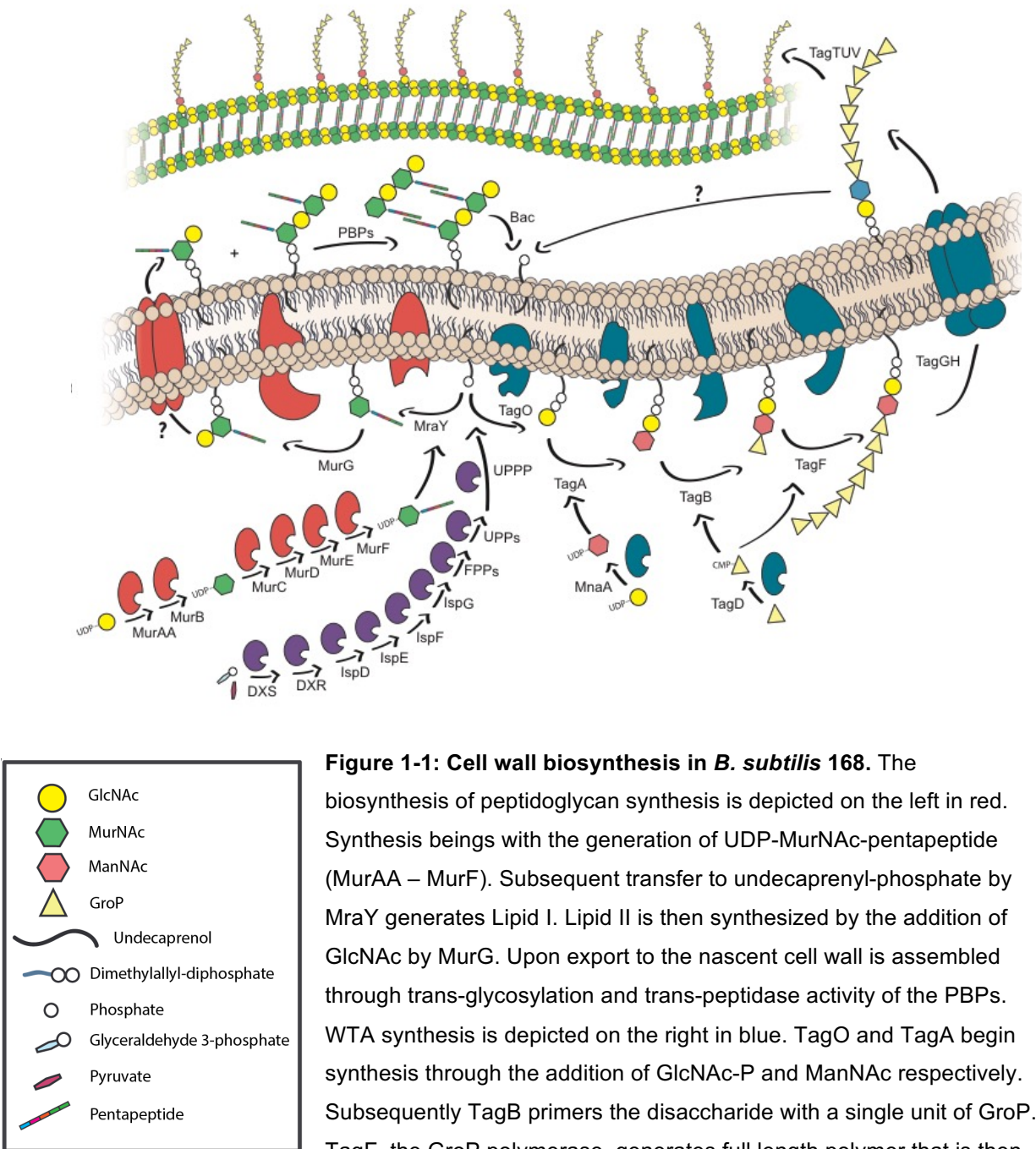


Figure 1-1: Cell wall biosynthesis in *B. subtilis* 168. The biosynthesis of peptidoglycan synthesis is depicted on the left in red. Synthesis begins with the generation of UDP-MurNAc-pentapeptide (MurAA – MurF). Subsequent transfer to undecaprenyl-phosphate by *MraY* generates Lipid I. Lipid II is then synthesized by the addition of GlcNAc by *MurG*. Upon export to the nascent cell wall is assembled through trans-glycosylation and trans-peptidase activity of the PBPs. WTA synthesis is depicted on the right in blue. *TagO* and *TagA* begin synthesis through the addition of GlcNAc-P and ManNAc respectively. Subsequently *TagB* primers the disaccharide with a single unit of GroP. *TagF*, the GroP polymerase, generates full length polymer that is then exported by *TagGH*. *TagTUV* completes the transfer of WTA to PG. In purple are outlined enzymes responsible for isoprenoid synthesis in *B. subtilis* 168. *DXS* - *IspG* enzymatic steps generate dimethylallyl-diphosphate that is subsequently polymerized into undecaprenyl-phosphate through the consecutive action of *FPPs*, *UppS* and *UPPP*.

enzymes responsible for isoprenoid synthesis in *B. subtilis* 168. *DXS* - *IspG* enzymatic steps generate dimethylallyl-diphosphate that is subsequently polymerized into undecaprenyl-phosphate through the consecutive action of *FPPs*, *UppS* and *UPPP*.

linear glycan strands made up of the alternating sugar residues *N*-acetylmuramic acid (MurNAc) and *N*-acetylglucosamine (GlcNAc) coupled by a β -1,4 glycosidic linkage. Each MurNAc sugar residue within the glycan strand contains a linked stem peptide chain comprised of four alternating L- and D-amino acids, which in *Bacillus subtilis* is L-alanyl- γ -D-glytamyl-diaminopimelyl-D-alanyl-D-alanine. Utilizing these stem peptides, adjacent glycan strands can form peptidyl bridges thereby creating a 3D superstructure providing the cell with structural integrity (Bhavsar and Brown, 2006; Burge et al., 1977a; 1977b; Hancock, 1997).

Synthesis of peptidoglycan begins with the intracellular synthesis of the precursor lipid II, which is formed in a stepwise manner beginning with the synthesis of UDP-*N*-acetylmuramic acid (UDP-MurNAc) from UDP-*N*-acetylglucosamine (UDP-GlcNAc) and phosphoenolpyruvate, catalyzed by the enzymes MurAA and MurB (Barreteau et al., 2008). Once synthesized, UDP-MurNAc undergoes subsequent reactions introducing the pentapeptide moiety at the D-lactyl position of the sugar. The pentapeptide is formed by the successive enzymatic steps of MurC, MurD, MurE, and MurF that catalyzes the addition of L-ala D-glu, diaminopimelic acid (DAP) and the dipeptide, D-ala D-ala respectively (Bouhss et al., 2008). Once complete the fully synthesized MurNAc-pentapeptide becomes lipid linked by the action of MraY that catalyzes its transfer to undecaprenyl-phosphate, an essential lipid carrier for cell wall synthesis, forming lipid I (Bouhss et al., 2008). Synthesis of lipid II is then carried out by MurG that

catalyzes the addition of UDP-GlcNAc to the 4-hydroxyl group of the MurNAc lipid I sugar. Lipid II is subsequently transferred across the membrane to the nascent cell wall and polymerized using various penicillin-binding-proteins (PBPs) through trans-glycosylase and trans-peptidase activity (van Heijenoort, 2001) (Figure 1-1).

Wall Teichoic Acid

Unlike the Gram-negative cell wall, which is primarily comprised of peptidoglycan, the Gram-positive cell wall in addition to PG has equal parts wall teichoic acids, which are a group of chemically diverse, high charged, phosphate rich anionic polymer covalently bound to peptidoglycan (BURGER and GLASER, 1964). Although the role of WTA is not completely understood, many studies point to various potential functions in bacterial physiology including, virulence (Weidenmaier et al., 2004; Winstel et al., 2015), bacteriophage attachment (Young, 1967), bio-film formation (Holland et al., 2011), metal deposition (Beveridge and Murray, 1980), cation chelation (Beveridge and Murray, 1980), cell shape (D'Elia et al., 2006a) and potential phosphate reservation (Grant, 1979). The identification of the genes responsible for the biosynthesis of WTA was first performed by searching for temperature-sensitive mutants that were impaired in teichoic acid synthesis (Brandt and Karamata, 1987; Pooley et al., 1991). These seminal studies coupled with biochemistry, informatics and

structural determination has led to our current understanding of the WTA biosynthetic pathway (Figure 1-1). In *B. subtilis* 168 the first step in WTA synthesis is the formation of an undecaprenyl-pyrophosphate disaccharide on the cytoplasmic side of the cell membrane where the two sugar molecules, GlcNAc and ManNAc, are added in succession by TagO and TagA. Both enzymes use the UDP activated version of their respective sugars, adding them onto the lipid carrier undecaprenyl-phosphate (Soldo et al., 2002; 1999). Indeed, this is the same lipid carrier used for PG synthesis. TagB, the WTA primase, subsequently adds a glycerol-3-phosphate (GroP) unit onto the lipid linked disaccharide (Bhavsar et al., 2005). The WTA polymerase TagF then adds GroP residues to form a polymer of a defined length (Sewell et al., 2009). The substrate for both TagB and TagF is an activated form of the sugar, CDP-glycerol, which is a product of TagD (Fong et al., 2006). Once polymerization is completed by TagF the polymer is flipped from the cytoplasmic side of the membrane to the extracellular surface by TagGH, an ABC transporter, at which point the polymer is covalently attached to peptidoglycan (Schirner et al., 2011). Until recently the enzymes responsible for the transfer of WTA to PG was unknown. Utilizing a MreB cytoskeleton pull down assay, Kawai Y., and colleagues, have identified three putative, and functionally redundant WTA transferases, TagT, TagU and TagV that are the products of the *lytR*, *ywtF*, *yvhJ* genes (Kawai et al., 2011).

As mentioned above, both WTA and PG synthesis are anchored to the lipid linked carrier undecaprenyl-phosphate (Und-P). Once synthesis and proper localization on the extracellular surface is complete, undecaprenyl-pyrophosphate is released, which can then be de-phosphorylated by undecaprenyl-phosphate phosphatase and recycled to act once again as a lipid carrier for subsequent rounds of either PG or WTA synthesis (Bhavsar and Brown, 2006).

Undecaprenyl-phosphate Synthesis

Both wall teichoic acid polymers and precursors of peptidoglycan synthesis are synthesized on the indispensable lipid carrier undecaprenyl-phosphate. Seminal biochemical studies have shown that Und-P is generated by linking 11 isopentenyl pyrophosphate (IPP) units, which for many years was thought to be the product of a mevalonate dependent biosynthetic pathway across *all organisms*. In recent years however it has been brought to light that an alternate, mevalonate-independent pathway, also exists for isopentenyl-pyrophosphate synthesis (Lichtenthaler, 2000; Rohdich et al., 2003; Rohmer, 1999). The alternate, DOXP pathway, utilizes glyceraldehyde 3-phosphate and pyruvate as a starting material. Both the DOXP and mevalonate pathway result in the production of isopentenyl-pyrophosphate (Rohmer, 1999). Farnesyl pyrophosphate synthase (FPPs) is a short-chain *trans*-prenyl-transferase that utilizes isopentenyl pyrophosphate to generate farnesyl pyrophosphate (FPP)

(Hosfield et al., 2004; Liang et al., 2002). Subsequently undecaprenyl pyrophosphate synthase (UppS), a long-chain *cis*-prenyl-transferase, is primed with 1 unit of FPP and through 8 consecutive 1'-4 condensations of IPP, generating undecaprenyl pyrophosphate (Und-PP) (Apfel et al., 1999; Liang et al., 2002). Upon dephosphorylation of Und-PP, by the nonessential enzyme UPPP, Und-P can be utilized for both peptidoglycan and wall teichoic acid synthesis (Tatar et al., 2007).

Peptidoglycan and Wall Teichoic Acid Synthesis is Intricately Linked

Outlined above are the biosynthetic pathways of peptidoglycan, wall teichoic acid and undecaprenyl-phosphate synthesis. Though these pathways can be thought of as distinct, it is important to note that cross-talk between these pathways exists. One such example is the balancing act that occurs between PG and WTA synthesis as a result on both pathways dependence on Und-P. It has been demonstrated that shutting down WTA synthesis can lead to increased PG production (D'Elia et al., 2009). Additionally it has been demonstrated that wall teichoic acids are spatial and temporal regulators for proper localization of PBPs that are responsible for late stage PG assembly (Atilano et al., 2010). Such connections between these distinct pathways can have great implications for cell wall drug discovery. They can lead not only to new therapeutic approaches such as combination therapies combining WTA and PG inhibitors (Farha et al., 2013);

but can also lead to unique screening approaches in the discovery of new antibiotics.

High Throughput Techniques in Antibacterial Drug Discovery

Traditionally, antibacterial screening campaigns fall into one of two categories; target based, and whole-cell phenotypic approaches. Both of these approaches have their own advantages and pitfalls (Brown and Wright, 2016; Farha and Brown, 2015; Payne et al., 2007; Silver, 2011; Swinney and Anthony, 2011) .

Screening campaigns employing a target base approach typically involve looking for inhibitors of a specific enzyme/target in a cell-free *in vitro* system. The greatest advantage of this approach is the quick identification of chemical matter that is on target; i.e. the mode of action (MOA) of hits is determined by the primary screen. However, a stringent bottleneck occurs when one tries to translate the *in vitro* inhibition observed into a whole-cell system. Bacterial cell surfaces make for phenomenal permeability barriers blocking most *in vitro* inhibitors from ever coming into contact with their intracellular targets (Cox and Wright, 2013; Silver, 2011). Complementary to this barrier are well developed efflux systems that actively pump unwanted chemical matter outside the cell (Nikaido, 1996). Indeed, this well developed system is one reason why targeting extracellular targets such as the PBPs has been so successful (Lewis, 2013).

Whole-cell phenotypic based campaigns are largely comprised of small molecule screens for antibacterial activity. Though such an approach obviates the bottlenecks associated with permeability and efflux, it too suffers from its own obstacles. Often whole-cell phenotypic screens suffer from too large a number of actives, many of which demonstrate non-specific toxicity making prioritization of chemical matter onerous (Silver, 2011). Compounding this problem are the hurdles associated with mode of action studies. With ~ 300 essential genes in both *E. coli* (Gerdes et al., 2003) and *S. aureus* (Forsyth et al., 2002), matching an inhibitor to its respective target is no small task.

Increasingly it is becoming evident that neither of these conventional approaches on their own serves us well for new antibacterial drug discovery. As such, the field is moving towards an integrative approach involving the development of whole-cell phenotypic screens that are directed towards a subset or specific target. Indeed, moving towards this integrated approach can harness the power of both conventional approaches while mitigating many of their individual shortcomings. Integrated strategies developed in cell wall drug discovery include screens for high-copy suppression (Li et al., 2004), comparative screens between wild-type and engineered rescue strains (Testa and Johnson, 2012), promoter-reporter target based screening (Czarny et al., 2014), and screens for changes in phenotype (resistance or sensitivity) caused by blockages in a specific

pathway (Swoboda et al., 2009; Wang et al., 2013). Outlined below are two examples that are elaborated and built upon throughout this thesis.

A Promoter-Reporter System for the Detection of Lesions in Cell Wall Synthesis

Nearly all cell wall active agents have been discovered using screens for growth inhibition, followed by time consuming and cumbersome secondary screens for activity directed towards the cell wall. Greatly lacking in the field are primary screening assays that are sensitive in detecting cell wall active compounds while avoiding off-target nuisance compounds. One way to develop such a primary screen is to harness the power of reporter-based strains that respond to cell wall stress. Many reporters have now been developed that respond to essential steps in PG synthesis; including a *vanH* promoter-reporter fusion to *lacZ* (Ulijasz et al., 1996). Such systems however suffer from only reporting on a subset of cell wall targets such as inhibition of trans-glycosylation (Mani et al., 1998). In recent years our lab has developed the P_{ywaC} reporter system that demonstrates a comprehensive response to inhibition of multiple pathways that converge on cell wall assembly, including PG, isoprenoid and WTA synthesis (D'Elia et al., 2009). Below outlined is the discovery and proof-of-principal of the P_{ywaC} reporter system.

D'Elia and colleagues in search for a novel promoter-reporter system, conducted a genome-wide search for promoters in *Bacillus subtilis* 168 that are up-regulated to TagD depletions by way of microarray analysis (D'Elia et al., 2009). During this study it was determined that one hundred and seventy-six genes were significantly activated in response to depletions in WTA synthesis. These genes were subsequently cross referenced with an existing data set that looked for stimulation of transcriptional activity by known antibiotics. Such efforts resulted in the shortlisting of ten genes all of which were highly up-regulated in response to TagD depletion. Of these ten, five showed up-regulation in response to cell wall-active antibiotics. All ten genes were highly up-regulated by TagD depletion and were well conserved among Gram-positive bacteria. Real time promoter-reporter systems were generated by fusing the promoters of each short-listed gene to *lux* genes providing a luminescence signal. These reporter systems were introduced into *tagB*, *tagD*, and *tagF* conditional mutants and luminescence was monitored under both induced and non-induced conditions. Of the short listed genes, the promoter of *ywaC* showed to be the most promising as lesions in teichoic acid biosynthesis caused between a 4 and 20-fold increase in luminescence (D'Elia et al., 2009).

To further validated the P_{*ywaC*} real-time reporter system and assess its suitability for high throughput screening, the system was tested against a commercially available library of 1,120 small molecules that contained previously approved

drugs and 167 antibiotics. It was clear that P_{ywaC} responded almost exclusively to cell wall-active antibiotics; particularly bacitracin, ramoplanin, vancomycin, and fosfomycin. Interestingly it was also noted that the reporter system was activated in response to fosmidomycin, an inhibitor of IspC, which is a committed step of isoprenoid synthesis (D'Elia et al., 2009).

Unique Dispensability Pattern Found in the WTA Biosynthetic Pathway Leads to a Platform for Drug Discovery

Recent technologies such as the development of genomic libraries has allowed for the deeper understanding of bacterial physiology. Such studies are continually elucidating the inherent complexities found within cell wall synthesis due in part to the numerous interconnected biosynthetic pathways that are both spatially and temporally regulated. Various studies have focused on unraveling the complexities of teichoic acid genetics in *B. Subtilis* 168. It has been demonstrated that late acting genes, namely *tagB*, *tagD*, and *tagF* are essential to cellular viability (Bhavsar et al., 2001; 2004). However it has also been shown that TagO, the enzyme responsible for catalyzing the first step in the biosynthetic pathway is dispensable (D'Elia et al., 2006a; 2006b). In subsequent work it was also been shown that deletion of *tagO* relieves the essentiality of the late acting biosynthetic genes (Lazarevic and Karamata, 1995; Soldo et al., 2002). This is indeed a synthetic-viable interaction (Figure 1-3).

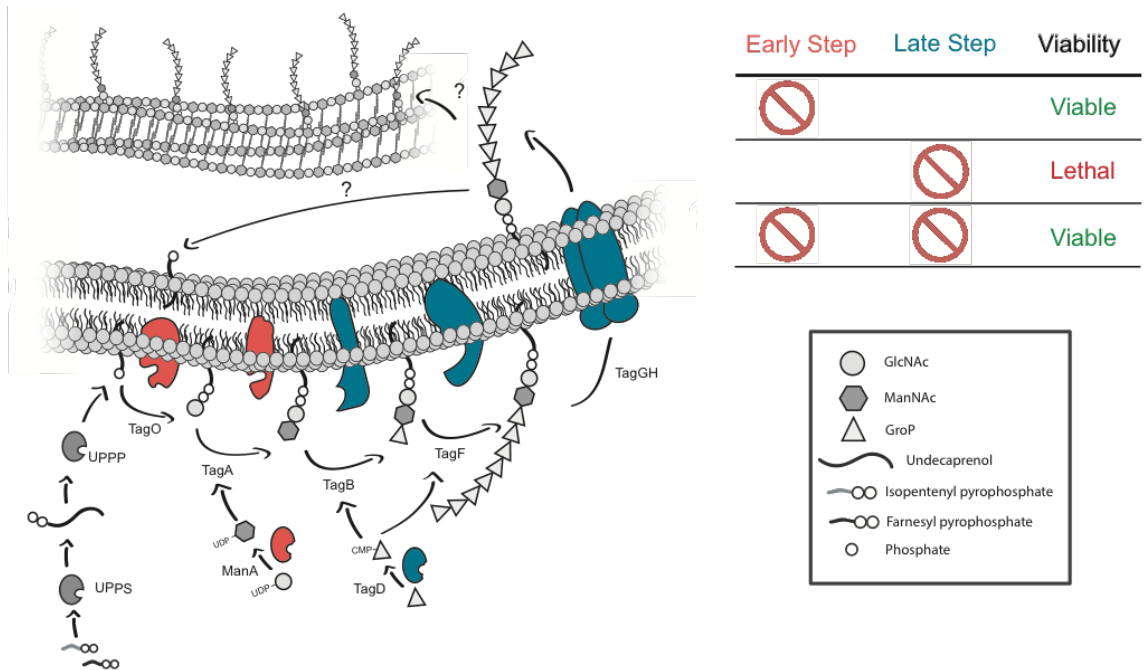


Figure 1-3: Dispensability pattern of Wall Teichoic Acid (WTA) biosynthesis in *B. subtilis* 168. The WTA biosynthetic pathway is divided into early (pink) and late (blue) steps. Gene products involved in early step synthesis (TagO, TagA) are dispensable for viability. Late acting gene products (TagB, TagD, TagF, TagGH) are essential and as such crucial for viability. Upon the introduction of a lesion in early step synthesis, late acting gene products become dispensable. As such lesion in late steps become no longer essential for viability under such conditions.

One can imagine how this powerful phenotype could be exploited for the discovery of wall teichoic acid inhibitors. Indeed, there have been numerous late stage WTA discovery campaigns which harnessed the power of this synthetic-viable interaction through the implementation of whole-cell phenotypic screening. The earliest example of such a study was performed by Swoboda and coworkers, who performed a high-throughput 55,000 small molecule screen against wild-type

S. aureus (RN4220) and the corresponding $\Delta tarO$ strain (Swoboda et al., 2009). Indeed, shortlisting small molecules that had antibacterial activity against wild-type *S. aureus* and had attenuated activity in a $\Delta tarO$ background led to the enrichment of late stage WTA inhibitors. Swoboda and coworkers identified 45 such compounds, the most potent of which was 1835F03; in subsequent work this molecule is referred to as targocil (Schirner et al., 2011; Swoboda et al., 2009). Targocil showed good antibacterial activity against RN4220 and some MRSA backgrounds but showed no activity against other Gram-positives such as *B. subtilis* 168 (Swoboda et al., 2009). The target of targocil was elucidated to be TarGH (the homolog of the *B. subtilis* 168 TagGH ABC transporter). In efforts to conclusively demonstrate this, researchers showed that heterologous complementation of TarGH using the *B. subtilis* 168 TagGH in *S. aureus* completely alleviated its activity (Schirner et al., 2011). This was only possible due to the fact that targocil is a *S. aureus* specific inhibitor and does not act upon TagGH, the *B. subtilis* 168 counterpart.

Objectives and Outline of This Thesis

Chemical-genetics, a term coined in the 1990's, aims to systematically use chemical matter to study how perturbations of a proteins function can distort a biological system as a whole. With rapid progression of such studies the amount of information regarding the interconnectedness of cellular networks has

exploded. The overarching objective of this thesis is to determine whether or not the 'connectedness' found between cell wall biosynthetic pathways (namely WTA, PG and isoprenoid synthesis) can be harnessed to develop 'unusual / unconventional' drug discovery platforms. Techniques and workflows outlined in subsequent chapters are unique in nature as they capture the power of whole-cell-phenotypic and target based screening while obviating many of their individual pitfalls. Such screening approaches could not be possible without the field of chemical-genetics. Indeed, the ultimate goal of this thesis is to demonstrate the credence of such approaches by utilizing them to discover and characterize novel classes of cell wall inhibitors.

Chapter 2 builds upon previously published work describing the discovery of the P_{ywaC} reporter. Outlined is the implementation of this reporter strain in a high-throughput manner to perform whole-cell reporter based screening for cell wall actives. The highly selective nature of the P_{ywaC} reporter led to the shortlisting of only 46 inhibitors from a library of 26,000 small molecules. Indeed, this was a manageable number of molecules to further characterize using more conventional techniques. Such work resulted in the discovery of 9 cell-wall active molecules. Outlined further in chapter 2 is the use of a newly developed *B. subtilis* 168 library of essential gene knockdowns that successfully identified the direct target of one of these cell wall actives.

As described above, the synthetic-viable WTA phenotype has led to the discovery of late stage inhibitors such as targocil. Rather than continuing on the same path, chapter 3 outlines an innovative antagonism based approach to 'screen for life'. Harnessing the same complex dispensability pattern, a chemical-chemical antagonism combination screen was developed using targocil -- the TarGH *S. aureus* specific inhibitor. One can imagine that small molecules that antagonize the action of targocil would be inhibitors of early step and WTA substrate producing enzymes. The study outlined in chapter 3 begins with screening a large library of 140,000 compounds, which resulted in a significant enrichment of inhibitors of the enzyme UppS – the prenyl-transferase responsible for undecaprenyl phosphate production. Indeed, Und-P is a substrate for the first step of WTA synthesis. With a strong connection between late stage WTA antagonism and Und-P it was of interest to determine what other targets would show antagonistic phenotypes with targocil.

Chapter 4 addresses this question by studying the mode of action of bepridil. Bepridil too shows strong antagonism with targocil, inhibits an essential target, but shows no affect on UppS activity *in vitro*. Though the exact mechanism of bepridil is still unknown, work outlined in chapter 4 points towards the first few lipid-linked steps of peptidoglycan synthesis. Overall, this thesis outlines effective and innovative approaches toward the identification of novel cell wall active compounds.

REFERENCES:

- Apfel, C.M., Takács, B., Fountoulakis, M., Stieger, M., Keck, W., 1999. Use of Genomics To Identify Bacterial Undecaprenyl Pyrophosphate Synthetase: Cloning, Expression, and Characterization of the Essential uppS Gene. *J. Bacteriol.* 181, 483–492. doi:10.1016/0003-9861(76)90504-X
- Atilano, M.L., Pereira, P.M., Yates, J., Reed, P., Veiga, H., Pinho, M.G., Filipe, S.R., 2010. Teichoic acids are temporal and spatial regulators of peptidoglycan cross-linking in *Staphylococcus aureus*. *Proc. Natl. Acad. Sci. U.S.A.* 107, 18991–18996. doi:10.1073/pnas.1004304107
- Barreteau, H., Kovac, A., Boniface, A., Sova, M., Gobec, S., Blanot, D., 2008. Cytoplasmic steps of peptidoglycan biosynthesis. *FEMS Microbiol. Rev.* 32, 168–207. doi:10.1111/j.1574-6976.2008.00104.x
- Beveridge, T.J., Murray, R.G., 1980. Sites of metal deposition in the cell wall of *Bacillus subtilis*. 141, 876–887.
- Bhavsar, A.P., Beveridge, T.J., Brown, E.D., 2001. Precise deletion of tagD and controlled depletion of its product, glycerol 3-phosphate cytidyltransferase, leads to irregular morphology and lysis of *Bacillus subtilis* grown at physiological temperature. 183, 6688–6693. doi:10.1128/JB.183.22.6688-6693.2001
- Bhavsar, A.P., Brown, E.D., 2006. Cell wall assembly in *Bacillus subtilis*: how spirals and spaces challenge paradigms. *Molecular Microbiology* 60, 1077–1090. doi:10.1111/j.1365-2958.2006.05169.x
- Bhavsar, A.P., Erdman, L.K., Schertzer, J.W., Brown, E.D., 2004. Teichoic acid is an essential polymer in *Bacillus subtilis* that is functionally distinct from teichuronic acid. 186, 7865–7873. doi:10.1128/JB.186.23.7865-7873.2004
- Bhavsar, A.P., Truant, R., Brown, E.D., 2005. The TagB protein in *Bacillus subtilis* 168 is an intracellular peripheral membrane protein that can incorporate glycerol phosphate onto a membrane-bound acceptor in vitro. *J. Biol. Chem.* 280, 36691–36700. doi:10.1074/jbc.M507154200
- Boucher, H.W., Talbot, G.H., Bradley, J.S., Edwards, J.E., Gilbert, D., Rice, L.B., Scheld, M., Spellberg, B., Bartlett, J., 2009. Bad bugs, no drugs: no ESKAPE! An update from the Infectious Diseases Society of America. *Clin. Infect. Dis.* 48, 1–12. doi:10.1086/595011
- Bouhss, A., Trunkfield, A.E., Bugg, T.D.H., Mengin-Lecreulx, D., 2008. The biosynthesis of peptidoglycan lipid-linked intermediates. *FEMS Microbiol. Rev.* 32, 208–233. doi:10.1111/j.1574-6976.2007.00089.x
- Brandt, C., Karamata, D., 1987. Thermosensitive *Bacillus subtilis* mutants which lyse at the non-permissive temperature. *J. Gen. Microbiol.* 133, 1159–1170. doi:10.1099/00221287-133-5-1159
- Brown, E.D., Wright, G.D., 2016. Antibacterial drug discovery in the resistance era. *Nature* 529, 336–343. doi:10.1038/nature17042

- Bugg, T.D.H., Braddick, D., Dowson, C.G., Roper, D.I., 2011. Bacterial cell wall assembly: still an attractive antibacterial target. *Trends Biotechnol.* 29, 167–173. doi:10.1016/j.tibtech.2010.12.006
- Burge, R.E., Adams, R., Balyuzi, H.H., Reaveley, D.A., 1977a. Structure of the peptidoglycan of bacterial cell wall I. II. *J. Mol. Biol.* 117, 955–974.
- Burge, R.E., Fowler, A.G., Reaveley, D.A., 1977b. Structure of the peptidoglycan of bacterial cell walls. I. *J. Mol. Biol.* 117, 927–953.
- Burger, M.M., Glaser, L., 1964. The Synthesis of Teichoic Acids. I. Polyglycerol Phosphate. *J. Biol. Chem.* 239, 3168–3177.
- Clatworthy, A.E., Pierson, E., Hung, D.T., 2007. Targeting virulence: a new paradigm for antimicrobial therapy. *Nat Chem Biol* 3, 541–548. doi:10.1038/nchembio.2007.24
- Cox, G., Wright, G.D., 2013. Intrinsic antibiotic resistance: mechanisms, origins, challenges and solutions. *Int. J. Med. Microbiol.* 303, 287–292. doi:10.1016/j.ijmm.2013.02.009
- Czarny, T.L., Perri, A.L., French, S., Brown, E.D., 2014. Discovery of Novel Cell Wall-Active Compounds Using P_{ywaC}, a Sensitive Reporter of Cell Wall Stress, in the Model Gram-Positive Bacterium *Bacillus subtilis*. *Antimicrob. Agents Chemother.* 58, 3261–3269. doi:10.1128/AAC.02352-14
- D'Elia, M.A., Millar, K.E., Beveridge, T.J., Brown, E.D., 2006a. Wall teichoic acid polymers are dispensable for cell viability in *Bacillus subtilis*. *J. Bacteriol.* 188, 8313–8316. doi:10.1128/JB.01336-06
- D'Elia, M.A., Millar, K.E., Bhavsar, A.P., Tomljenovic, A.M., Hutter, B., Schaab, C., Moreno-Hagelsieb, G., Brown, E.D., 2009. Probing teichoic acid genetics with bioactive molecules reveals new interactions among diverse processes in bacterial cell wall biogenesis. *Chem. Biol.* 16, 548–556. doi:10.1016/j.chembiol.2009.04.009
- D'Elia, M.A., Pereira, M.P., Chung, Y.S., Zhao, W., Chau, A., Kenney, T.J., Sulavik, M.C., Black, T.A., Brown, E.D., 2006b. Lesions in teichoic acid biosynthesis in *Staphylococcus aureus* lead to a lethal gain of function in the otherwise dispensable pathway. *J. Bacteriol.* 188, 4183–4189. doi:10.1128/JB.00197-06
- Davies, J., 2006. Where have All the Antibiotics Gone? *Can J Infect Dis Med Microbiol* 17, 287–290.
- Farha, M.A., Brown, E.D., 2015. Unconventional screening approaches for antibiotic discovery. *Ann. N. Y. Acad. Sci.* 1354, 54–66. doi:10.1111/nyas.12803
- Farha, M.A., Leung, A., Sewell, E.W., D'Elia, M.A., Allison, S.E., Ejim, L., Pereira, P.M., Pinho, M.G., Wright, G.D., Brown, E.D., 2013. Inhibition of WTA Synthesis Blocks the Cooperative Action of PBPs and Sensitizes MRSA to β -Lactams *Antimicrob. Agents Chemother.* 8, 226–233. doi:10.1021/cb300413m
- Fong, D.H., Yim, V.C.-N., D'Elia, M.A., Brown, E.D., Berghuis, A.M., 2006. Crystal structure of CTP:glycerol-3-phosphate cytidylyltransferase from *Staphylococcus aureus*: examination of structural basis for kinetic mechanism. *Biochim. Biophys. Acta* 1764, 63–69. doi:10.1016/j.bbapap.2005.10.015

- Forsyth, R.A., Haselbeck, R.J., Ohlsen, K.L., Yamamoto, R.T., Xu, H., Trawick, J.D., Wall, D., Wang, L., Brown-Driver, V., Froelich, J.M., C, K.G., King, P., McCarthy, M., Malone, C., Misiner, B., Robbins, D., Tan, Z., Zhu Zy, Z.-Y., Carr, G., Mosca, D.A., Zamudio, C., Foulkes, J.G., Zyskind, J.W., 2002. A genome-wide strategy for the identification of essential genes in *Staphylococcus aureus*. *Molecular Microbiology* 43, 1387–1400.
- Gerdes, S.Y., Scholle, M.D., Campbell, J.W., Balázs, G., Ravasz, E., Daugherty, M.D., Somera, A.L., Kyrpides, N.C., Anderson, I., Gelfand, M.S., Bhattacharya, A., Kapratl, V., D'Souza, M., Baev, M.V., Grechkin, Y., Mseeh, F., Fonstein, M.Y., Overbeek, R., Barabási, A.-L., Oltvai, Z.N., Osterman, A.L., 2003. Experimental determination and system level analysis of essential genes in *Escherichia coli* MG1655. *J. Bacteriol.* 185, 5673–5684. doi:10.1128/JB.185.19.5673-5684.2003
- Grant, W.D., 1979. Cell wall teichoic acid as a reserve phosphate source in *Bacillus subtilis*. 137, 35–43.
- Hancock, I.C., 1997. Bacterial cell surface carbohydrates: structure and assembly. *Biochem. Soc. Trans.* 25, 183–187.
- Holland, L.M., Conlon, B., O'Gara, J.P., 2011. Mutation of tagO reveals an essential role for wall teichoic acids in *Staphylococcus epidermidis* biofilm development. *Microbiology (Reading, Engl.)* 157, 408–418. doi:10.1099/mic.0.042234-0
- Hosfield, D.J., Zhang, Y., Dougan, D.R., Broun, A., Tari, L.W., Swanson, R.V., Finn, J., 2004. Structural basis for bisphosphonate-mediated inhibition of isoprenoid biosynthesis. *J. Biol. Chem.* 279, 8526–8529. doi:10.1074/jbc.C300511200
- Kawai, Y., Marles-Wright, J., Cleverley, R.M., Emmins, R., Ishikawa, S., Kuwano, M., Heinz, N., Bui, N.K., Hoyland, C.N., Ogasawara, N., Lewis, R.J., Vollmer, W., Daniel, R.A., Errington, J., 2011. A widespread family of bacterial cell wall assembly proteins. *EMBO J.* 30, 4931–4941. doi:10.1038/emboj.2011.358
- Lazarevic, V., Karamata, D., 1995. The tagGH operon of *Bacillus subtilis* 168 encodes a two-component ABC transporter involved in the metabolism of two wall teichoic acids. *Molecular Microbiology* 16, 345–355.
- Lewis, K., 2013. Platforms for antibiotic discovery. *Nat Rev Drug Discov* 12, 371–387. doi:10.1038/nrd3975
- Li, X., Zolli-Juran, M., Cechetto, J.D., Daigle, D.M., Wright, G.D., Brown, E.D., 2004. Multicopy suppressors for novel antibacterial compounds reveal targets and drug efflux susceptibility. *Chem. Biol.* 11, 1423–1430. doi:10.1016/j.chembiol.2004.08.014
- Liang, P.-H., Ko, T.-P., Wang, A.H.-J., 2002. Structure, mechanism and function of prenyltransferases. *Eur. J. Biochem.* 269, 3339–3354.
- Lichtenthaler, H.K., 2000. Non-mevalonate isoprenoid biosynthesis: enzymes, genes and inhibitors. *Biochem. Soc. Trans.* 28, 785–789.
- Ling, L.L., Schneider, T., Peoples, A.J., Spoering, A.L., Engels, I., Conlon, B.P., Mueller, A., Schäberle, T.F., Hughes, D.E., Epstein, S., Jones, M., Lazarides, L., Steadman, V.A., Cohen, D.R., Felix, C.R., Fetterman, K.A., Millett, W.P., Nitti, A.G., Zullo, A.M., Chen, C., Lewis, K., 2015. A new antibiotic kills pathogens without detectable resistance. *Nature* 517,

455–459. doi:10.1038/nature14098

Livermore, D.M., 2012. Current Epidemiology and Growing Resistance of Gram-Negative Pathogens. *The Korean Journal of Internal Medicine* 27, 128–142. doi:10.3904/kjim.2012.27.2.128

Mani, N., Sancheti, P., Jiang, Z.D., McNaney, C., DeCenzo, M., Knight, B., Stankis, M., Kuranda, M., Rothstein, D.M., Sanchet, P., Knighti, B., 1998. Screening systems for detecting inhibitors of cell wall transglycosylation in *Enterococcus*. *J. Antibiot.* 51, 471–479.

Nathan, C., 2015. Cooperative development of antimicrobials: looking back to look ahead. *Nat. Rev. Microbiol.* 13, 651–657. doi:10.1038/nrmicro3523

Nikaido, H., 1996. Multidrug efflux pumps of gram-negative bacteria. *J. Bacteriol.* 178, 5853–5859.

Payne, D.J., Gwynn, M.N., Holmes, D.J., Pompliano, D.L., 2007. Drugs for bad bugs: confronting the challenges of antibacterial discovery. *Nat Rev Drug Discov* 6, 29–40. doi:10.1038/nrd2201

Pooley, H.M., Abellan, F.X., Karamata, D., 1991. A conditional-lethal mutant of *Bacillus subtilis* 168 with a thermosensitive glycerol-3-phosphate cytidyltransferase, an enzyme specific for the synthesis of the major wall teichoic acid. *J. Gen. Microbiol.* 137, 921–928.

Rohdich, F., Zepeck, F., Adam, P., Hecht, S., Kaiser, J., Laupitz, R., Gräwert, T., Amslinger, S., Eisenreich, W., Bacher, A., Arigoni, D., 2003. The deoxyxylulose phosphate pathway of isoprenoid biosynthesis: studies on the mechanisms of the reactions catalyzed by IspG and IspH protein. *Proc. Natl. Acad. Sci. U.S.A.* 100, 1586–1591. doi:10.1073/pnas.0337742100

Rohmer, M., 1999. The discovery of a mevalonate-independent pathway for isoprenoid biosynthesis in bacteria, algae and higher plants†. *Natural Product Reports* 16, 565–574. doi:10.1039/A709175C

Schirner, K., Stone, L.K., Walker, S., 2011. ABC Transporters Required for Export of Wall Teichoic Acids Do Not Discriminate between Different Main Chain Polymers. *ACS chemical biology*. doi:10.1021/cb100390w

Sewell, E.W., Brown, E.D., 2013. Taking aim at wall teichoic acid synthesis: new biology and new leads for antibiotics. *J. Antibiot.* doi:10.1038/ja.2013.100

Sewell, E.W.C., Pereira, M.P., Brown, E.D., 2009. The wall teichoic acid polymerase TagF is non-processive in vitro and amenable to study using steady state kinetic analysis. *J. Biol. Chem.* 284, 21132–21138. doi:10.1074/jbc.M109.010215

Silver, L.L., 2011. Challenges of antibacterial discovery. *Clin. Microbiol. Rev.* 24, 71–109. doi:10.1128/CMR.00030-10

Silver, L.L., 2006. Does the cell wall of bacteria remain a viable source of targets for novel antibiotics? *Biochem. Pharmacol.* 71, 996–1005. doi:10.1016/j.bcp.2005.10.029

Soldo, B., Lazarevic, V., Karamata, D., 2002. tagO is involved in the synthesis of all anionic cell-wall polymers in *Bacillus subtilis* 168. *Microbiology (Reading, Engl.)* 148, 2079–2087.

- Soldo, B., Lazarevic, V., Pagni, M., Karamata, D., 1999. Teichuronic acid operon of *Bacillus subtilis* 168. *Molecular Microbiology* 31, 795–805.
- Spellberg, B., 2014. The future of antibiotics. *Crit Care*.
- Swinney, D.C., Anthony, J., 2011. How were new medicines discovered? *Nat Rev Drug Discov* 10, 507–519. doi:10.1038/nrd3480
- Swoboda, J.G., Meredith, T.C., Campbell, J., Brown, S., Suzuki, T., Bollenbach, T., Malhowski, A.J., Kishony, R., Gilmore, M.S., Walker, S., 2009. Discovery of a small molecule that blocks wall teichoic acid biosynthesis in *Staphylococcus aureus*. *ACS Chem Biol*. 4, 875–883. doi:10.1021/cb900151k
- Tatar, L.D., Marolda, C.L., Polischuk, A.N., van Leeuwen, D., Valvano, M.A., 2007. An *Escherichia coli* undecaprenyl-pyrophosphate phosphatase implicated in undecaprenyl phosphate recycling. *Microbiology (Reading, Engl.)* 153, 2518–2529.
- Testa, C.A., Johnson, L.J., 2012. A whole-cell phenotypic screening platform for identifying methylerythritol phosphate pathway-selective inhibitors as novel antibacterial agents. *Antimicrob. Agents Chemother.* 56, 4906–4913. doi:10.1128/AAC.00987-12
- Ulijasz, A.T., Grenader, A., Weisblum, B., 1996. A vancomycin-inducible lacZ reporter system in *Bacillus subtilis*: induction by antibiotics that inhibit cell wall synthesis and by lysozyme. 178, 6305–6309.
- van Heijenoort, J., 2001. Formation of the glycan chains in the synthesis of bacterial peptidoglycan. *Glycobiology* 11, 25R–36R.
- Wang, H., Gill, C.J., Lee, S.H., Mann, P., Zuck, P., Meredith, T.C., Murgolo, N., She, X., Kales, S., Liang, L., Liu, J., Wu, J., Santa Maria, J., Su, J., Pan, J., Hailey, J., Mcguinness, D., Tan, C.M., Flattery, A., Walker, S., Black, T., Roemer, T., 2013. Discovery of wall teichoic acid inhibitors as potential anti-MRSA β -lactam combination agents. *Chem. Biol.* 20, 272–284.
- Weidenmaier, C., Kokai-Kun, J.F., Kristian, S.A., Chanturiya, T., Kalbacher, H., Gross, M., Nicholson, G., Neumeister, B., Mond, J.J., Peschel, A., 2004. Role of teichoic acids in *Staphylococcus aureus* nasal colonization, a major risk factor in nosocomial infections. *Nature Medicine* 10, 243–245. doi:doi:10.1038/nm991
- Winstel, V., Kühner, P., Salomon, F., Larsen, J., Skov, R., Hoffmann, W., Peschel, A., Weidenmaier, C., 2015. Wall Teichoic Acid Glycosylation Governs *Staphylococcus aureus* Nasal Colonization. *MBio* 6, e00632. doi:10.1128/mBio.00632-15
- Wright, G.D., 2007. The antibiotic resistome: the nexus of chemical and genetic diversity. *Nat. Rev. Microbiol.* 5, 175–186. doi:10.1038/nrmicro1614
- Young, F.E., 1967. Requirement of glucosylated teichoic acid for adsorption of phage in *Bacillus subtilis* 168. *Proc. Natl. Acad. Sci. U.S.A.* 58, 2377–2384.
- Zhu, W., Zhang, Y., Sinko, W., Hensler, M.E., Olson, J., Molohon, K.J., Lindert, S., Cao, R., Li, K., Wang, K., Wang, Y., Liu, Y.-L., Sankovsky, A., de Oliveira, C.A.F., Mitchell, D.A., Nizet, V., McCammon, J.A., Oldfield, E., 2013. Antibacterial drug leads targeting isoprenoid biosynthesis. *Proc. Natl. Acad. Sci. U.S.A.* 110, 123–128. doi:10.1073/pnas.1219899110

CHAPTER TWO - P_{ywaC} , a sensitive reporter of cell wall stress

PREFACE

A portion of the work found in this chapter has been previously published:

Czarny, T.L., Perri, A.L., French S., Brown E.D. (2014) Discovery of novel cell wall-active compounds using P_{ywaC}, a sensitive reporter of cell wall stress, in the model gram-positive bacterium *Bacillus subtilis*. *Antimicrobial Agents and Chemotherapy*, June 2014 vol. 58 no. 6 3261-3269.

Work reproduced with permission. Copyright © American Society for Microbiology, *Antimicrobial Agents and Chemotherapy*, vol. 58, 2014, 3261-3269

Work outlining the identification of UppS as the target of MAC-0170636 was performed in collaboration with Dr. Jason Peters, a postdoctoral fellow in the lab of Dr. Carol Gross (UCSF). This work is in final review as part of a collaborative manuscript outlining the generation of the CRISPRi knockdown collection and its use as tool for drug discovery.

Jason M. Peters*, Alexandre Colavin*, Handuo Shi*, Tomasz L. Czarny, Matthew H. Larson, Spencer Wong, John S. Hawkins, Candy H. S. Lu, Byoung-Mo Koo, Elizabeth Marta, Anthony L. Shiver, Evan H. Whitehead, Jonathan S. Weissman, Eric D. Brown, Lei S. Qi, Kerwyn Casey Huang, Carol A. Gross (2016) A Comprehensive, CRISPR-based Approach to Functional Analysis of Essential Genes in Bacteria. *Cell (in press)*

* *Joint first authors*

Experiments presented in this chapter were performed by me with the exception of:

- (1) Primary P_{ywaC} screen & DISC(3) follow-up (Perri, A.L.)
- (2) Imaging of prepared samples using bright-field microscopy (French, S.).
- (3) The CRISPRi library of essential gene knockdowns in *B. subtilis* 168, along with the UppS overexpression strain were developed by Dr. Jason Peters.

SUMMARY

While screening for enzyme inactivation and lethality in whole cell assays has shown success in the discovery of probes and antibiotics; both have disadvantages. The merits of both methods have been outlined extensively in chapter 1. Here we demonstrate a powerful alternative using a whole-cell promoter-reporter system that in addition to whole cell activity also has the potential to elucidate target. Herein we report on a pilot screen of 26,000 small molecules to identify cell wall-active chemicals in real time using an autonomous luminescence gene cluster driven by the promoter of *ywaC*. The gene product of which, encodes a guanosine tetra(penta)phosphate synthetase that is expressed under cell wall stressing conditions. We subsequently utilized growth inhibition, membrane permeabilization and osmotic suppression studies to identify 9 cell wall actives. Of the nine, the target of MAC-0170636 was elucidated using a chemical-genetic approach looking for chemical sensitization to a knock-down library of 289 essential genes in *B. subtilis* 168. Undecaprenyl pyrophosphate synthase (UppS) was identified as the potential target of MAC-0170636 using this approach. Further confirmation of target was obtained using phenotypic and enzymatic studies.

INTRODUCTION

With the discovery of penicillin in 1929, the first antibacterial agent to be widely used in the clinic, the cell wall is one of the earliest targets exploited in antibacterial drug discovery. Indeed, cell wall-active agents have been a rich reservoir for efficacious antibiotics. These drugs are typically bactericidal in nature and target extra-cytoplasmic functions in bacterial cells, obviating a requirement for cell penetration. Although intensively explored, the cell wall still has many untapped targets and provides new opportunities for the discovery of novel anti-bacterial chemical matter (Brown and Wright, 2005; Falconer and Brown, 2009; Sewell and Brown, 2013). Indeed, nearly all cell wall active agents have been discovered using screens for growth inhibition, followed by cumbersome secondary screens for activity directed at the cell wall. What's lacking are selective primary screening assays for the sensitive detection of cell wall active compounds while avoiding off-target and nuisance compounds. The bacterial cell wall is an essential macromolecular structure with key roles in numerous functions including maintenance of cell shape, growth and division (Hancock, 1997). The Gram-positive cell wall is comprised of two main components; peptidoglycan (PG) and wall teichoic acid (WTA), in roughly equal quantities. Both are synthesized on the lipid carrier undecaprenyl phosphate (Bhavsar and Brown, 2006). Existing antibacterials targeting the cell wall are largely inhibitors of PG synthesis, however, WTA and undecaprenol synthesis

are emerging as promising new targets (Farha et al., 2013a; Swoboda et al., 2009; Tidten-Luksch et al., 2012; Wang et al., 2013).

Previous work from our laboratory identified the up-regulation of gene *ywaC* upon inhibition of wall teichoic acid (WTA) synthesis (D'Elia et al., 2009). So identified, we constructed a promoter-reporter system by fusing the promoter of *ywaC* to the *lux* genes, providing a real time luminescence signal. The system was tested against an extensive panel of antibiotics and showed exquisite selectivity for antibiotics targeting cell wall biosynthesis (D'Elia et al., 2009). Thus, the *ywaC* promoter reporter system was able to sense cell wall stress in *B. subtilis* resulting from the perturbation of PG, WTA and undecaprenol synthesis. The gene *ywaC* encodes a largely-uncharacterized protein that in recent years has been shown to have GTP pyrophosphokinase activity (Nanamiya et al., 2008). This class of enzyme synthesizes guanosine tetra(penta) phosphate or (p)ppGpp, a well known bacterial “alarmone” that influences gene expression during cell stress. In addition, studies using promoter census searches have revealed that *ywaC* is a member of the σ^W regulon, which includes genes that are up-regulated in response to cell wall-active antibiotics (Cao et al., 2002a). Indeed, other promoter reporter-based systems have been used, in several bacterial hosts, to detect the presence of cell wall inhibitors (Cao et al., 2002b; Hong et al., 2002; Laciola et al., 2013; Lai and Kirsch, 1996; Mani et al., 1998; Mascher et al., 2004; Ulijasz et al., 1996). For the most part, these systems respond only to

compounds that block PG synthesis and thus are insensitive, for example, to WTA and undecaprenol synthesis.

Herein we describe the development and implementation of a kinetic whole cell screen using the P_{ywaC} -*lux* promoter-reporter system. Using a library of some 26,000 diverse synthetic compounds, we show that the real time assay is robust, highly sensitive and amenable to high throughput screening. Further, the cell-based screen was extremely effective in enriching for cell wall-active chemical matter. Secondary assays of the actives derived from this screen identified 9 novel compounds that target cell wall biogenesis in the model Gram-positive *B. subtilis* 168 (Figure 2-1).

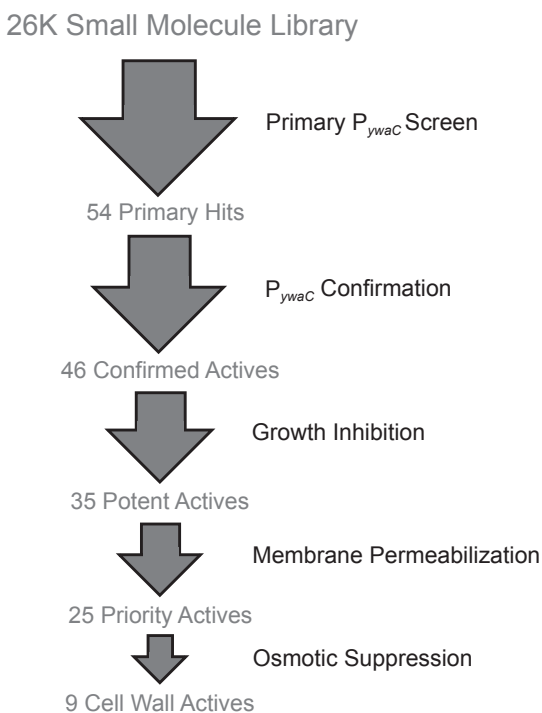


Figure 2-1. Screening workflow. A diverse collection of 26,000 synthetic compounds was screened using the P_{ywaC} reporter system and generated 54 active compounds. Activity was

confirmed for 46 compounds upon retest. Confirmed actives were subject to growth inhibition studies using *B. subtilis* to reveal 35 potent actives. Subsequently, a membrane permeabilization counter screen was used to exclude membrane-active compounds and yielded 25 priority actives. Of these, the activity of 9 compounds phenocopied known cell wall antibiotics and P_{ywaC} activity could be suppressed with the inclusion of osmoprotectants (MSM) in the growth medium and produced morphological defects in *B. subtilis*. These constituted novel cell wall actives.

Targeted genomic editing in living organisms has become a powerful hypothesis generating tool for drug discovery research. With the introduction of genomic editing using engineered nucleases it is quickly becoming a mainstream technique used by researchers in various fields (Sander and Joung, 2014). In recent years a method for repressing gene expression based on Cas9, an RNA-guided DNA endonuclease, from a type II CRISPR (Clustered Regularly Interspaced Short Palindromic Repeats) system has been developed in *E. coli*, titled CRISPR interference (CRISPRi) (Qi et al., 2013). Catalytically inactivated Cas9 endonuclease, when coexpressed with a single guide RNA (sgRNA), generates a DNA recognition complex that can interfere with transcriptional elongation by sterically blocking RNA polymerase. Systematic and precise control of gene expression can be obtained by modifying the 20nt base-pairing region found in the sgRNA sequence to selectively bind at specific locations of the chromosome. This causes selective recruitment of inactivated Cas9, which subsequently causes selective repression of RNA polymerase by sterically hindering its DNA binding site (Figure 2-2).

Motivated by previous studies utilizing libraries of sensitized strains to identify drug targets and genetic interactions (Lee et al., 2011; Xu et al., 2010); we employed a recently constructed library of essential gene knockdowns in *B. subtilis* 168, developed using the CRISPRi system, to identify the target of MAC-0170636, one of the 9 cell-wall actives (Peters, JM., Czarny T., *et al.*, *unpublished*). The two components of the system, sgRNA and catalytically inactive Cas9 as described above, are integrated on the chromosome at the *lacA* and *amyE* loci respectively. Using this system, repression levels of targeted genes can be controlled by induction of Cas9 expression since it is under the control of a xylose-inducible promoter (Figure 2-2). Increased Cas9 expression leads to further knockdown of the targeted gene. The constructed library contains 289 clones each with unique sgRNAs that systematically target all 289 known or proposed genes.

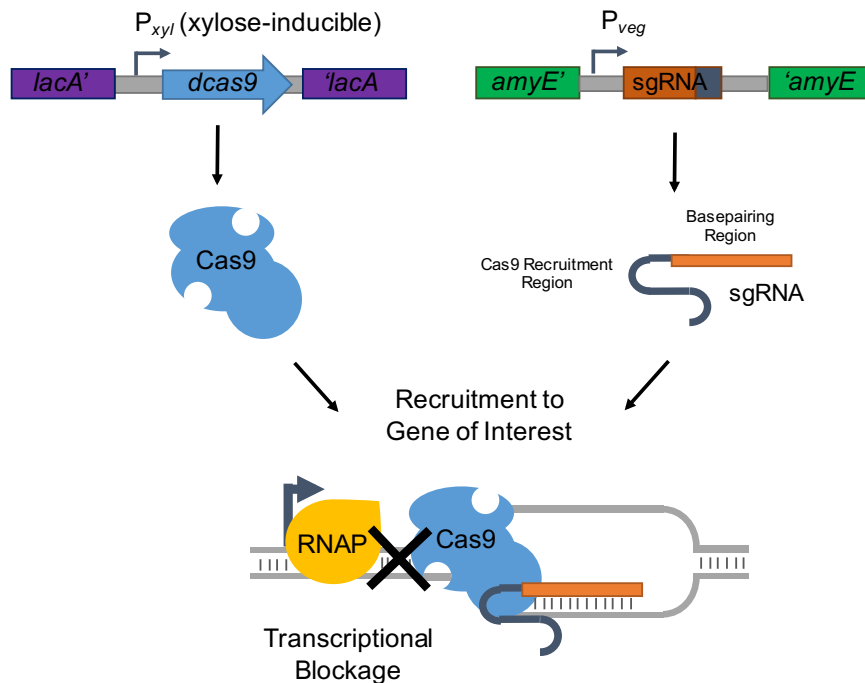


Figure 2-2: Mechanism of gene inactivation using the CRISPRi system in *B. subtilis* 168.

CRSPRi is a two component system comprising of an inactivated Cas9 endonuclease and single guide RNA (sgRNA) integrated at the *lacA* and *amyE* loci respectively. Cas9 is under control of a xylose inducible promoter and sgRNA is constitutively expressed. sgRNA encode both a Cas9 recruitment hairpin and a basepairing region which is responsible for targeting of Cas9 sgRNA complex to the 5' end of the gene of interest. Upon recruitment of the Cas9 sgRNA complex transcriptional activity of RNA polymerase (RNAP) is sterically blocked. Levels of transcriptional activity can be modulated by regulating the amount of Cas9 being expressed using xylose. Increased levels of Cas9 lead to increased levels of transcriptional blockage.

The clone responsible for knocking down the gene product undecaprenyl pyrophosphate synthase (UppS) showed the highest sensitization to MAC-0170636 at sub-MIC concentrations. UppS is an integral part of undecaprenyl phosphate synthesis across many Gram-positive and Gram-negative species and is intriguing as a target for drug discovery (Zhu et al., 2013). The target of MAC-

0170636 was further confirmed and characterized using an enzymatic *in vitro* assay employing recombinant UppS in combination with compelling phenotypic studies.

RESULTS

Amenability of the P_{ywaC} reporter system to high-throughput screening

Our lab originally reported on studies of the P_{ywaC} reporter to identify interactions among WTA, PG and undecaprenyl synthesis in *B. subtilis* 168 while helping explain the complexity of teichoic acid gene dispensability (D'Elia et al., 2009). Here, we have optimized the P_{ywaC} reporter system for high-throughput screening (HTS), harnessing its capacity to enrich for perturbants of cell wall synthesis. In modifying the previous reported method, a kinetic assay was developed where luminescence was measured continuously for 19 hours on solid LB-agar containing compound at a desired screening concentration of 10 µM. As an obligate aerobe, our engineered *B. subtilis* 168 strain posed an interesting screening challenge. Typically, HTS assays of bacteria are performed in liquid media, however, shaking is required for reproducible growth of our reporter strain in such conditions. Further, the kinetic nature of our assay meant that multiple reads were required. Because multimode readers are commonly integrated with non-shaking incubation chambers we needed an alternative solution. We found that solid agar provided an ideal growth condition and generated a robust reporter signal that was highly amenable to kinetic luminescence detection. In

further optimizing the assay three key parameters were evaluated – inoculum of cell culture, the temporal window in which luminescence was measured and the compound screening concentration. Ranging inoculums were tested to identify an optimal starting density in which most cell wall active compounds up-regulated the transcriptional response of P_{ywaC} . At 6×10^6 CFU ml^{-1} all cell wall inhibitors tested yielded at least a 2.1-fold increase.

To probe the sensitivity of our assay system we turned to conventional cell wall-active compounds of diverse mechanism, for example, targeting both the membrane and extracellular steps in PG synthesis, as well as the 1-deoxy-D-xylulose-5-diphosphate (DOXP) isoprenoid biosynthesis pathway (Table 2-1). In addition to cell wall-active compounds we found that the report system was sensitive to membrane-active chemicals. Sensitivity of the P_{ywaC} promoter-reporter was defined by the minimum activation concentration (MAC) and was compared to the minimum inhibitory concentration (MIC) for known antibiotics. MAC values were evaluated based on a statistical increase of 4 standard deviations (2.1 fold) over the low control (1% DMSO). Nearly all molecules had MIC/MAC ratios greater than 1, demonstrating that the reporter system was capable of detecting activity at concentrations below their MIC for most compounds. Particularly noteworthy was the high sensitivity for vancomycin, fosmidomycin and various cephalosporins where the ratios greater than 10 were seen. Nearly all of the above compounds showed meaningful activation of the

reporter at or below 10 μM . Thus we chose this concentration for our high throughput screen.

Table 2-1. Evaluation of the sensitivity of the HTS optimized P_{ywaC} reporter system against select cell wall associated and membrane perturbing compounds.

Compound	Mode of Action	MAC (μM)	MIC (μM)	MIC/MAC
Carbenicillin	Transpeptidase inhibition	0.21	1.65	7.86
Nafcillin	Transpeptidase inhibition	0.75	1.51	2.01
Cephalothin	Transpeptidase inhibition	1.58	1.58	1.00
Cefoxitin	Transpeptidase inhibition	1.46	5.85	4.01
Cefuroxime	Transpeptidase inhibition	0.74	23.60	31.90
Ceftazidime	Transpeptidase inhibition	9.15	29.3	3.20
Cefotaxime	Transpeptidase inhibition	1.37	10.9	7.96
Ceftriaxone	Transpeptidase inhibition	0.56	18.0	32.14
Vancomycin	Transpeptidase inhibition	0.01	0.42	42.00
Fosfomycin	MurA inhibition	145.00	145.00	1.00
D-Cycloserine	Alanine racemase inhibition	7.19	3.59	0.50
Tunicamycin	MraY & TagO inhibition	0.12	0.24	2.00
Bacitracin	Undecaprenol recycling	3.56	112.4	31.57
Fosmidomycin	DOXP Reductoisomerase	6.81	109.00	16.01
Daptomycin	Membrane potential, LTA	1.24	0.39	0.31
Polymyxin B	Membrane permeability	3.84	7.68	2.00
EDTA	Membrane permeability	548.00	2190.00	4.00

1. Sensitivity of the P_{ywaC} reporter system was determined against select compounds by evaluating the minimum inhibitory concentration (MIC) and minimum P_{ywaC} activating concentration (MAC) and generating MIC : MAC ratios. High MIC : MAC ratios represent sensitivity of the reporter below MIC of the corresponding compound.

Kinetic screening of a 26,000 member small molecule library for P_{ywaC} activation

A diverse collection of some 26,000 synthetic compounds, commercially sourced from Chembridge and Maybridge Chemicals, was screened against the HTS optimized P_{ywaC} reporter system at a concentration of 10 μM in duplicate for a

duration of 19 hours, taking luminescence reads every 60 minutes. There was, of course, no theoretical ceiling on luminescence resulting from reporter gene activation. Nevertheless, fosmidomycin (10 μ M) provided practical control for our screen. Fosmidomycin targets the DOXP pathway, specifically the reductoisomerase IspC. The latter is essential for the production of prenyl precursors for the synthesis of undecaprenyl phosphate -- the lipid species that supports both PG and WTA membrane associated biosynthesis. Neat DMSO (1%) was chosen as a low control as this was the final concentration of DMSO present in each well containing compound in analysis. (Figure 2-3A) shows an example time course for reporter luminescence in response to fosmidomycin and illustrates a strong and broad peak of luminescence that is characteristic of the reporter system. The increase in luminescence signal, in response to fosmidomycin, correlates with that of growth. A maximum is reached as cells begin entering stationary phase. Interestingly at this point the negative control (1 % DMSO) shows an increase in luminescence. This tailing effect can be attributed to nutrient starvation as YwaC is part of a class of enzymes that synthesizes (p)ppGpp, a well known bacterial "alarmone" that is produced during cell stress, including amino acid starvation. In our analysis of compound data, the maximum relative light units (RLU) values were recorded and normalized to the DMSO controls on the corresponding screening plate. This generated a fold-increase value corresponding to the activation of the compound relative to that recorded for the 1 % DMSO control. The inclusion of fosmidomycin as a control

allowed us to monitor the robustness of the reporter throughout the screen (Figure 2-3B).

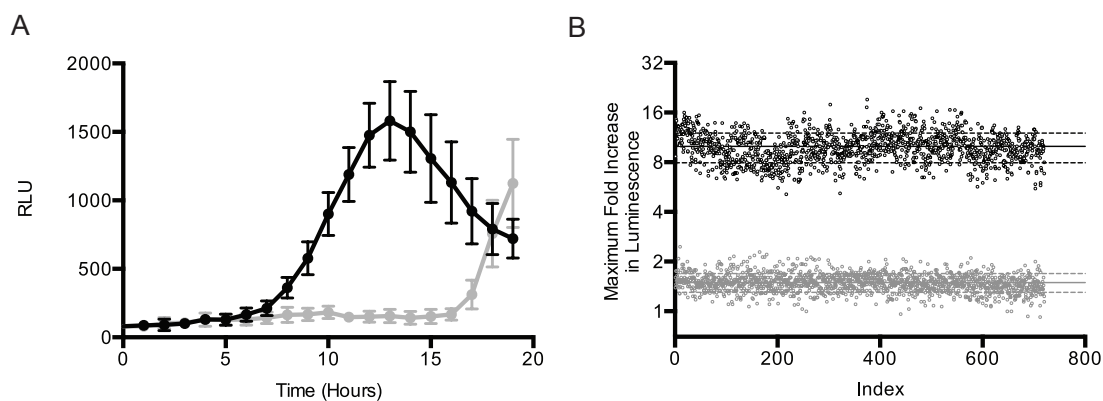


Figure 2-3: Assessing the robustness of the P_{ywaC} reporter HTS assay. (A) A representative time course of the luminescence response (relative light units, RLU) for the positive control compound fosmidomycin at a concentration of 10 μ M (black circles). Also shown is the luminescence on addition of 1 % DMSO (grey circles). (B) Fosmidomycin was used as a control compound on each screening plate. Shown is the maximal P_{ywaC} response recorded in response to 10 μ M fosmidomycin for each of these control wells (open black circles) relative to that of a 1 % neat DMSO treatment (open grey circles). Solid black and grey horizontal lines correspond to the average of the fosmidomycin and DMSO activation respectively. Broken black and grey horizontal lines correspond to \pm one standard deviation away from the mean of activation due to fosmidomycin and DMSO respectively.

Figure 2-4A shows a plot of the data for the 26,000 compounds where the fold-luminescence of replicates are plotted against one another and reveal strong repeatability of the assay duplicates. A statistical analysis of the data revealed a standard deviation of 0.57 about the mean of the 1 % DMSO control; instead of a statistical cut-off we elected to choose a threshold (3.5) that made for a manageable number of actives. The threshold of 3.5-fold increase led to 81

active compounds in the primary screen. Figure 2-4B shows an analysis of the duration of luminescence increases of 3.5-fold or more and revealed that several of our actives resulted from a single spike in luminescence. Where this behavior was quite different, for example, from our control compound fosmidomycin, we suspected that these spikes might be fleeting luminescence artifacts. To guard against possible artifacts the 81 primary actives were further evaluated to ensure that the increases were sustained for at least 2 consecutive kinetic time points (2 hours). That analysis led to 54 actives. These compounds were cherry picked and subjected to a retest under primary screening conditions. The result was 46 confirmed actives.

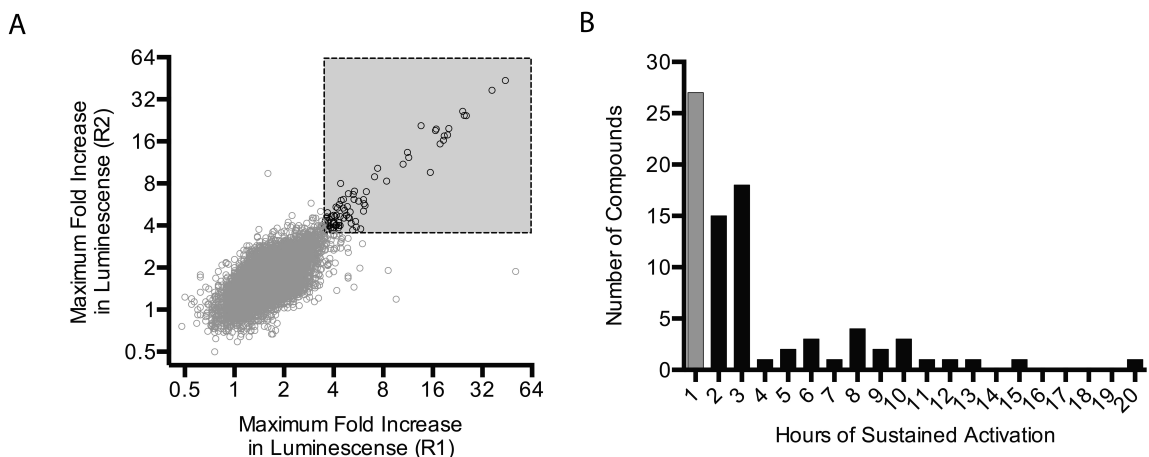


Figure 2-4. Replica plot and hit selection for the primary 26,000 small molecule P_{ywaC} kinetic screen. (A) Duplicate samples from the primary screen describe the maximum fold increase in luminescence achieved during the 19-hour kinetic read. With an arbitrary cutoff of 3.5-fold or greater in both replicates, the data shown in open black circles correspond to 81 compounds designated as actives while grey open circles are inactive. (B) The plot shows the duration of activation of the 81 molecules (P_{ywaC} activity above 3.5 fold). Some 54 compounds

(black bars) show sustained activity for at least two sequential kinetic reads. The remaining 27 (grey bar) show activity for only 1 time-point and were de-prioritized for further follow-up.

EC₅₀ and membrane permeabilization studies

Studies of dose dependent growth inhibition were conducted on the 46 confirmed active compounds using wild-type *B. subtilis* 168. Some 35 compounds showed clear growth inhibition, with EC₅₀ values between 0.05 and 80 μ M (Supplementary Table 2-1). Potency showed a modest correlation with P_{ywaC} response seen in the primary screen where molecules with potent EC₅₀ values (0-10 μ M) showed the strongest P_{ywaC} transcriptional activity (Figure 2-5).

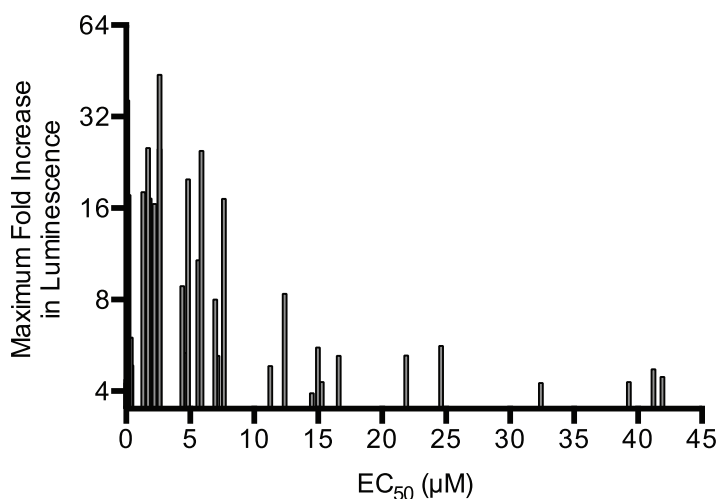


Figure 2-5. Correlation of potency and P_{ywaC} activity. EC₅₀ data of the inhibition of *B. subtilis* growth for 35 potent actives (x-axis) is plotted against maximal P_{ywaC} activity (y-axis).

As membrane-active compounds have been previously shown to increase P_{ywaC} transcriptional activity, a membrane permeabilization counter screen was performed on the 35 potent actives using the membrane potential-sensitive cyanine dye DiSC3. In this assay, membrane-active compounds lead to an increase or decrease in steady state fluorescence through perturbation of the proton motive force (Farha et al., 2013b). Of the 35 potent actives tested, 8 molecules were membrane-active (Supplementary Table 2-1). With two compounds unavailable for reorder, this left us with 25 priority actives for follow up to confirm activity on the cell wall.

P_{ywaC} transcriptional activity of cell wall active antibiotics can be suppressed by osmoprotectants

To determine whether or not the transcriptional response of P_{ywaC} could be suppressed by osmoprotectants when exposed to cell wall-active agents a panel of known cell wall-active antibiotics were tested in rich media in a dose dependent manner in the presence and absence of MSM (20 mM $MgCl_2$, 0.5 M Sucrose, 20 mM Maleic acid) (Leaver et al., 2009). Responses were monitored for compounds with diverse targets including transpeptidation (vancomycin, nafcillin), cytoplasmic synthesis of precursors (fosfomicin), and membrane associated steps (bacitracin, fruillimicin b, ramoplanin, moenomycin A, and tunicamycin). In the presence of osmoprotectants the reporter was suppressed for all of the cell wall-active compounds tested (Figure 2-6).

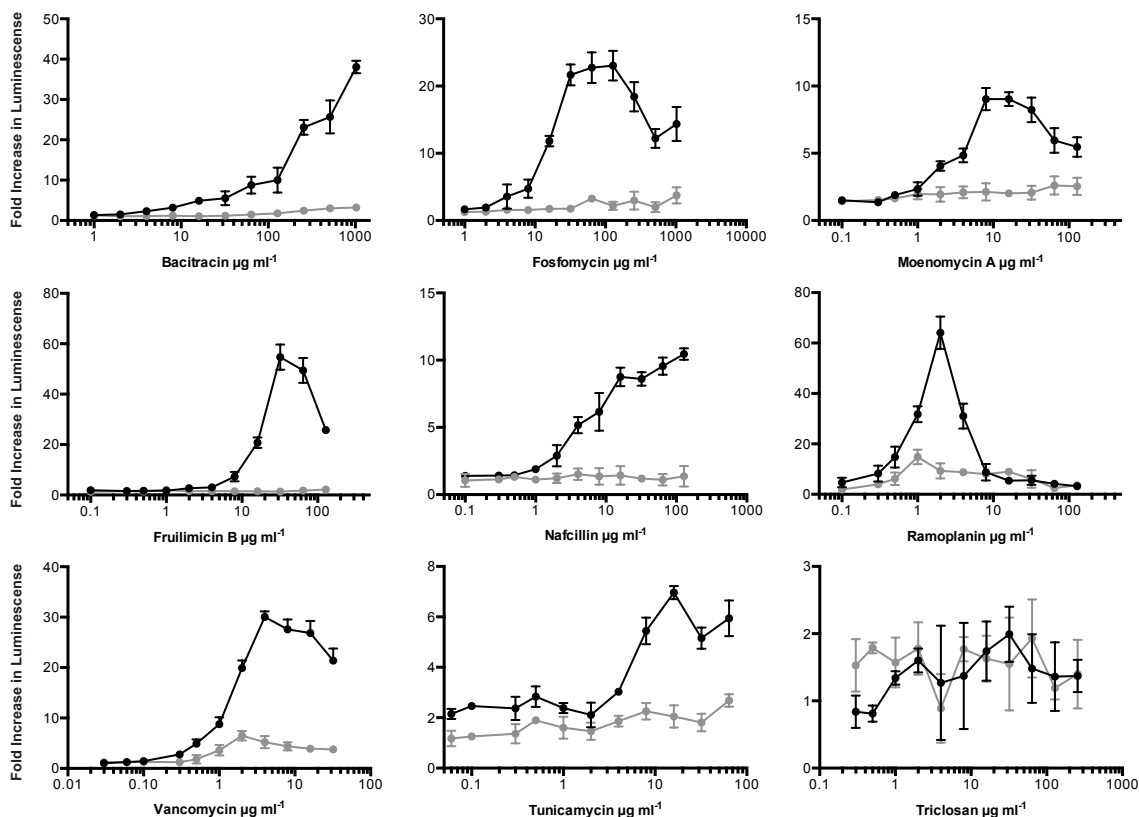


Figure 2-6. P_{ywaC} promoter-reporter response to a panel of antibiotics in presence and absence of osmoprotective medium. Peak response of the P_{ywaC} reporter was measured in presence (grey circles) and absence (black circles) of osmoprotectants (MSM) for a panel of largely cell wall-active antibiotics at a range of concentrations. Fold increase in luminescence was calculated as the normalized luminescence (RLU/OD₆₀₀) value of the reporter strain divided by the normalized luminescence value without antibiotic at the same time point.

The 25 priority actives were reordered and liquid chromatography mass spectrometry (LC/MS) confirmed the purity (>80 %) and identity of each. Having demonstrated the suppression of reporter luminescence for known cell wall active compounds, we endeavored to explore this phenotype for the priority actives.

P_{ywaC} reporter activity was monitored in a dose dependent manner a 19-hour time course on solid LB-agar from 0.5 µM to 256 µM in the presence and absence of

osmoprotectant (MSM). Of the 25 compounds 9 showed signature luminescence responses that were concentration dependent and could be at least partially suppressed by osmoprotectants (Figure 2-7), suggesting that these compounds are active against the bacterial cell wall biosynthetic machinery (Table 2-2).

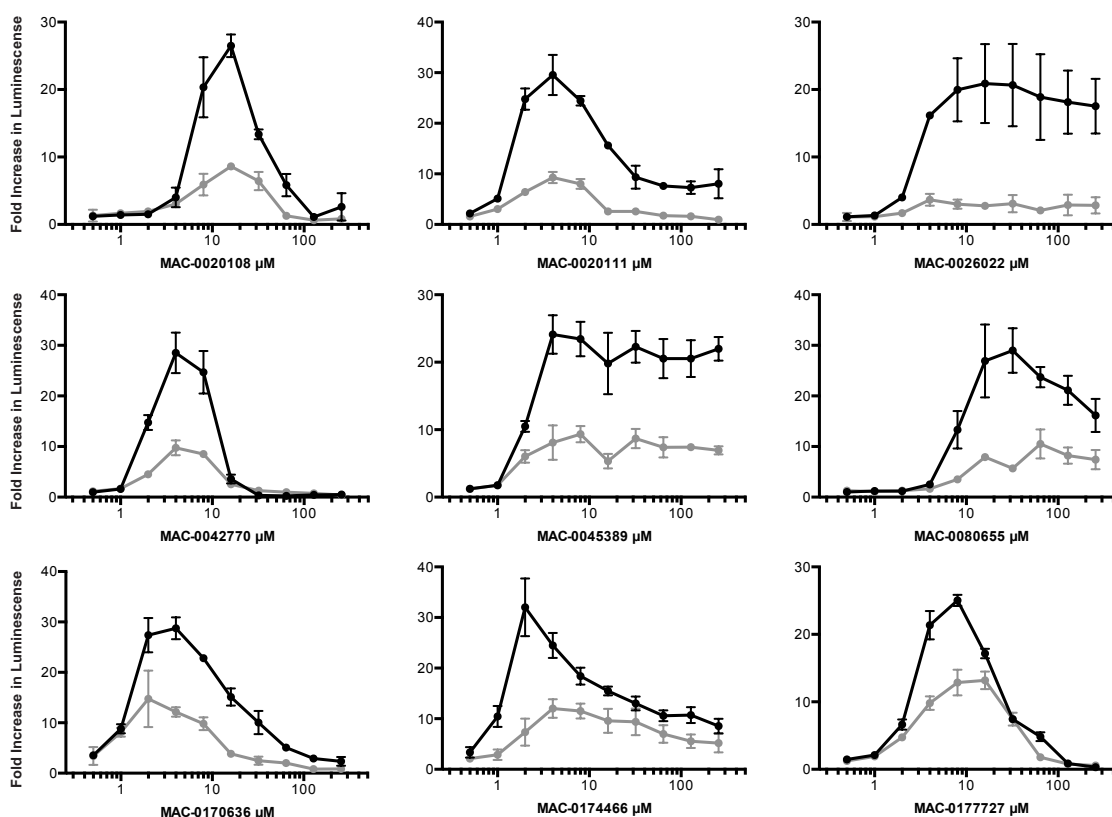
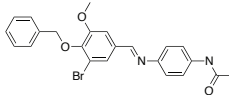
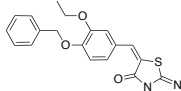
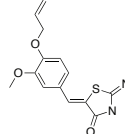
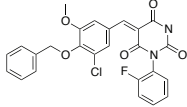
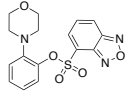
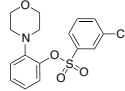
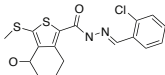
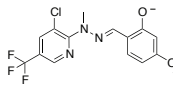
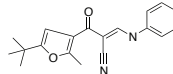


Figure 2-7. Dose response of the P_{ywac} promoter-reporter in the absence and presence of osmoprotectants leads to 9 novel, cell wall-active inhibitors. Peak response of the P_{ywac} reporter was measured in the presence (grey circles) and absence (black circle) of osmoprotectants (MSM) for 25 priority actives of which 9 pheno-copied known cell wall antibiotics deeming them cell wall actives. Fold increase in luminescence was calculated by dividing the RLU value in the presence of inhibitor over the 1 % DMSO control.

Table 2-2: Nine cell wall-active lead compounds.

Compound	MIC (μM)	MAC (μM)	MIC/MAC	Fold Suppression (-MSM/+MSM)	Structure
MAC-0170636	4	0.5	8	4.05	
MAC-0174466	2	0.5	4	4.36	
MAC-0080655	32	4	8	5.10	
MAC-0177727	16	1	16	2.69	
MAC-0020108	32	4	8	4.55	
MAC-0020111	8	1	8	8.42	
MAC-0026022	16	2	8	45.88	
MAC-0042770	8	2	4	3.25	
MAC-0045389	4	2	2	3.70	

¹For each compound the minimum inhibitory concentration (MIC) against *B. subtilis* 168 along with the minimum activating concentration (MAC) against the P_{ywaC} reporter is recorded. MIC / MAC ratios greater-than one demonstrate sensitivity of the reporter below MIC concentrations. Fold suppression of P_{ywaC} activity in response to the compound in osmoprotectants was calculated by dividing the increase in luminescence in the absence of osmoprotectants by the increase in luminescence in the presence of osmoprotectants. High fold suppression values depict suppression of the corresponding molecules activity against cell wall biosynthesis in the presence of osmoprotectants.

P_{ywaC} actives show morphological effects against *B. subtilis* 168 at sub-MIC concentrations

With the 9 compounds pheno-copying known cell wall-active antibiotics, we sought further confirmation through microscopic examination. Dose dependent studies were performed with each of the 9 compounds from sub-MIC through to MIC concentrations. The fraction of abnormal cells in treatment populations were observed to be inversely proportional to cell culture density; demonstrating dose-dependent filamentous morphology characteristic of cell wall-active molecules (Supplementary Figure 2-2). All 9 of the compounds showed an induction of morphological changes at sub-MIC concentrations in a dose-dependent manner (Supplementary Figure 2-1) four of which are highlighted in Figure 2-8. We conclude that these 9 compounds are likely cell wall-active.

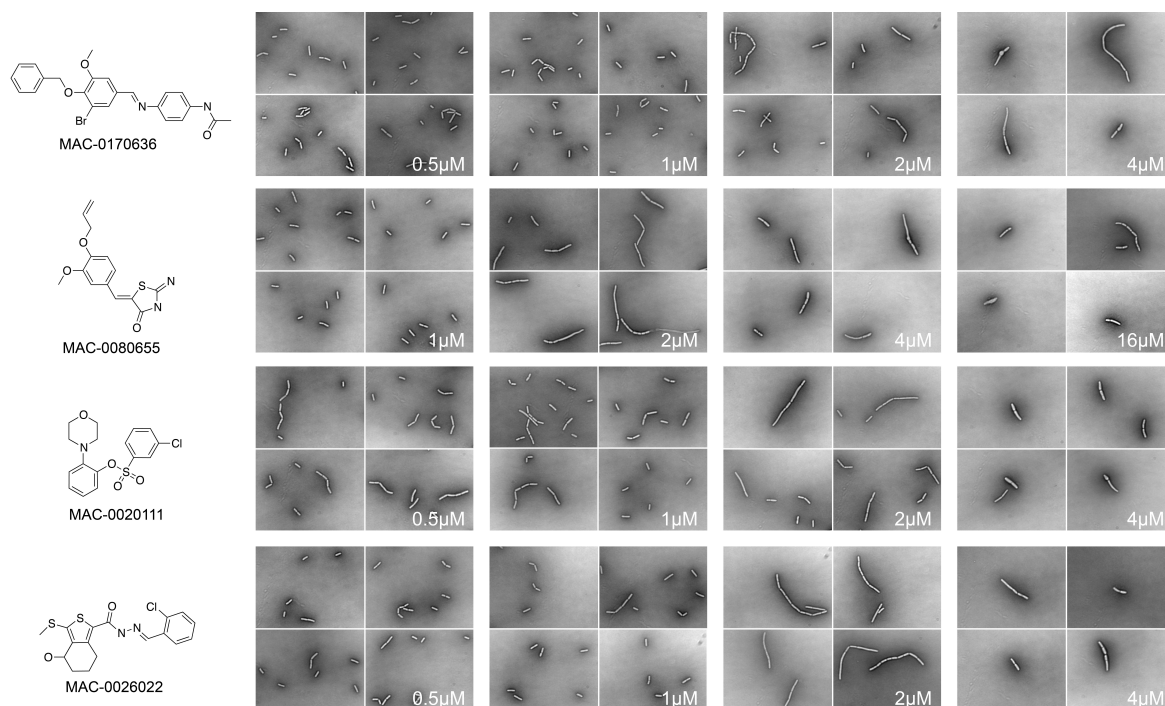


Figure 2-8. Morphological studies of *B. subtilis* 168 in the presence of 9 novel cell wall actives. *B. subtilis* 168 was grown to mid-exponential phase and visualized in the presence of 9 novel cell wall-active compounds, 4 of which are shown here, (see Supplementary Figure 2-1 for full set of micrographs) at sub-MIC concentrations in a dose dependent manner.

Sensitization of the *B. subtilis* 168 CRISPRi essential knockdown library identifies the target of MAC-0170636

To comprehensively assess the direct target of the nine cell wall actives we took a chemical-genetic approach to look for sensitization in a collection of precise essential gene knock-downs generated using the CRISPRi method in *Bacillus subtilis* 168 (Peters JM., Czarny T., *et al*, *unpublished*). The Gross Lab at University of California San Francisco has built a library of strains expressing computationally-optimized sgRNAs that target all 289 known or proposed

essential genes in *B. subtilis* 168 (Peters JM., Czarny T., *et al*, *unpublished*).

We employed a solid based pinning approach to array the 289 knockdown strains and 95 wild-type control strains in quadruplicate (1536 density), on rich solid media containing each inhibitor at sub MIC concentrations ($1/2$, $1/4$, and $1/8^{\text{th}}$ MIC). Plates were grown at 30 °C overnight and subsequently imaged using a transmissive scanner. Integrated density of each colony was computationally analyzed using FIJI and R. Edge effects on the plate were removed by normalizing all data to the mean of the middle two quartiles as previously described (Mangat et al., 2014). Only MAC-0170636 showed any meaningful / specific sensitization profiles. Our solid-based genome wide screening approach identified *uppS* as the most sensitized knockdown strain to MAC-0170636. A screening concentration of 1 µg/mL provided the clearest results as lower concentrations showed no sensitization and higher concentrations showed non-specific sensitization. Data corresponding to MAC-0170636 at $1/4$ MIC is depicted in Figure 2-9.

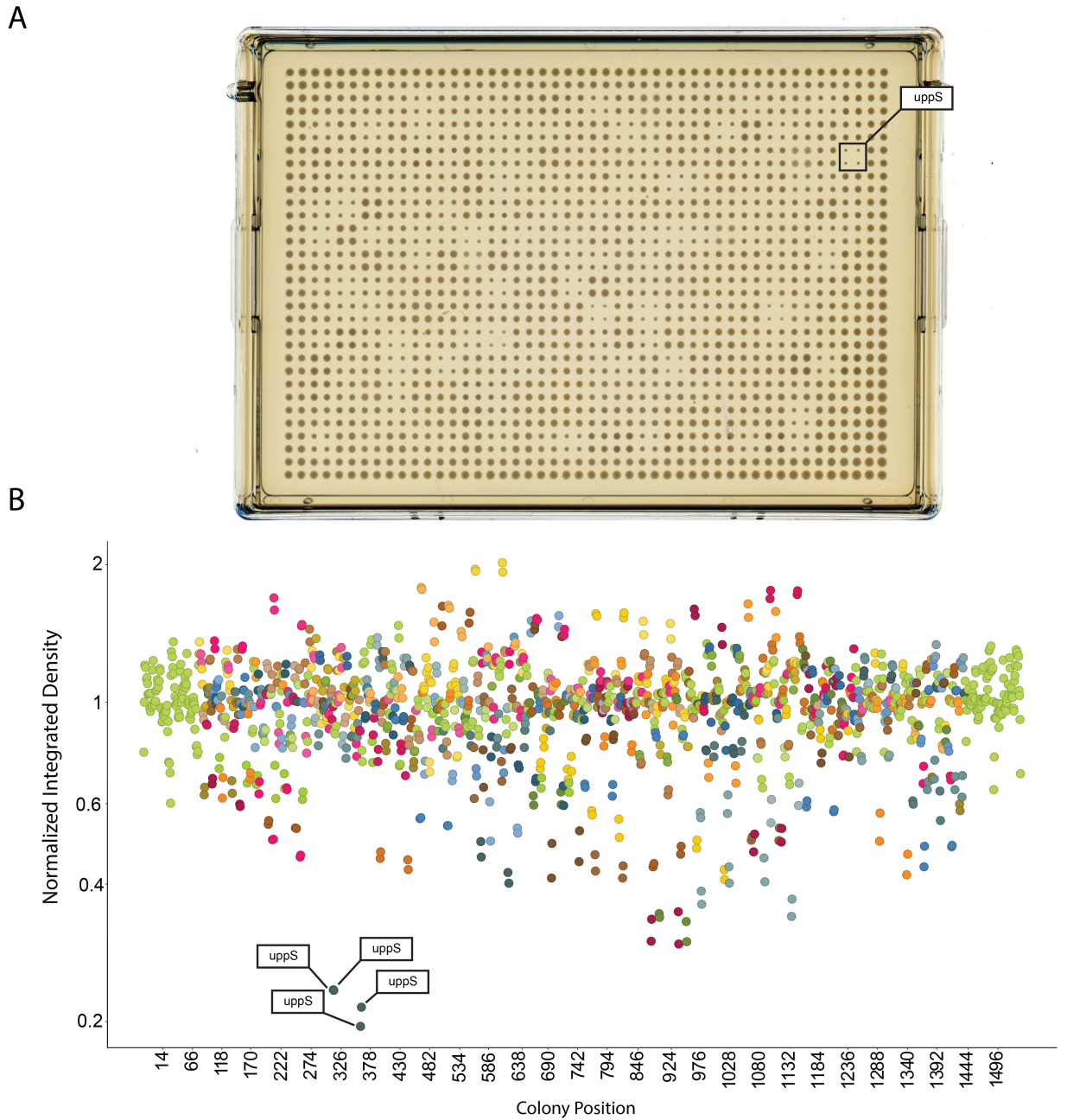


Figure 2-9: Sensitization of the *B. subtilis* 168 CRISPRi essential knockdown library to the presence of MAC-0170636. (A) The CRISPRi essential knockdown collection was pinned in quadruplicate on solid media containing MAC-0170636 at 1 $\mu\text{g}/\text{mL}$. The library was grown overnight at 30 $^{\circ}\text{C}$, and imaged using a transmissive scanner. **(B)** Colony density was analyzed for each clone and then normalized to the mean density of the middle two quartiles of the data. Normalized density and colony plate position (1 to 1536) are depicted on the Y and X-axis

respectively. Data is colored uniquely based on targeted gene. Colonies and data correlating to *uppS* are highlighted.

Over-expression and knockdown of UppS results in suppression and sensitization to MAC-0170636 respectively

To phenotypically confirm results found using the CRISPRi knockdown library, we generated an IPTG inducible *B. subtilis* 168 clone overexpressing UppS. Pspank-*uppS* was integrated at *amyE* and subsequently knocked out at its native locus using a *KanR* cassette. Upon induction with 1mM IPTG, an 8-fold increase in MIC of MAC-0170636 was observed (Figure 2-9). Additionally, we tested whether CRISPRi knockdown of *uppS* could be further sensitized upon *dcas9* induction in response to increasing xylose concentrations as Cas9 expression is controlled by a xylose inducible promoter. Indeed, this was the case. With basal knockdown levels, 0.0 % xylose, we observed a 4-fold decrease in the MIC of MAC-0170636. Upon *dcas9* induction with 0.05 % xylose a 32-fold decrease in MIC was observed (Figure 2-10). Concentrations of xylose higher than 0.05 % lead to erratic and unreproducible growth.

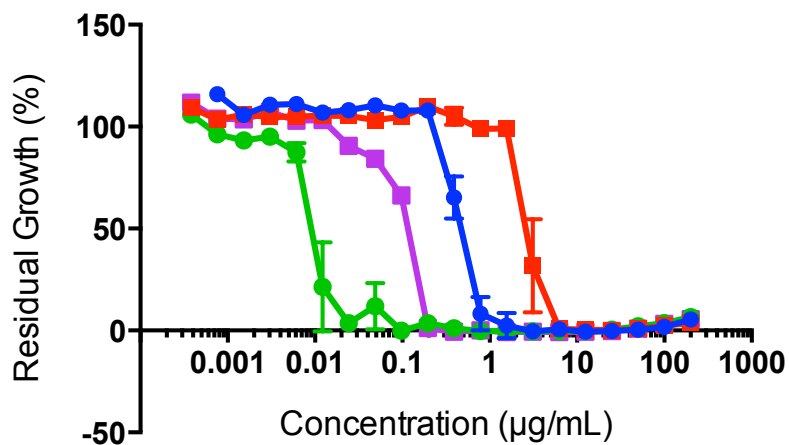


Figure 2-10: Susceptibility of wild type and engineered *B. subtilis* 168 strains to MAC-0170636. Wild type data is depicted in blue. Suppressed activity in the UppS overexpression strain (induced with 1mM IPTG) is presented in red. Purple and green data points depict sensitization of the engineered UppS knockdown strain at basal (0 % xylose) and induced (0.05 % xylose) states respectively. Residual growth represents relative fitness to each strain and condition exposed to no drug.

Intrinsic resistance of *S. aureus* provides further validation of UppS as the target of MAC-0170636

In determining the effectiveness of MAC-0170636 against the clinically relevant pathogen *S. aureus*, MIC determinations were conducted in both Newman and MRSA backgrounds (Christianson et al., 2007) (Figure 2-11). With no activity in either background we postulated that the significant differences in protein sequence (55% identity) is responsible for resistance. To test this hypothesis, we expressed UppS from *S. aureus* Newman as the sole source of UppS in *B. subtilis* 168. Native *B. subtilis* 168 *uppS* was knocked out using a KanR cassette while being complemented with *uppS* from *S. aureus* at the amyE locus using the Pspank system (Quisel et al., 2001). A second strain was also engineered to

complement with *uppS* from *B. subtilis* 168 to serve as an expression control. We found that these engineered cells expressing *S. aureus* UppS were completely resistant to MAC-0170636 (Figure 2-11).

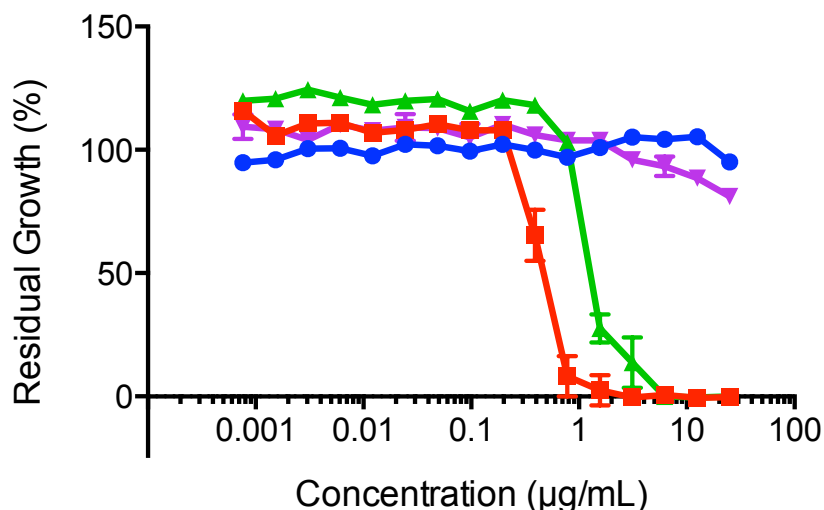


Figure 2-11: UppS from *S. aureus* as the sole source of UppS in *B. subtilis* 168 confers resistance to MAC-0170636. Activity profiles of MAC-0170636 were conducted against both wild type *B. subtilis* 168 (red) and *S. aureus* Newman (blue) strains. Data obtained using engineered *B. subtilis* 168 strains containing native UppS knockouts complemented with either UppS from *S. aureus* and *B. subtilis* 168 are depicted in purple and green respectively.

MAC-0170636 inhibits recombinant UppS *in vitro*

To further confirm that UppS is the direct drug target, we tested MAC-0170636 ability to inhibit purified *B. subtilis* UppS using a coupled enzyme assay that detects the release of pyrophosphate during subsequent additions of isopentenyl pyrophosphate. Pyrophosphate generated during the reaction is cleaved by pyrophosphatase to generate 2 units of inorganic phosphate. Inorganic phosphate is then used in the phosphorylation, and breakdown, of 2-amino-6-

mercapto-7-methyl- purine ribonucleoside (MESG) by purine nucleoside phosphorylase (PNP) (Figure 2-12). This cleavage of MESG is measured by means of increased absorbance at 360 nm. We found a concentration-dependent decrease in UppS activity upon the addition of MAC-017063 with an IC_{50} of $0.8\mu\text{M}$ (Figure 2-13). Details regarding characterization and expression of *B. subtilis* 168 UppS are outlined in chapter 3.

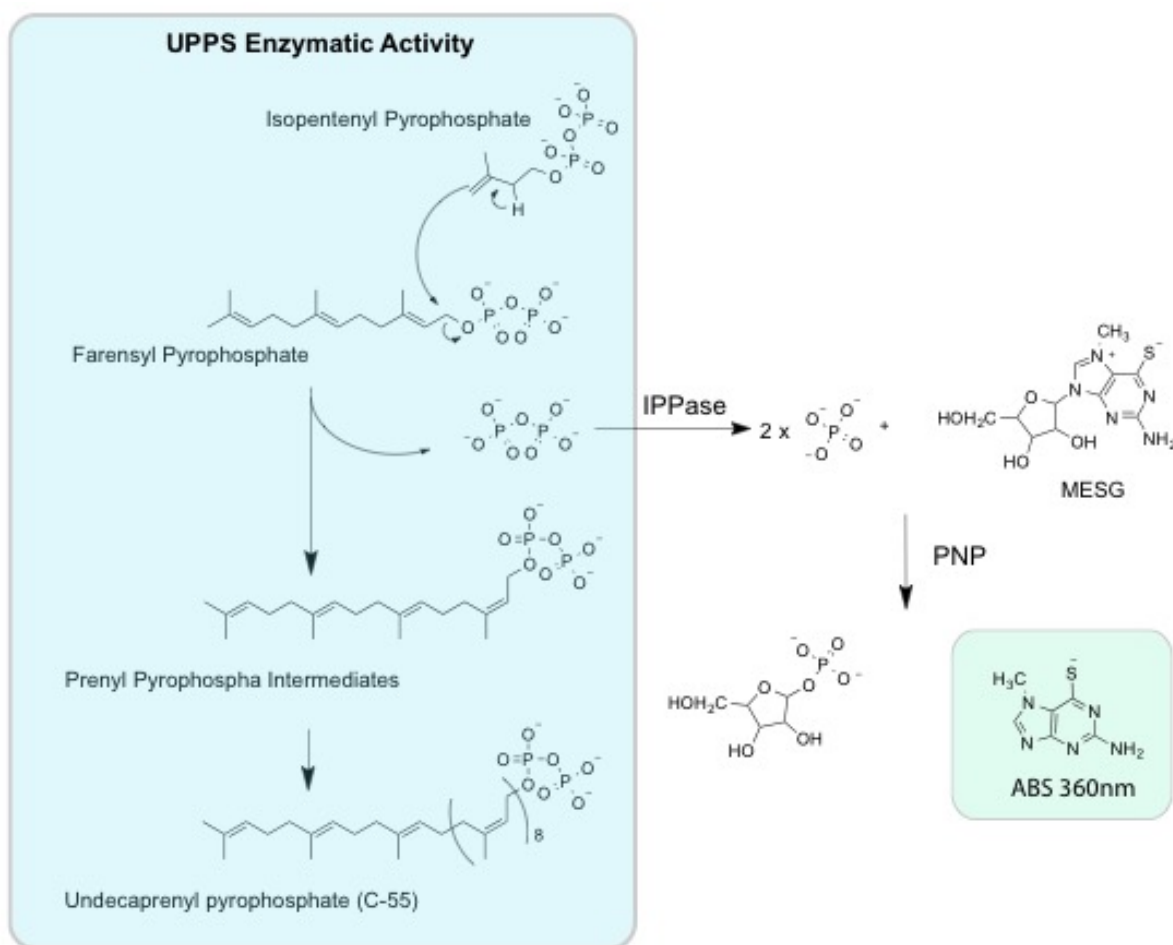


Figure 2-12: Monitoring *in vitro* activity of UppS using a coupled pyrophosphate detection assay. Enzymatic activity of UppS is highlighted in blue. UppS is primed with a single unit of farnesyl pyrophosphate (FPP) and catalyzes the subsequent addition of an isopentenyl pyrophosphate (IPP) unit generating a prenyl pyrophosphate intermediate and releasing

pyrophosphate as a byproduct of the reaction. UppS catalyzes a further 8 rounds of isopentenyl pyrophosphate addition to generate the C-55 lipid undecaprenyl pyrophosphate. Pyrophosphate produced which each subsequent addition of IPP is cleaved by pyrophosphatase (IPPase) to generate 2 units of inorganic phosphate. Inorganic phosphate is used in the phosphorylation, and breakdown, of 2-amino-6-mercapto-7-methyl- purine ribonucleoside (MESG) by purine nucleoside phosphorylase (PNP). This cleavage of MESG is measured by means of increased absorbance at 360 nm (highlighted in green).

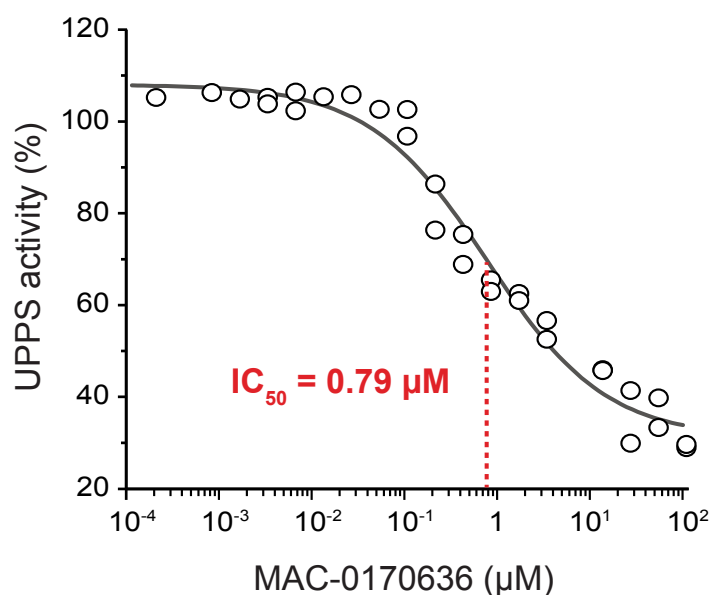


Figure 2-13: Assessing inhibitory activity of MAC-0170636 *in vitro*. A kinetic pyrophosphate detection assay was used to assess inhibition of MAC-0170636 *in vitro*. Reactions with varying concentrations of MAC-0170636 were conducted in the presence of: 0.2 mM 2-amino-6-mercapto-7-methyl- purine ribonucleoside (MESG), 0.625 U of purine ribonucleoside phosphorylase (PNP), 0.2 U of inorganic pyrophosphatase (PyroP), 0.125 µg of purified UppS enzyme, 0.82 µM farnesyl pyrophosphate (FPP) (1xKM) and 65 µM isopentenyl pyrophosphate IPP (5x KM).

DISCUSSION

In the work presented here, we have made use of the specific response of the *B. subtilis ywaC* promoter to cell wall antibiotics to develop a real time high-throughput assay for the identification of novel chemical matter that targets cell wall biosynthesis. In conducting a pilot screen, we identified 9 novel cell wall actives using additional filters -- mainly membrane activity and osmotic suppression. Additionally, using a chemical-genetic approach, we identified the direct target of one of the nine compounds (MAC-0170636). The enzymatic target UppS was identified in the genome wide experiment and subsequently confirmed using various phenotypic assay and an enzymatic *in vitro* study.

Optimized for solid growth media, the P_{ywaC} -*lux* promoter-reporter system was a robust and sensitive reporter for the action of known cell wall-active antibiotics with various mechanisms of action, including both intra- and extra-cellular steps in PG synthesis, as well as the DOXP pathway for isoprenoid biosynthesis. The sensitivity of the reporter was revealed by comparison of the MIC to MAC. Indeed, exquisite sensitivity for some cell wall antibiotics was seen, in some cases at concentrations 30-fold less than the MIC. Other cell wall reporter-based strains have previously been developed that respond to inhibition of essential steps in PG synthesis; including a *vanH* promoter-reporter fusion to *lacZ*. Such systems, however, only report on a subset of cell wall targets such as inhibition of transglycosylation (Mani et al., 1998). In contrast, the P_{ywaC} reporter described

herein has a nearly comprehensive response to cell wall synthesis inhibition with demonstrated sensitivity for multiple pathways that converge on cell wall assembly, including PG, isoprenoid and WTA biosynthesis.

A pilot-scale screen using the P_{ywaC} -*lux* promoter-reporter system of 26,000 diverse synthetic compounds revealed 54 actives, 46 of which confirmed on retest. Some 35 of these had potent whole cell activity against *B. subtilis* and were further evaluated with a counter screen for off-target membrane-active compounds using DiSC₃, a fluorescence reporter of membrane polarization in bacteria (Farha et al., 2013b). This left 25 priority actives that were reordered, checked for quality and identity, and tested in a dose-dependent response of P_{ywaC} -*lux* promoter-reporter system in the presence and absence of osmoprotectants. Some 9 of the 25 compounds showed signature luminescence responses that were concentration dependent and suppressed by osmoprotectants. All 9 of these chemicals are most likely novel cell wall-active compounds. The latter assay was inspired by evidence dating back more than 40 years establishing that cell wall deficient cells, induced by genetic mutation or chemical perturbation, could be rescued with osmoprotectants and divalent cations (Boylan et al., 1972; Burmeister and Hesseltine, 1968; Gilpin et al., 1973; Murray et al., 1998; Richard W Gilpin, 1976; Young et al., 1970). In recent years it was shown that a stable L-form of *B. subtilis*, lacking a cell wall, could be generated by the depletion of the *murE* operon and a single mutation in *ispA*

when cultured in rich media supplemented with high concentrations of sucrose and Mg^{2+} (Leaver et al., 2009). As such we hypothesized that activity of P_{ywaC} induced by cell wall actives could be suppressed in the presence of osmoprotectants similarly to that of chemical and or genetic blocks in cell wall synthesis. Such suppression phenotypes were used to prioritize novel compounds for cell wall mode of action studies. In examining known cell wall antibiotics in dose and temporal studies we found that the transcriptional activity of the P_{ywaC} reporter system can indeed be suppressed in the presence of osmoprotectants.

Morphological changes due to the exposure of cell wall active agents on various bacterial species has been well documented over the years showing varied morphological phenotypes, which include blebbing, rounding long filamentation along with the increase in division septa (Amini, 2009; Greenwood and O'Grady, 1973; Lorian, 1975; Zhanel et al., 1992; Zimmerman and Stapley, 1976). To determine if the 9 compounds thought to be selectively targeting cell wall biosynthesis showed similar phenotypes, imaging studies for these compounds was performed at sub-MIC and MIC concentrations. All 9 of the compounds showed an induction of morphological changes at sub-MIC concentrations and in a dose-dependent manner. Interestingly MAC-0080655 gives rise to long filamentous cells at low concentrations however when approaching the MIC cells become shorter and spheroplasts begin to appear. Such morphological

dependence on concentration has previously been described with β -lactams in *Escherichia coli* (Greenwood and O'Grady, 1973).

In recent years' antibiotic drug discovery has embraced chemical genetic approaches to aid in target identification of potential lead compounds (Roemer et al., 2012). Inspired by systematic genome-wide mutant libraries developed and used in yeast fitness profiling analogous tools have been built in both Gram-positive and Gram-negative bacterial organisms. Such libraries including the Keio collection (Yamamoto et al., 2009), which encompasses nearly 4,000 non-essential gene knockouts in *E. coli*, have been successfully used to study the genetic interactions of antibiotics and known chemicals (Nichols et al., 2011). However, due to the fact that unlike yeast, prokaryotic bacteria are haploid in nature, deletions in essential targets cannot be generated. New interference technology utilizing inactivated endonucleases found as part of the type II CRISPR system have shown great promise in bacterial systems (Qi et al., 2013) and has recently been utilized in the construction of a genome-wide essential knockdown library in *Bacillus subtilis* 168 (Peters JM., Czarny T., et al, *unpublished*). Using this library, we employed a chemical-genetic sensitization strategy to look for the enzymatic target to our newly discovered 9 cell wall actives. The power of this strategy lies within the ability to identify direct targets rather than associated targets as such found in studies profiling non-essential deletion collections. Clones that contain sgRNA basepairing region

corresponding to the 5' region of the target should be sensitized in the presence of drug at sub-MIC concentrations. Within our collection of 9 cell wall actives only one showed a clear sensitization profile (MAC-0170636). Potentially limiting are the differing levels of Cas9 expression required for meaningful gene product knockdown in the cell. Though titration can be obtained by induction of Cas9 using xylose these experiments would require large and costly quantities of active compounds. Whole genome profiles of all 9 compounds were conducted in the absence of inducer leading to ~ 4-fold decrease in gene product expression (Peters JM, Czarny T., *et al*, *unpublished*). With induction of Cas9 (1% xylose) up to 1000-fold decreases in gene product expression can be observed (Peters JM, Czarny T., *et al*, *unpublished*). Profiles of MAC-0170636 at $\frac{1}{4}$ the MIC (1 μ g/mL) showed the most profound sensitization to the knockdown of UppS. Responsible for the synthesis of undecaprenol pyrophosphate, UppS acts by means of polymerizing isopentenyl pyrophosphate (IPP) units using farnesyl pyrophosphate (FPP) as a primer (Chang et al., 2004). Indeed other genes did show sensitization to MAC-0170636 namely genes relating to peptidoglycan synthesis, wall teichoic acid synthesis, and cell division. All of the processes sensitized to MAC-0170636 rely on stable undecaprenyl phosphate levels within the cell underlying the other observed gene sensitizations.

In confirming the results obtained from the chemical-genetic screen, we performed careful phenotypic confirmation of the CRISPRi *uppS* knock down

strain. Upon MIC determination of MAC-017636 with basal (0 % Xylose) and induced (0.05 % Xylose) levels of Cas9 expression, 4 and 32-fold reduction of MIC were observed respectively. With this correlated dependence of MIC on the amount of UppS found in the cell, we further postulated that we should be able to high copy suppress the activity of MAC-017636. As such we engineered a *B. subtilis* 168 strain overexpressing UppS and did indeed observe an 8-fold increase in MIC upon induction. Though these results pointed to an interaction between MAC-017636 and UppS, further experiments were required to determine that the interaction between MAC-017636 and UppS was direct. We took an *in vitro* approach to study the enzymatic activity of UppS in the presence and absence of MAC-017636. Activity of UppS was measured using a coupled spectrophotometric phosphate release assay measuring the breakdown of MESG at 360nm. Indeed, upon dosing with MAC-017636 we observed a concentration-dependent decrease in UppS activity (IC_{50} of 0.79 μ M).

With undecaprenyl phosphate (Und-P) being required for all membrane associated steps of cell wall biogenesis in both Gram-positive and Gram-negative pathogens; targeting isoprenoid biosynthesis is an intriguing approach forward for antibiotic drug discovery. UppS is of special interest as isoprenoid biosynthesis upstream of UppS is not conserved amongst all pathogens. To date there have been no validated antibiotics targeting UppS, however, there are some interesting leads (Zhu et al., 2013) (Farha et al., 2015). To determine

whether or not MAC-017636 showed any promising activity against the clinically relevant pathogen *S. aureus* MICs were determined for both Newan and a community acquired methicillin resistant strain. MAC-017636 unfortunately showed no activity against either. We hypothesized that the significant difference in gene sequence between UppS from *S. aureus* and *B. subtilis* 168 (55 % sequence identity) was responsible for resistance. As such we engineered a strain of *B. subtilis* 168 expressing UppS from *S. aureus* as its sole source of UppS. Indeed our engineered *B. subtilis* 168 showed a resistance profile similar to that of *S. aureus*. This not only provided supporting evidence that the difference in structure was responsible for resistance but also further corroborates that UppS is the true target of MAC-017636.

The P_{ywaC} reporter screen takes a whole cell approach and with the unique ability to report on biological activity at sub-MIC concentrations. Thus the assay has the potential to discover cell wall-active compounds that would otherwise be discarded from conventional screens for viability. While the P_{ywaC} promoter-reporter could be a valuable follow-up tool to enrich for cell wall-targeted chemicals among whole cell-active collections, it is arguably best used as a primary screening tool with the rare capacity to report on previously untapped chemical space. Such sensitivity could be particularly useful, for example, in search for novel natural product inhibitors, where high-throughput efforts typically use crude / semi-pure extracts which may contain molecules of interest at sub-

inhibitory concentrations. In addition unlike typical whole cell screening approaches the P_{ywaC} promoter-reporter system obviates follow up on uninteresting, and generally reactive, nuisance compounds while reporting specifically on inhibitors perturbing cell wall biosynthesis. As such, our efforts have generated 9 novel cell wall-actives, which of MAC-017636 inhibits UppS. These molecules are ripe for further mode of action in the context of cell wall assembly. Though MAC-017636 showed no activity against *S. aureus* it is a prime candidate for SAR development to broaden its spectrum of activity.

METHODS

Solid based P_{ywaC} screening methodology

Screens of P_{ywaC} transcriptional activity were performed in 96-well microtitre plates (catalog no. 6005688; Perkin Elmer), in duplicate using a stand-alone Biomek FX workstation (Beckman Coulter Inc) for setup. The night before screening, a single colony of the strain EB1385(D'Elia et al., 2009) was grown in 5 mL of Luria-Bertani (LB) broth supplemented with erythromycin (0.5 $\mu\text{g}/\text{mL}$). On the day of screening, cells were harvested at an OD_{600} of 3.0. The cells were then diluted into fresh LB broth supplemented with antibiotic to a final OD_{600} of 0.02. To each well of a 96-well microtitre plate, 1 μL of compound (1 mM in 100 % DMSO) was added. 99 μL of liquid (warmed) 0.5 % LB-agar supplemented with antibiotic were subsequently transferred to the 96-well microtitre plates containing compound. The liquid LB-agar was allowed to solidify at room temperature for 2 hours. After 2 hours at room temperature, 20 μL of cells at a final OD_{600} of 0.02 were spotted on the surface of the solid LB-agar. Plates were allowed to dry for approximately 1 hour before the start of the assay. Assay luminescence was read using an EnVision Multilabel plate reader (Perkin Elmer) with an emission wavelength of 492 nm over the course of 19 hours. Fosmidomycin (10 μM) was used as the high control and neat dimethyl sulfoxide (DMSO) was used as the low control. In instances where osmotic suppression assays were performed LB media was supplemented with MSM (20 mM MgCl_2 , 0.5 M Sucrose, 20 mM maleic acid).

Calculation of the fold increase in luminescence was determined for each sample by dividing the luminescence values of the sample by the average of the low controls on the corresponding assay plate at the corresponding time point.

Determination of minimal inhibitory concentration (MIC)

The minimal inhibitory concentration (MIC) defines the lowest concentration of a compound required to inhibit growth of a particular strain. A single colony of the the strain being profiled was grown in 5 ml of LB broth. Following 16 hours of growth, the overnight culture was diluted 100-fold into fresh LB broth. Once the cells reached an OD₆₀₀ of 0.3-0.5, the cells were diluted 10,000-fold into fresh LB. The MICs of various antibacterial agents were determined for each of the strains by adding 198 µl of the diluted cells to wells of a clear 96-well microtitre plate (catalog no. 3370, Corning Costar) containing compound at 2-fold dilutions. The plates were incubated at 30 °C with aeration for 16 hours. Optical density was measured at 600 nm with a Spectra-max Plus instrument (Molecular Devices).

EC₅₀ determination

A dose-response assessment (50 % inhibitory concentration [EC₅₀]) was determined for each priority active obtained from the primary screen using a cell-based assay for growth inhibition. The assay was conducted as described for the

MIC determinations in liquid LB media. Inhibitors were added at half-logarithmic dilutions from 100 μM to 0.001 μM . EC_{50} values were determined by use of nonlinear least-squares regression using GraFit Workspace (Erithacus Software Limited).

Cytoplasmic membrane permeability assay

Cytoplasmic membrane permeabilization was determined by using the membrane-potential-sensitive cyanine dye DiSC₃(5) (Sims et al., 1974). Strain EB6 was grown at 30 °C with shaking to mid-logarithmic phase ($\text{OD}_{600} = 0.5 - 0.6$). Cells were harvested by centrifugation at 16,000 $\times g$, washed once with buffer (150 mM Tris-HCl, pH 7.2), and re-suspended in assay buffer (10 mM Tris-HCl, pH 7.2) to an OD_{600} of 0.04. A 100 μL cell suspension was placed in each well of a clear 96-well microtitre plate (catalog no. 3370, Corning Costar). The cell suspension was incubated with 0.4 μM DiSC₃(5) until DiSC₃(5) uptake was maximal (as indicated by a stable reduction in fluorescence due to fluorescence quenching as the dye became concentrated in the cell by the membrane potential). The desired concentration of test compound was subsequently added and the fluorescence reading was monitored using a Synergy HT multi-mode microplate reader (Biotek) at an excitation wavelength of 622 nm and an emission wavelength of 670 nm. The maximal fluorescence increase due to the disruption of the cytoplasmic membrane was recorded. A blank with only cells and the dye was used to subtract the background.

Morphological studies of *B. subtilis*

Cultures were prepared as previously described in MIC determination, then chemically fixed in a 1:10 (v/v) culture-to-20 mM HEPES (pH 6.8) with 1.5 % glutaraldehyde solution. Samples were fixed at 4 °C overnight to limit *de novo* cell wall biosynthesis during fixation. After which, samples were negatively stained with 1.5 % nigrosin, flushed with N₂ gas to remove bubbles, and gently heated at 55 °C to bring cells to a common focal plane. Samples were visualized using brightfield microscopy with an inverted Nikon Eclipse TE-200 at 1000x magnification with a Plan Fluor Apo 100x objective. Micrographs were acquired using the open-source microscopy package Micro Manager (Edelstein et al., 2001).

***B. subtilis* 168 CRISPRi library profiling of MAC-017636**

Glycerol stocks of the library (in 96-well format, 4 plates total) were pinned onto PLUSPLATES (Cat. PLU-001, Singer Instruments, UK) containing LB Agar and incubated at 30 ° C overnight. Once grown the library was up-scaled to 384 format using a Singer Rotor (Singer Instruments, UK) on PLUSPLATES containing LB Agar. Plates were incubated at 30 ° C overnight. The library was up-scaled again the next day to 1536 format using the same method. The 1536 density *B. subtilis* CRISPRi library was pinned onto PLUSPLATES containing LB agar supplemented with sub-MIC ($1/2$, $1/4$ and $1/8^{\text{th}}$ MIC) concentrations of MAC-017636. Plates were grown overnight at 30 ° C and scanned using a transmissive

scanner (Epson Perfection V700, Epson USA). Images were analyzed using FIJI and R as previously described (French S., et al, *submitted Molecular Biology of the Cell*). Data was visualized using Spotfire (Tibco Software Inc., USA).

Overexpression and purification of UppS from *B. subtilis* 168

The gene *uppS* (GeneBank Sequence NC_000964.3) was cloned into the pET-19b vector (Novagene) modified to encode an engineered Tobacco Etch Virus (TEV) protease cleavage site. Primers used to generate construct are listed below. UppS was over-expressed in *E. coli* BL21 (Rosetta) using auto-induction (Studier, 2005). Cells were harvested by centrifugation at 6000 x *g* for 25 minutes at 4°C. Cells were suspended in lysis buffer containing 50 mM NaH₂PO₄ (pH 8.0), 300 mM NaCl, 10 mM imidazole, 250 KU rLysozyme (Novagen) and an EDTA-free protease inhibitor tablet (Roche Diagnostics). Cells were lysed using a cell disrupter (Constant Systems Limited, Daventry UK). Lysates were cleared by centrifugation at 30,000 x *g* for 30 minutes at 4 °C. Nickel-affinity chromatography was performed on the lysates using a 30 mL free flow gravity column and 5 mL of Ni-NTA agarose (Sigma). Once loaded column was washed with buffer (10 column volumes) containing 50mM NaH₂PO₄ (pH 8.0), 300 mM NaCl, 20 mM Imidazole. The his-tagged UppS was then eluted in elution buffer containing 50 mM NaH₂PO₄ (pH 8.0), 300mM NaCl, 250mM Imidazole. Elution fractions were dialyzed overnight against 20 mM Tris · HCl (pH 8.0), 300 mM NaCl, and 1 mM DTT. Once dialyzed the elution fraction was concentrated using

Amicon Ultra centrifugation filters (10 kDa cut-off) and quantified using a NanoDrop (Thermo Scientific).

uppS FWD: CTAGCATATG CTCAACATACTCAAAAATTG

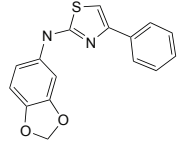
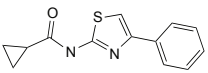
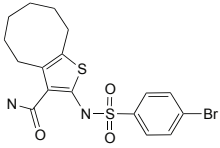
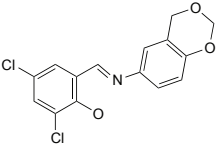
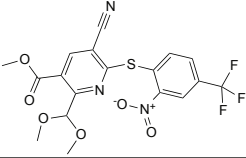
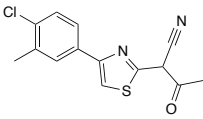
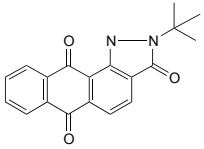
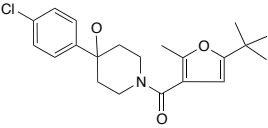
uppS REV: CTAGCTACGAG CTAAATTCCGCCAAA

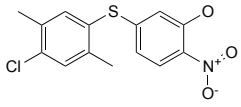
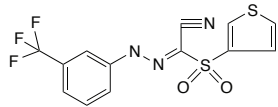
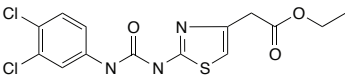
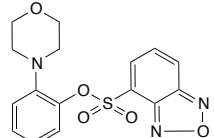
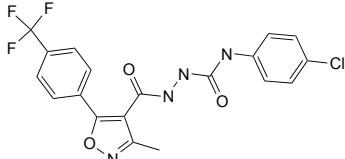
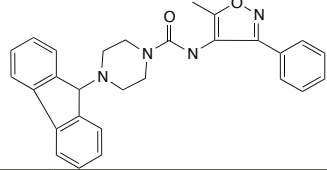
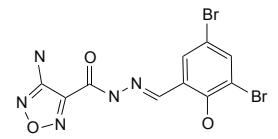
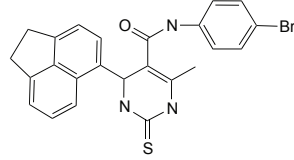
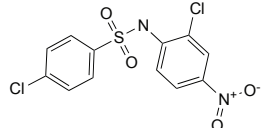
Inhibition kinetics for MAC-0170636 against UppS

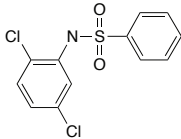
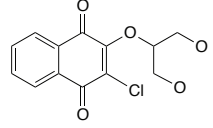
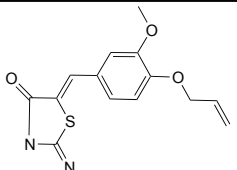
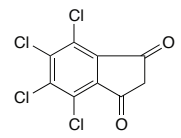
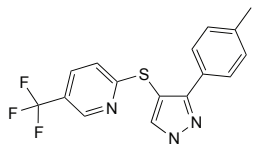
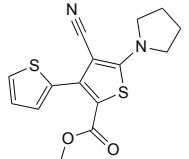
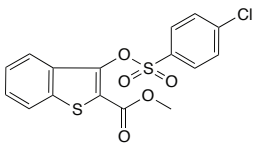
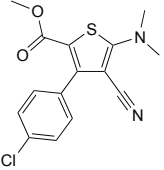
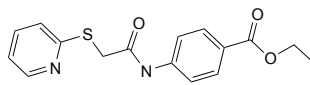
A Kinetic EnzCheck pyrophosphate assay (Life Technologies) was used to assess inhibition of MAC-0170636 *in vitro* with accordance to the manufacturers suggested guidelines. The IC₅₀ value was determined in 100 µL reaction volumes using a flat bottom 96-well plate (Costar 3370) in duplicate. Reactions with varying concentrations of MAC-0170636 were conducted with a final concentration of 1 % DMSO in the presence of: 0.2 mM 2-amino-6-mercapto-7-methyl- purine ribonucleoside (MESG), 0.625 U of purine ribonucleoside phosphorylase (PNP), 0.2 U of inorganic pyrophosphatase (PyroP), 0.125 µg of purified UppS enzyme, 0.82 µM farenstyl pyrophosphate (FPP) (1xKM) and 65 µM isopentenyl pyrophosphate IPP (5x KM). Data was fit using GraFit V5 software (Erithacus Software).

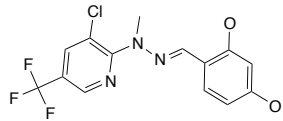
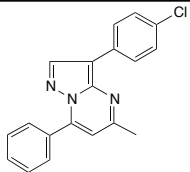
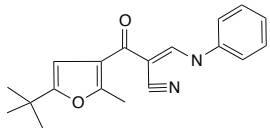
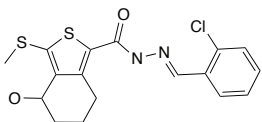
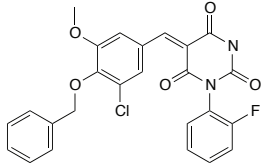
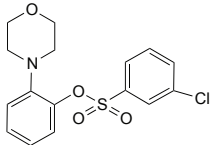
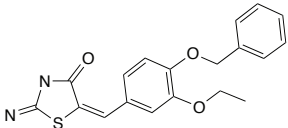
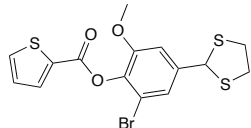
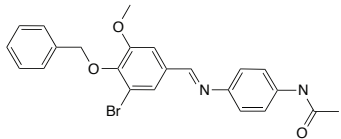
SUPPLEMENTAL DATA

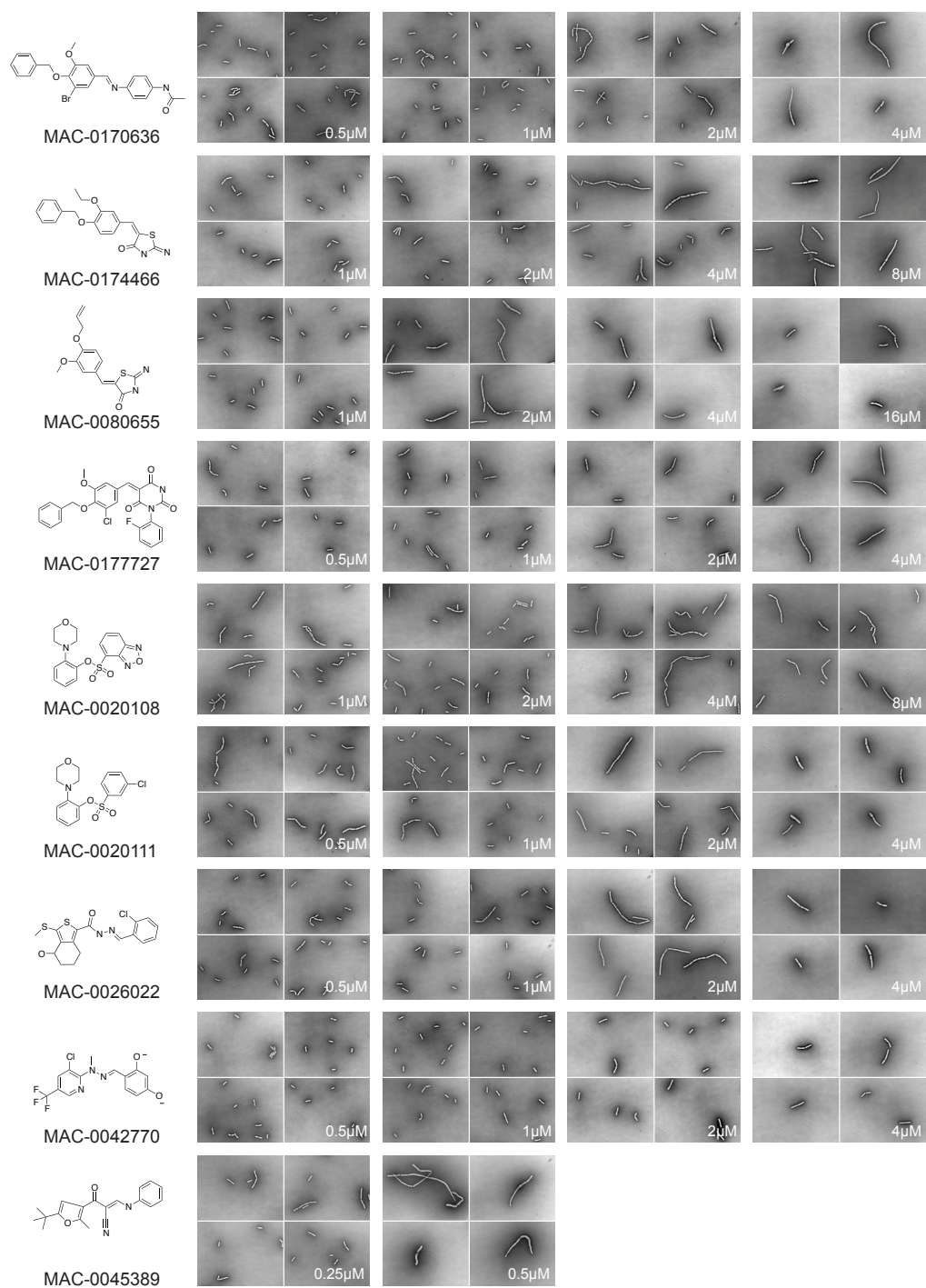
S Table 2-1: Thirty-five potent actives.

Compound	Average Max Fold Increase in Luminescence	EC ₅₀ (μM)	Membrane activity	Structure
MAC-0175574	4.10	14.51	—	
MAC-0038612	4.25	0.01	—	
MAC-0079448	4.91	32.40	—	
MAC-0002436	5.03	15.29	+	
MAC-0048802	4.29	39.30	—	
MAC-0011589	4.37	0.01	+	
MAC-0173768	4.77	1.93	—	
MAC-0019019	4.78	41.90	+	

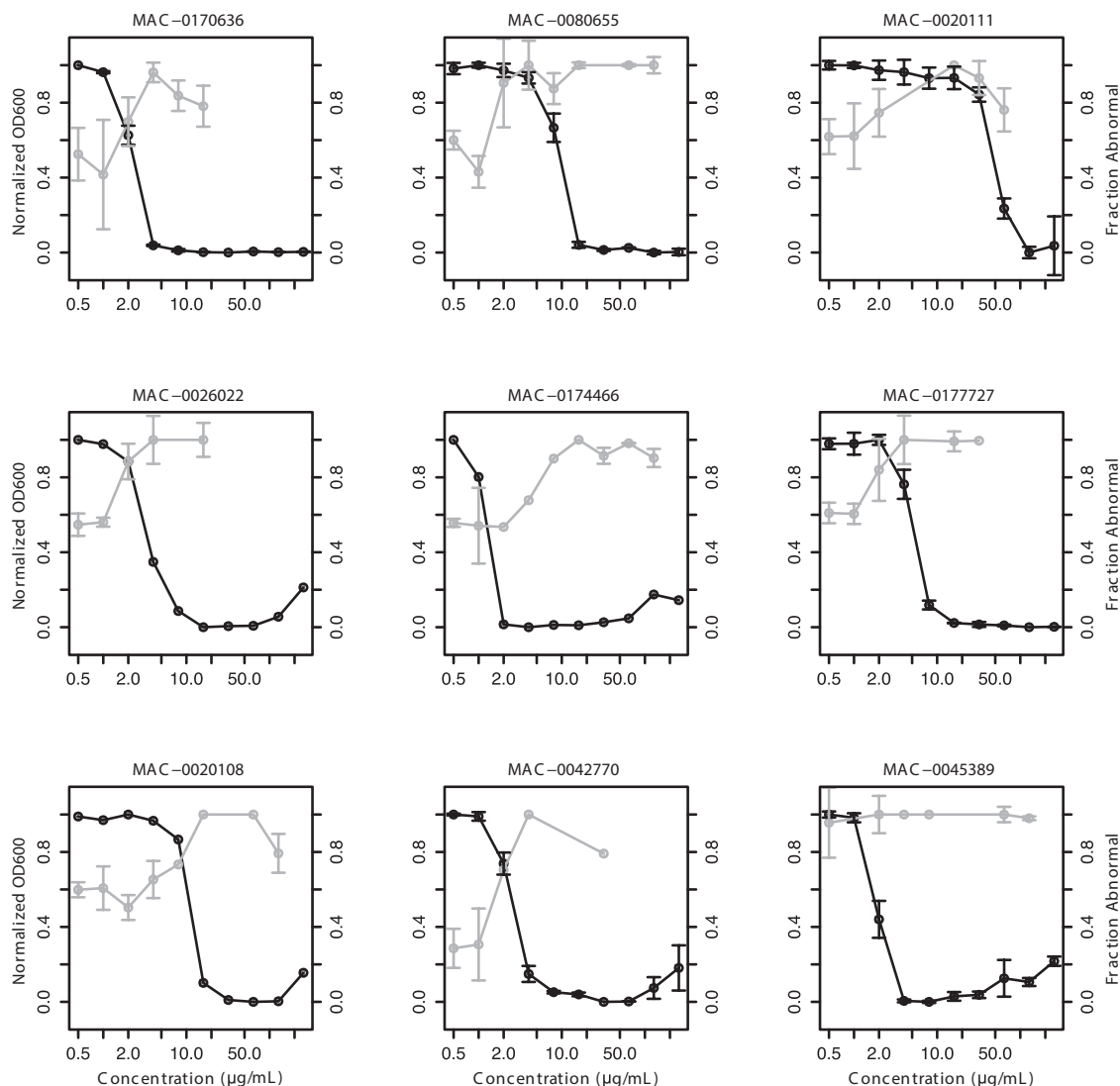
MAC-0005082	4.79	41.20	+	
MAC-0043328	5.01	11.27	-	
MAC-0158780	4.87	0.42	+	
MAC-0020108	5.58	7.13	-	
MAC-0047200	5.74	16.61	-	
MAC-0158121	5.25	21.90	+	
MAC-0172913	5.97	4.58	-	
MAC-0173775	5.85	14.98	-	
MAC-0002472	6.66	24.60	+	

MAC-0171005	6.21	0.36	—	
MAC-0036740	8.00	6.97	—	
MAC-0080655	8.36	12.38	—	
MAC-0036904	8.85	4.38	—	
MAC-0048182	10.79	5.65	—	
MAC-0025760	11.85	2.53	—	
MAC-0004444	16.53	2.22	+	
MAC-0025767	17.44	1.38	—	
MAC-0161641	17.16	7.63	—	

MAC-0042770	18.13	1.84	—	
MAC-0175940	18.73	0.18	—	
MAC-0045389	18.22	1.34	—	
MAC-0026022	19.91	4.84	—	
MAC-0177727	24.70	5.90	—	
MAC-0020111	25.02	2.62	—	
MAC-0174466	25.31	1.71	—	
MAC-0005103	36.86	0.08	—	
MAC-0170636	43.88	2.60	—	



S Figure 2-1: Morphological studies of *B. subtilis* 168 in the presence of 9 novel cell wall actives. *B. subtilis* 168 was grown to mid-exponential phase and visualized in the presence of 9 novel cell wall-active compounds at sub-MIC concentrations in a dose dependent manner.



S FIG 2-2. Dose-dependent morphological variation. The estimated fraction of abnormal cells is displayed alongside conventional MIC curves for each cell wall- active compound. A clear dose-response in cell morphology is evident, with the morphological response often inversely related to culture density. Fractions of abnormal cells are calculated in ImageJ, with abnormality defined as cellular area that varies by more than 3 standard deviations from the mean area of an untreated cell population. The contrast from the negative stain allows for rapid and accurate detection of cell margins, with a watershed algorithm applied to ensure that septated cells are counted as separate entities when linked at the poles. Past the MIC, it becomes challenging to accumulate enough cells to be statistically relevant within a treatment well, due to cell death. In cases where cell numbers were limited under microscopy, the acquired images were pooled as a single treatment, and no standard deviations are presented.

REFERENCES

- Amini, B., 2009. Effect of different sub MIC concentrations of penicillin, vancomycin and ceftazidime on morphology and some biochemical properties of *Staphylococcus aureus* and *Pseudomonas aeruginosa* isolates. Iranian Journal of Microbiology 1.
- Bhavsar, A.P., Brown, E.D., 2006. Cell wall assembly in *Bacillus subtilis*: how spirals and spaces challenge paradigms. Molecular Microbiology 60, 1077–1090. doi:10.1111/j.1365-2958.2006.05169.x
- Boylan, R.J., Mendelson, N.H., Brooks, D., Young, F.E., 1972. Regulation of the bacterial cell wall: analysis of a mutant of *Bacillus subtilis* defective in biosynthesis of teichoic acid. 110, 281–290.
- Brown, E.D., Wright, G.D., 2005. New targets and screening approaches in antimicrobial drug discovery. Chem. Rev. 105, 759–774. doi:10.1021/cr030116o
- Burmeister, H.R., Hesseltine, C.W., 1968. Induction and propagation of a *Bacillus subtilis* L form in natural and synthetic media. 95, 1857–1861.
- Cao, M., Kobel, P.A., Morshedi, M.M., Wu, M.F.W., Paddon, C., Helmann, J.D., 2002a. Defining the *Bacillus subtilis* sigma(W) regulon: a comparative analysis of promoter consensus search, run-off transcription/microarray analysis (ROMA), and transcriptional profiling approaches. J. Mol. Biol. 316, 443–457. doi:10.1006/jmbi.2001.5372
- Cao, M., Wang, T., Ye, R., Helmann, J.D., 2002b. Antibiotics that inhibit cell wall biosynthesis induce expression of the *Bacillus subtilis* sigma(W) and sigma(M) regulons. Molecular Microbiology 45, 1267–1276.
- Chang, S.-Y., Ko, T.-P., Chen, A.P.-C., Wang, A.H.-J., Liang, P.-H., 2004. Substrate binding mode and reaction mechanism of undecaprenyl pyrophosphate synthase deduced from crystallographic studies. Protein Sci. 13, 971–978. doi:10.1110/ps.03519904
- Christianson, S., Golding, G.R., Campbell, J., Canadian Nosocomial Infection Surveillance Program, Mulvey, M.R., 2007. Comparative genomics of Canadian epidemic lineages of methicillin-resistant *Staphylococcus aureus*. J. Clin. Microbiol. 45, 1904–1911. doi:10.1128/JCM.02500-06
- D'Elia, M.A., Millar, K.E., Bhavsar, A.P., Tomljenovic, A.M., Hutter, B., Schaab, C., Moreno-Hagelsieb, G., Brown, E.D., 2009. Probing teichoic acid genetics with bioactive molecules reveals new interactions among diverse processes in bacterial cell wall biogenesis. Chem. Biol. 16, 548–556. doi:10.1016/j.chembiol.2009.04.009
- Edelstein, A., Amodaj, N., Hoover, K., Vale, R., Stuurman, N., 2001. Computer Control of Microscopes Using μ Manager, Current protocols in John Wiley & Sons, Inc., Hoboken, NJ, USA. doi:10.1002/0471142727.mb1420s92
- Falconer, S.B., Brown, E.D., 2009. New screens and targets in antibacterial drug discovery. Current Opinion in Microbiology 12, 497–504. doi:10.1016/j.mib.2009.07.001

- Farha, M.A., Czarny, T.L., Myers, C.L., Worrall, L.J., French, S., Conrady, D.G., Wang, Y., Oldfield, E., Strynadka, N.C.J., Brown, E.D., 2015. Antagonism screen for inhibitors of bacterial cell wall biogenesis uncovers an inhibitor of undecaprenyl diphosphate synthase. *Proc. Natl. Acad. Sci. U.S.A.* 201511751. doi:10.1073/pnas.1511751112
- Farha, M.A., Leung, A., Sewell, E.W., D'Elia, M.A., Allison, S.E., Ejim, L., Pereira, P.M., Pinho, M.G., Wright, G.D., Brown, E.D., 2013a. Inhibition of WTA Synthesis Blocks the Cooperative Action of PBPs and Sensitizes MRSA to β -Lactams 8, 226–233. doi:10.1021/cb300413m
- Farha, M.A., Verschoor, C.P., Bowdish, D., Brown, E.D., 2013b. Collapsing the proton motive force to identify synergistic combinations against *Staphylococcus aureus*. *Chem. Biol.* 20, 1168–1178. doi:10.1016/j.chembiol.2013.07.006
- Gilpin, R.W., Young, F.E., Chatterjee, A.N., 1973. Characterization of a stable L-form of *Bacillus subtilis* 168. 113, 486–499.
- Greenwood, D., O'Grady, F., 1973. Comparison of the responses of *Escherichia coli* and *Proteus mirabilis* to seven beta-lactam antibiotics. *J. Infect. Dis.* 128, 211–222.
- Hancock, I.C., 1997. Bacterial cell surface carbohydrates: structure and assembly. *Biochem. Soc. Trans.* 25, 183–187.
- Hong, H.-J., Paget, M.S.B., Buttner, M.J., 2002. A signal transduction system in *Streptomyces coelicolor* that activates the expression of a putative cell wall glycan operon in response to vancomycin and other cell wall-specific antibiotics. *Molecular Microbiology* 44, 1199–1211.
- Lacriola, C.J., Falk, S.P., Weisblum, B., 2013. Screen for agents that induce autolysis in *Bacillus subtilis*. *Antimicrob. Agents Chemother.* 57, 229–234. doi:10.1128/AAC.00741-12
- Lai, M.H., Kirsch, D.R., 1996. Induction signals for vancomycin resistance encoded by the vanA gene cluster in *Enterococcus faecium*. *Antimicrob. Agents Chemother.* 40, 1645–1648.
- Leaver, M., Domínguez-Cuevas, P., Coxhead, J.M., Daniel, R.A., Errington, J., 2009. Life without a wall or division machine in *Bacillus subtilis*. *Nature* 457, 849–853. doi:10.1038/nature07742
- Lee, S.H., Jarantow, L.W., Wang, H., Sillaots, S., Cheng, H., Meredith, T.C., Thompson, J., Roemer, T., 2011. Antagonism of chemical genetic interaction networks resensitize MRSA to β -lactam antibiotics. *Chem. Biol.* 18, 1379–1389. doi:10.1016/j.chembiol.2011.08.015
- Lorian, V., 1975. Some effects of subinhibitory concentrations of antibiotics on bacteria. *Bull N Y Acad Med* 51, 1046–1055.
- Mangat, C.S., Bharat, A., Gehrke, S.S., Brown, E.D., 2014. Rank Ordering Plate Data Facilitates Data Visualization and Normalization in High-Throughput Screening. *J Biomol*

Screen 1087057114534298. doi:10.1177/1087057114534298

- Mani, N., Sancheti, P., Jiang, Z.D., McNaney, C., DeCenzo, M., Knight, B., Stankis, M., Kuranda, M., Rothstein, D.M., Sanchet, P., Knighti, B., 1998. Screening systems for detecting inhibitors of cell wall transglycosylation in *Enterococcus*. *J. Antibiot.* 51, 471–479.
- Mascher, T., Zimmer, S.L., Smith, T.-A., Helmann, J.D., 2004. Antibiotic-inducible promoter regulated by the cell envelope stress-sensing two-component system LiaRS of *Bacillus subtilis*. *Antimicrob. Agents Chemother.* 48, 2888–2896. doi:10.1128/AAC.48.8.2888-2896.2004
- Murray, T., Popham, D.L., Setlow, P., 1998. *Bacillus subtilis* cells lacking penicillin-binding protein 1 require increased levels of divalent cations for growth. 180, 4555–4563.
- Nanamiya, H., Kasai, K., Nozawa, A., Yun, C.-S., Narisawa, T., Murakami, K., Natori, Y., Kawamura, F., Tozawa, Y., 2008. Identification and functional analysis of novel (p)ppGpp synthetase genes in *Bacillus subtilis*. *Molecular Microbiology* 67, 291–304. doi:10.1111/j.1365-2958.2007.06018.x
- Nichols, R.J., Sen, S., Choo, Y.J., Beltrao, P., Zietek, M., Chaba, R., Lee, S., Kazmierczak, K.M., Lee, K.J., Wong, A., Shales, M., Lovett, S., Winkler, M.E., Krogan, N.J., Typas, A., Gross, C.A., 2011. Phenotypic Landscape of a Bacterial Cell. *Cell* 144, 143–156. doi:10.1016/j.cell.2010.11.052
- Qi, L.S., Larson, M.H., Gilbert, L.A., Doudna, J.A., Weissman, J.S., Arkin, A.P., Lim, W.A., 2013. Repurposing CRISPR as an RNA-guided platform for sequence-specific control of gene expression. *Cell* 152, 1173–1183. doi:10.1016/j.cell.2013.02.022
- Quisel, J.D., Burkholder, W.F., Grossman, A.D., 2001. In vivo effects of sporulation kinases on mutant Spo0A proteins in *Bacillus subtilis*. *J. Bacteriol.* 183, 6573–6578. doi:10.1128/JB.183.22.6573-6578.2001
- Richard W Gilpin, S.S.N., 1976. Time-Lapse Photography of *Bacillus subtilis* L-Forms Replicating in Liquid Medium 127, 1018.
- Roemer, T., Davies, J., Giaever, G., Nislow, C., 2012. Bugs, drugs and chemical genomics. *Nat Chem Biol* 8, 46–56. doi:10.1038/nchembio.744
- Sander, J.D., Joung, J.K., 2014. CRISPR-Cas systems for editing, regulating and targeting genomes. *Nature Biotechnology* 32, 347–355. doi:10.1038/nbt.2842
- Sewell, E.W., Brown, E.D., 2013. Taking aim at wall teichoic acid synthesis: new biology and new leads for antibiotics. *J. Antibiot.* doi:10.1038/ja.2013.100
- Sims, P.J., Waggoner, A.S., Wang, C.H., Hoffman, J.F., 1974. Studies on the mechanism by which cyanine dyes measure membrane potential in red blood cells and phosphatidylcholine vesicles. *Biochemistry* 13, 3315–3330.
- Studier, F.W., 2005. Protein production by auto-induction in high density shaking cultures.

Protein Expr. Purif. 41, 207–234.

- Swoboda, J.G., Meredith, T.C., Campbell, J., Brown, S., Suzuki, T., Bollenbach, T., Malhowski, A.J., Kishony, R., Gilmore, M.S., Walker, S., 2009. Discovery of a small molecule that blocks wall teichoic acid biosynthesis in *Staphylococcus aureus*. 4, 875–883. doi:10.1021/cb900151k
- Tidten-Luksch, N., Grimaldi, R., Torrie, L.S., Frearson, J.A., Hunter, W.N., Brenk, R., 2012. IspE inhibitors identified by a combination of in silico and in vitro high-throughput screening. PLoS ONE 7, e35792. doi:10.1371/journal.pone.0035792
- Ulijasz, A.T., Grenader, A., Weisblum, B., 1996. A vancomycin-inducible lacZ reporter system in *Bacillus subtilis*: induction by antibiotics that inhibit cell wall synthesis and by lysozyme. 178, 6305–6309.
- Wang, H., Gill, C.J., Lee, S.H., Mann, P., Zuck, P., Meredith, T.C., Murgolo, N., She, X., Kales, S., Liang, L., Liu, J., Wu, J., Santa Maria, J., Su, J., Pan, J., Hailey, J., Mcguinness, D., Tan, C.M., Flattery, A., Walker, S., Black, T., Roemer, T., 2013. Discovery of wall teichoic acid inhibitors as potential anti-MRSA β -lactam combination agents. Chem. Biol. 20, 272–284. doi:10.1016/j.chembiol.2012.11.013
- Xu, H.H., Trawick, J.D., Haselbeck, R.J., Forsyth, R.A., Yamamoto, R.T., Archer, R., Patterson, J., Allen, M., Froelich, J.M., Taylor, I., Nakaji, D., Maile, R., Kedar, G.C., Pilcher, M., Brown-Driver, V., McCarthy, M., Files, A., Robbins, D., King, P., Sillaots, S., Malone, C., Zamudio, C.S., Roemer, T., Wang, L., Youngman, P.J., Wall, D., 2010. *Staphylococcus aureus* TargetArray: comprehensive differential essential gene expression as a mechanistic tool to profile antibacterials. Antimicrob. Agents Chemother. 54, 3659–3670. doi:10.1128/AAC.00308-10
- Yamamoto, N., Nakahigashi, K., Nakamichi, T., Yoshino, M., Takai, Y., Touda, Y., Furubayashi, A., Kinjyo, S., Dose, H., Hasegawa, M., Datsenko, K.A., Nakayashiki, T., Tomita, M., Wanner, B.L., Mori, H., 2009. Update on the Keio collection of *Escherichia coli* single-gene deletion mutants. Mol Syst Biol 5, 335. doi:10.1038/msb.2009.92
- Young, F.E., Haywood, P., Pollock, M., 1970. Isolation of L-forms of *Bacillus subtilis* which grow in liquid medium. 102, 867–870.
- Zhanel, G.G., Hoban, D.J., Harding, G.K., 1992. Subinhibitory antimicrobial concentrations: A review of in vitro and in vivo data. Can J Infect Dis 3, 193–201.
- Zhu, W., Zhang, Y., Sinko, W., Hensler, M.E., Olson, J., Molohon, K.J., Lindert, S., Cao, R., Li, K., Wang, K., Wang, Y., Liu, Y.-L., Sankovsky, A., de Oliveira, C.A.F., Mitchell, D.A., Nizet, V., McCammon, J.A., Oldfield, E., 2013. Antibacterial drug leads targeting isoprenoid biosynthesis. Proc. Natl. Acad. Sci. U.S.A. 110, 123–128. doi:10.1073/pnas.1219899110
- Zimmerman, S.B., Stapley, E.O., 1976. Relative morphological effects induced by cefoxitin and other beta-lactam antibiotics in vitro. Antimicrob. Agents Chemother. 9, 318–326.

**CHAPTER THREE - A small molecule screening platform for the discovery
of inhibitors of undecaprenyl diphosphate synthase**

PREFACE

Majority of the work presented in this chapter is published (open access) at ACS Infectious Disease.

Tomasz L. Czarny, Eric D. Brown. (2016) A Small-Molecule Screening Platform for the Discovery of Inhibitors of Undecaprenyl Diphosphate Synthase. ACS Infectious Diseases. DOI: 10.1021/acsinfecdis.6b00044

Experiments presented in this chapter were solely designed and performed by me with the exception of:

- (1) Anthony Scalia, an undergraduate student who I was mentoring in the lab, helped in performing ~15 % of the 140,000 *B. subtilis* 168 primary screen.

SUMMARY

The bacterial cell wall has long been a celebrated target for antibacterial drug discovery due to its critical nature in bacteria and absence in mammalian systems. At the heart of the cell wall biosynthetic pathway lies undecaprenyl phosphate (Und-P); the lipid linked carrier upon which the bacterial cell-wall is built. As described in chapter 1, with most whole cell antibacterial drug discovery campaigns mode of actions studies are challenging and cumbersome. Herein we exploit the complex dispensability pattern found within WTA synthesis to develop a powerful workflow enriching for inhibitors of undecaprenyl diphosphate synthase (UppS). Interrogating a chemical collection of 142,000 small molecules resulted in the identification of 6 new inhibitors of UppS. To date inhibitors of UppS generally show off target effects on membrane potential due to their chemical nature. One of the 6 inhibitors identified, MAC-0547630, exhibits nanomolar inhibition against UppS without off target effects on membrane potential. Such characteristics make it a unique chemical probe for exploring the inhibition of UPPs in bacterial cell systems.

INTRODUCTION

The conserved nature of cell-wall biosynthesis among bacterial species, along with its absence in mammalian systems, has long made it a prevalent and well utilized target in antibacterial drug discovery (Bugg et al., 2011). Nevertheless, the preponderance of agents that inhibit extra-cytoplasmic steps of peptidoglycan synthesis, namely penicillin binding proteins (PBPs), has left much of the cell wall biosynthetic machinery of bacteria untapped for antibacterial therapies (Brown and Wright, 2005; Falconer and Brown, 2009; Sewell and Brown, 2013). One such target is undecaprenyl diphosphate synthase (UppS). UppS is a conserved enzyme belonging to a family of *cis*-prenyltransferases. Prenyltransferases are responsible for the production of many linear isoprenoids including steroids, terpenes and carotenoids (Ogura and Koyama, 1998). UppS catalyzes the synthesis of the C₅₅ lipid – undecaprenyl diphosphate (Und-PP) through 8 consecutive 1'-4 condensations of isopentenyl pyrophosphate (IPP) using the priming molecule farnesyl pyrophosphate (FPP) (Liang et al., 2002). Upon dephosphorylation of Und-PP; undecaprenyl phosphate (Und-P) is utilized by both Gram-positive and Gram-negative bacteria as an indispensable membrane anchor for the synthesis of nascent cell wall (van Heijenoort, 2007).

Cell wall biosynthesis is inherently complex containing many interconnected biosynthetic pathways that are both spatially and temporally regulated (Atilano et al., 2010; Bhavsar and Brown, 2006). These complexities and interactions can be

harnessed to generate unique high-throughput screening approaches for drug discovery (Brown and Wright, 2016; 2005; Farha and Brown, 2015). Arguably, one of the best examples of this is the idiosyncratic dispensability pattern found in genes coding for the wall teichoic acid (WTA) biosynthetic pathway (Figure 3-1) (D'Elia et al., 2006a; 2006b). In Gram-positives the cell wall is made up of equal parts (by weight) peptidoglycan and WTA, both of which are synthesized on the lipid carrier Und-P (Bhavsar and Brown, 2006). WTAs are a group of chemically diverse, highly charged, phosphate rich poly-anionic polymers covalently bound to peptidoglycan (Bhavsar and Brown, 2006). Though the exact function of WTA is unknown studies point to its importance in host colonization (Weidenmaier et al., 2004; Winstel et al., 2015), biofilm formation (Holland et al., 2011) and β -lactam resistance in methicillin-resistant *Staphylococcus aureus*, MRSA (Campbell et al., 2011; Farha et al., 2013a). Synthesized on the cytoplasmic side of the membrane, WTA synthesis is initiated by consecutive transfer of *N*-acetyl-glucosamine-1-phosphate and *N*-acetyl-mannosamine-1-phosphate to Und-P by the non-essential enzymes TagO and TagA respectively. The polymerization, export and attachment of the poly-glycerol-phosphate polymer is then performed by the remainder of the biosynthetic enzymes whose gene products are essential (D'Elia et al., 2006b). Intriguingly the essentiality of these late-acting gene products can be obviated by a deletion in either of the early step genes (*tagO* or *tagA*) (Figure 3-1) (D'Elia et al., 2006b). Indeed, this gene dispensability pattern has been well exploited in the search for late stage

WTA inhibitors. Efforts of such studies have been limited to comparative screens of wild-type and $\Delta tarO$ *S. aureus* growth inhibition, focusing on small molecules that lose whole cell activity in the $\Delta tarO$ background. Such screens have led to many inhibitors of the TarGH ABC transporter including targocil (Swoboda et al., 2009; Wang et al., 2013). Further, antagonism between late and early steps was used to discover the cryptic action of ticlopidine, a drug used to treat hypertension, on the TarO enzyme in *S. aureus* (Farha et al., 2013a). While the inhibition of TarO doesn't lead to growth inhibition, ticlopidine was found to reverse beta-lactam resistance in MRSA.

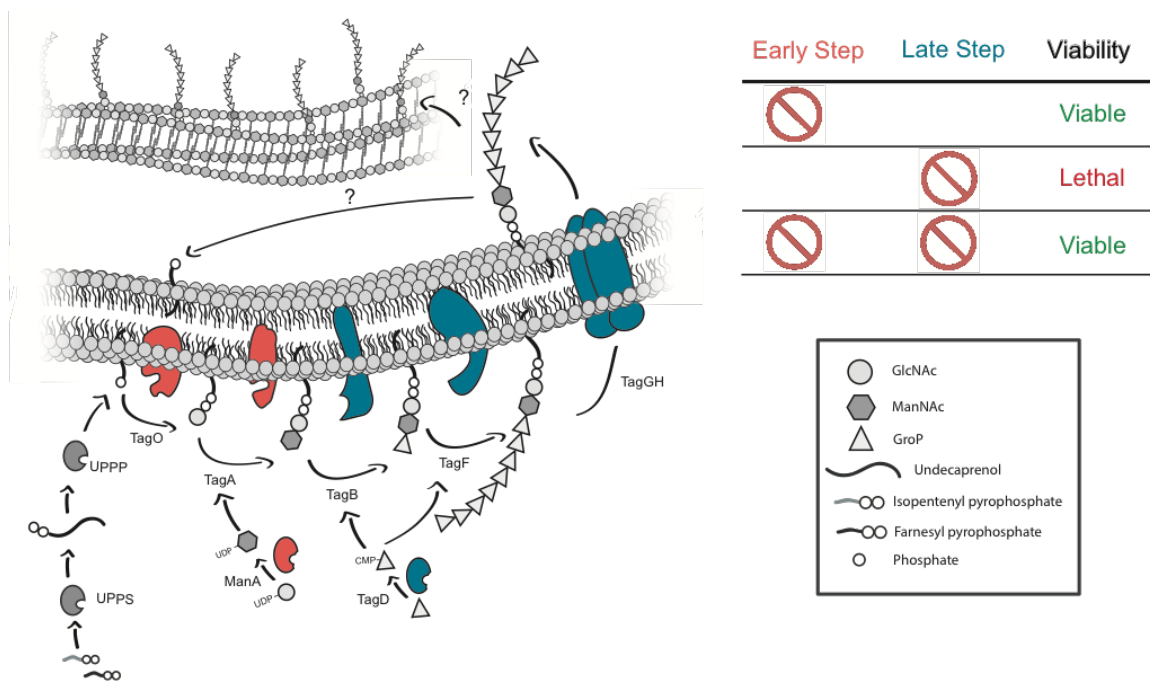


Figure 3-1: Dispensability pattern of Wall Teichoic Acid (WTA) biosynthesis in *B. subtilis* 168. The WTA biosynthetic pathway is divided into early (pink) and late (blue) steps. Gene products involved in early step synthesis (TagO, TagA) are dispensable for viability. Late acting

gene products (TagB, TagD, TagF, TagGH) are essential and as such crucial for viability. Upon the introduction of a lesion in early step synthesis, late acting gene products become dispensable. As such lesion in late steps become no longer essential for viability under such conditions.

As with all whole cell antibacterial drug discovery campaigns, target identification through mode of action (MOA) studies is cumbersome and time consuming. Further, whole cell screens for growth inhibition typically generate large numbers of active compounds that are troublesome to prioritize for downstream efforts. Harnessing powerful whole cell phenotypes such as the dispensability pattern found within WTA synthesis in the first few steps of screening reduces the need for MOA. As mentioned above inhibition of late stage WTA synthesis -- with compounds such as targocil -- results in a lethal phenotype. One can imagine that a screen for small molecules that antagonise targocil would lead to the discovery of early-step (TagO, TagA) and substrate producing (MnaA, UPPP, UppS) inhibitors. Based on this hypothesis, designed and optimized was a chemical-chemical based antagonism secondary screen, using targocil, which resulted in powerful enrichment of UppS inhibitors.

Starting with a chemical library comprised of ~142,000 diverse synthetic molecules, an initial screen for growth inhibition was optimized and executed against the model Gram-positive *B. subtilis* 168. This organism was chosen due to its amenable to high-throughput screening as a level 1 biosafety hazard. Additionally, unlike in *S. aureus*, inhibition of earl-step WTA synthesis results in a

sick phenotype. Therefore, a screen for growth-inhibition in this organism is uniquely sensitive to inhibitors of early-step WTA synthesis (D'Elia et al., 2006a). Indeed, such efforts led to the identification of 3,705 *B. subtilis* 168 growth inhibitory molecules.

Following the generation of a *B. subtilis* active collection, a chemical-chemical targocil antagonism screen was optimized and executed in *S. aureus*. This organism was chosen as targocil is a *S. aureus* specific inhibitor. This secondary screen allowed for prioritization of compounds that inhibit early-step synthesis and associated WTA enzymes. Upon screening the 3,705 *B. subtilis* 168 actives, 181 compounds were found to be antagonistic with targocil. As all early step and associated targets show severe sick phenotypes in *B. subtilis* 168; growth inhibition at a single high concentration (125 μ M) on solid media was assessed. This led to 35 priority antagonists. Assessment of potency focused our efforts on elucidating the target of one of these compounds, MAC-0547630. Generation of spontaneous mutants in the presence of MAC-0547630, followed by whole genome sequencing, revealed single nucleotide polymorphisms (SNPs) in *uppS*. To assess the validity and enrichment for inhibitors of UppS using targocil antagonism, all 35 priority antagonists were assessed against an *in vitro* UppS enzyme screen. Six inhibitors of UppS were identified with varying levels of effectiveness including MAC-0547630. With a hit rate of 17%, this approach proved to be a powerful tool in the discovery of UppS inhibitors. Five of the 6

inhibitors were available for resupply and were followed up further in this study (Figure 3-2). Due to the chemical nature of the majority of UppS inhibitors (high logP and charged-hydrophobic structural characteristics), it has been demonstrated that they tend to have off target effects involving membrane potential (Feng et al., 2015). Though this can be an advantageous phenotype for antibiotics, such off target effects can be problematic when studying biological systems. However, one of the inhibitors described in this study (MAC-0547630) shows great promise as a probe due to its selective and nanomolar inhibition of UppS.

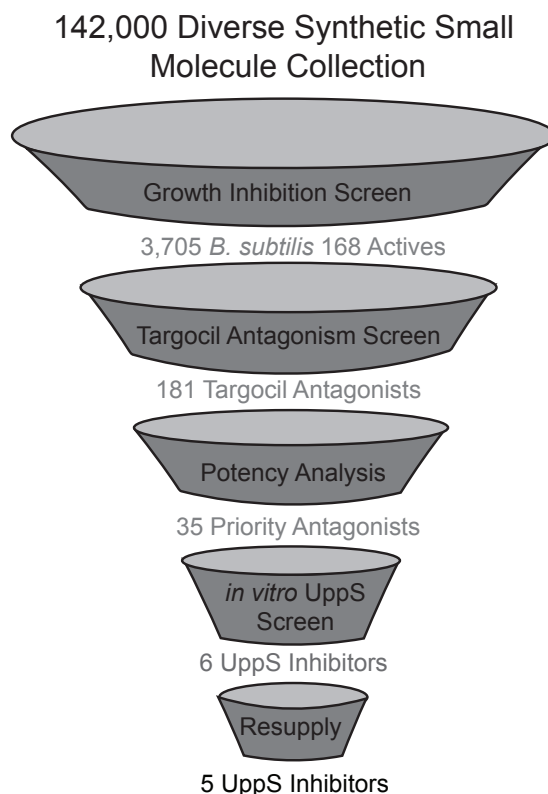


Figure 3-2. Screening workflow for identifying inhibitors of UppS. A collection of 142,000 diverse synthetic small molecules was screened for growth inhibition against the model Gram-

positive *B. subtilis* 168 resulting in 3,705 actives. Antagonism by these molecules of the late stage WTA inhibitor targocil was then assessed in *S. aureus* identifying 181 antagonists. Further study of the potency of these compounds led to the identification of 35 priority antagonists. A subsequent *in vitro* screen for undecaprenyl pyrophosphate synthase (UppS) inhibition resulted in 6 UppS inhibitors. Of these 5 compounds were available for resupply and further study.

RESULTS

High throughput screen of 142,000 compounds for *B. subtilis* 168 growth inhibition

Work began with a screen of a diverse collection of 142,000 synthetic compounds for growth inhibition of wild-type *B. subtilis* at a concentration of 10 μ M. Growth at 30 °C was measured by change in absorbance (600 nm) after 8 hours of incubation in specialized HiGrow microtiter shakers (DIGILAB, Marlborough, MA), set to 550 rpm. These conditions led to an optimal screening window which captured *B. subtilis* 168 at a late exponential growth phase (Figure 3-3). To assess the robustness of the HTS assay throughout the screen, high (1% DMSO) and low (10 μ M penicillin-G) controls were included on each screening plate. Screening data were normalized to remove plate-to-plate and well-positional variation as previously described (Mangat et al., 2014). Hits were selected using a statistical cutoff of 2 standard deviations below the mean of the full data set, resulting in a hit cutoff of 70% growth. That cutoff led to a hit rate of 2.61 % and a total of 3,705 *B. subtilis* 168 actives (Figure 3-2, Figure 3-4).

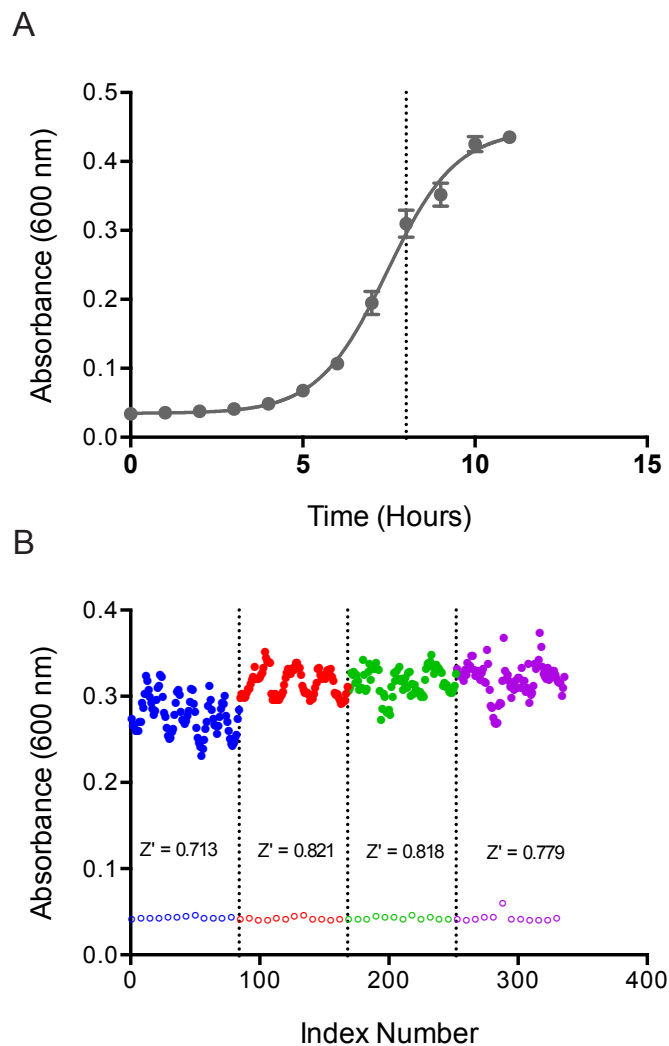


Figure 3-3: Optimized conditions for *B. subtilis* 168 growth inhibition screen. (A) A growth curve of *B. subtilis* 168 (EB6) was performed in 96-well format using HiGrow incubators (DigiLab, Marlborough MA) at 30 °C and 550 rpm. Absorbance was measured approximately every hour for 11 hours using an Envision multi-label reader (Perkin Elmer). Dotted line (8 hours) represents the chosen time-point for incubation during the growth inhibition screen. **(B)** The growth inhibition screening window was assessed at the chosen 8-hour time-point. High controls (1 % DMSO, depicted with filled in circles) and Low controls (10 μ M Penicillin G, depicted with open circles) were organized and plotted by plate. Index numbers 1-84, 85-168, 169-252, 253-336, present plates 1,2,3 and 4 respectively. Z' for each plate are depicted with an average Z' of 0.782.

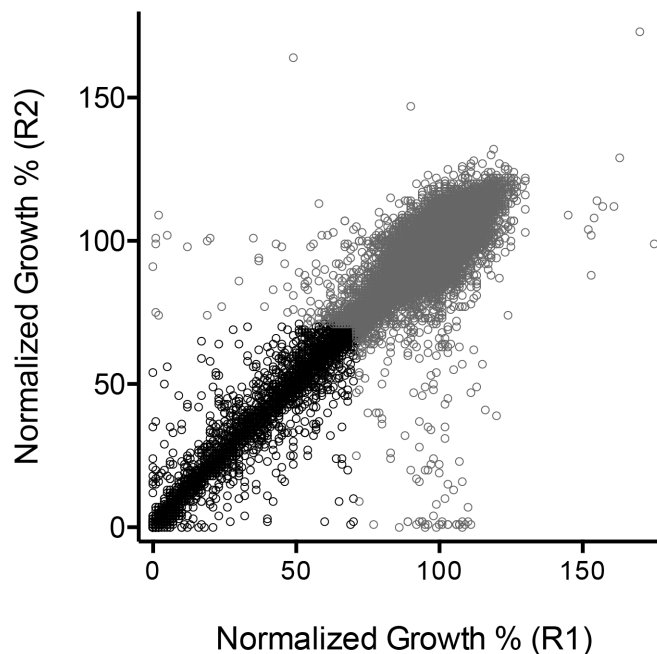


Figure 3-4: Replica plot of primary *B. subtilis* 168 growth inhibition screen. A collection of 142,000 diverse synthetic small molecules was screened at 10 μ M for growth inhibition of *B. subtilis* 168 in duplicate. Normalized growth, expressed as a percentage, for replicate 1 and 2 is depicted on the x and y-axis respectively. A statistical cut-off of 70 % was established for both replicates. Grey open circles represent inactive molecules and black open circles represent 3,705 *B. subtilis* 168 actives.

High throughput screen of 3,705 *B. subtilis* 168 actives for antagonists of targocil

As demonstrated by previously studies published in our lab, early step WTA inhibitors show whopping antagonism with targocil -- a late stage, *S. aureus* specific, WTA inhibitor (Farha et al., 2013a). Capitalizing on this information the design and optimization of a targocil antagonism screen ensued. Due to targocils high frequency of resistance it was imperative to find suitable screening

conditions where spontaneous mutants would be minimized resulting in a clean screen with few false positives. Indeed, *B. subtilis* 168 is not amenable to this powerful secondary screen since targocil is a *S. aureus* specific inhibitor. As such, the targocil antagonism screen was optimized in *S. aureus* Newman. 8x the MIC of targocil was chosen as a screening concentration to reduce the number of spontaneous resistant mutants. This screening concentration of targocil was tested for amenability in both 96-well and 384-well formats. Additionally, appropriate incubation times were assessed to minimize spontaneous suppressors. The most suitable condition tested for a high-throughput screen was 384-well format incubated for 12 hours (Figure 3-5).

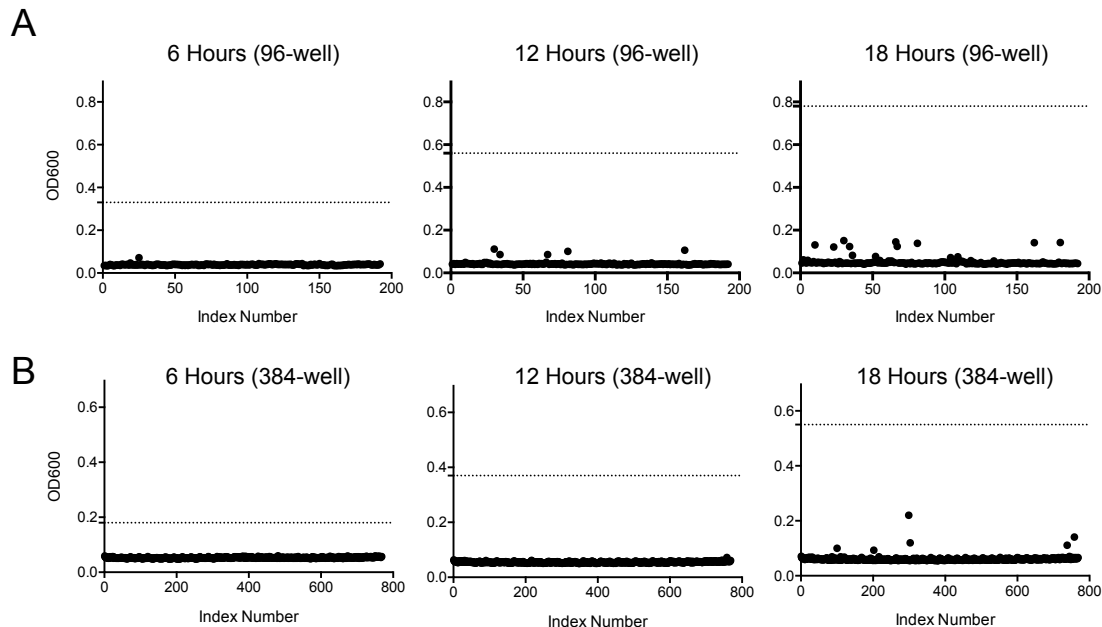


Figure 3-5: Optimization of the targocil antagonism screen. (A) Feasibility of a 96-well format screen was assessed by plating targocil at 8x MIC across two 96-well plates with an assay volume of 100 μ L. Plates were incubated at 37 $^{\circ}$ C and read at 6, 12, and 18 hours. Each well for

plate 1 was indexed from 1-96 and plate 2 was indexed 97-192 (x-axis). Absorbance at 600 nm is plotted on the y-axis as a viability readout. Data points emerging from the baseline are spontaneous mutants. Dashed lines represent average growth of *S. aureus* Newman solvent controls. **(b)** Feasibility of a 384-well format screen was assessed by plating 8x MIC targocil across two 384-well plates with an assay volume of 50 μ L. Plates were incubated at 37 °C and read at 6, 12, and 18 hours. Each well for plate 1 was indexed from 1-384 and plate 2 was indexed from 385 to 768 (x-axis). Absorbance at 600 nm was measured as a viability readout (y-axis). Data points emerging from the baseline are spontaneous mutants. Dashed lines represent average growth of *S. aureus* Newman solvent control.

Upon establishing suitable screening conditions, the 3,705 *B. subtilis* 168 actives were systematically screened at 20 μ M for antagonism with targocil at eight-times its MIC (16 μ g/mL) in 384-well format. High and low controls were used to assess the robustness of the screen and to normalize the screening data. Neat DMSO was used as a high (solvent) control and erythromycin was used as the low control. Data was analyzed on a plate-to-plate basis using the middle two quartiles of the data as baseline and the high controls as a theoretical ceiling for rescue (see methods). Compounds that restored growth >10 % over the middle two quartiles of the data were classified as targocil antagonists. Such a cut-off led to a manageable follow-up of 181 molecules, resulting in a hit rate of 4.8 % (Figure 3-2, Figure 3-6).

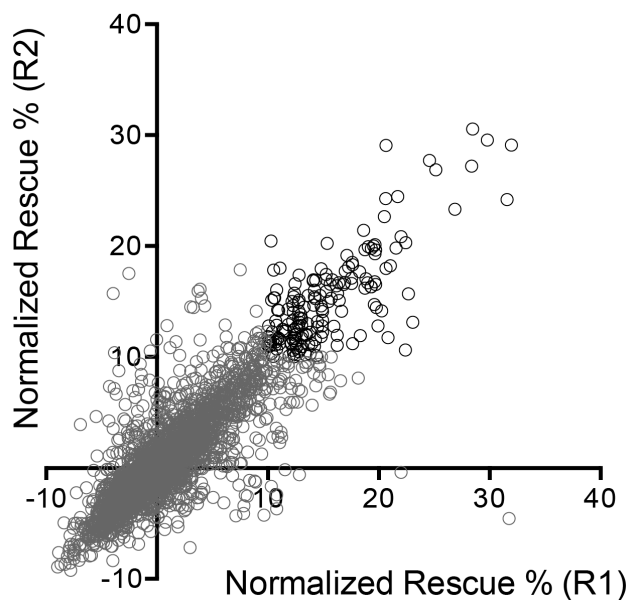


Figure 3-6: Replica plot depicting data from secondary targocil antagonism screen. The 3,705 actives were assessed for antagonistic interactions with targocil in *S. aureus* using our previously established method. These were assessed at 20 μM in duplicate in the presence of targocil at 16 $\mu\text{g}/\text{mL}$. Percentage suppression of growth inhibition (compared to growth without added compounds) for replicates 1 and 2 are depicted on the x and y-axis respectively. A suppression of 10 % or more of growth inhibition was used as a cut-off to identify 181 targocil antagonists (black open circles) and 3,524 non-interacting compounds (grey open circles).

Potency assessment of 181 targocil antagonists on solid media

Having discovered these compounds with liquid media screens, the potency was further assessed on solid, to prioritize compounds which are amenable to the generation of spontaneous mutants on solid media. Indeed, frequently compounds that are growth inhibitory in liquid media, lack sufficient potency on solid media for follow up. Thus the 181 antagonists were assessment of growth inhibition on solid media plugs at a concentration of 125 μM using an automated

colony pinning device to inoculate colonies as previously described (French et al., 2016). Thirty-five of the 181 compounds were completely growth inhibitory using this assay (Figure 3-2).

Spontaneously generated mutant to MAC-0547630 contains a SNP in *uppS*

MAC-0547630 was prioritized from the 35 priority antagonists due to its potent nature -- MIC of 0.1 µg/mL in *B. subtilis* 168. To try to determine the target of MAC-0547630 spontaneous mutants of *B. subtilis* 168 were generated on solid media by plating 6×10^7 CFU onto LB agar plates containing 4x, 8x and 16x MIC of MAC-0547630. Upon incubation for 72 hours at 30 °C a mutation frequency of 3×10^{-7} was observed. A highly resistant mutant dubbed 8x-2 was tested for cross resistance to other antibiotics. As no cross resistance was observed it was sent for whole genome next gen sequencing via an Illumina sequencer. Sequencing results were aligned to the previously published *B. subtilis* 168 genome (NC_000964) using bowtie alignment software (Langmead et al., 2009). Upon analysis a single SNP was observed in *uppS* with 69x coverage at 100 % frequency -- 1,721,683 T→A (Leu₁₅₇His).

Overexpression and establishment of kinetic parameters for UppS isolated from *B. subtilis* 168, *S. aureus*, and *E. coli*

With UppS as the potential target for MAC-0547630 it was not only imperative to obtain *in vitro* enzyme inhibition data for MAC-0547630 but also to test whether

or not any other of the 35 priority antagonists were inhibitors of UppS. As such recombinant UppS from *B. subtilis* 168 (UppS^{BS}), *E. coli* (UppS^{EC}), and *S. aureus* (UppS^{SA}) was purified. UppS from each organism was cloned into a pET-19b vector (Novagene) modified to encode an engineered Tobacco Etch Virus (TEV) protease cleavage site. *E. coli* BL21 (Rosetta) cells were used for induction. UppS from each organism was purified on a Ni-NTA agarose gravity fed column. UppS catalyzes a 1'-4 condensation of 8 molecules of isopentenyl diphosphate (IPP) with farnesyl diphosphate (FPP) to form undecaprenyl-pyrophosphate. With each subsequent condensation of IPP, during polymerization, pyrophosphate is released as a by-product. Using a coupled kinetic EnzCheck pyrophosphate detection assay (Life Technologies) pyrophosphate release was detected by kinetically following breakdown of 2-amino-6-mercapto-7-methyl-purine ribonucleoside (MESG) by monitoring the change in absorbance at 360 nm. Kinetic parameters including enzyme linearity and substrate KM's were established for all three recombinant enzymes (Figure 3-7)

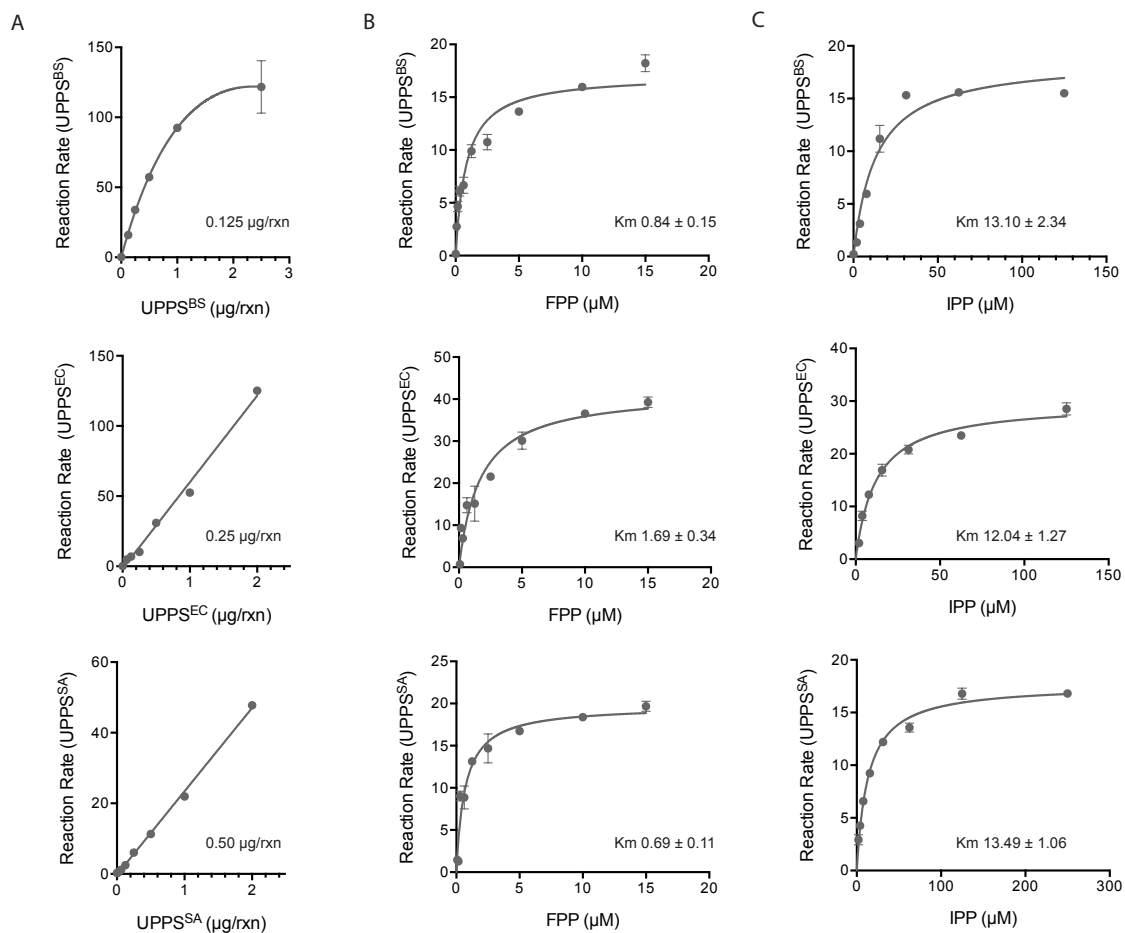


Figure 3-7. Establishing parameters for *in vitro* assessment of UPPS cloned from *B.*

***subtilis*, *E. coli*, and *S. aureus*.** (A) Establishing linearity with UPPS^{BS}, UPPS^{EC}, UPPS^{SA} concentration in EnzCheck pyrophosphate release assay. (B) Farnesyl pyrophosphate (FPP) KM determination in UPPS^{BS}, UPPS^{EC}, UPPS^{SA}. (C) Isopentenyl pyrophosphate (IPP) KM determination in UPPS^{BS}, UPPS^{EC}, UPPS^{SA}.

***In vitro* enzyme based screen for UppS inhibition**

With MAC-0547630's high probability of UppS inhibition, assessed were all 35 priority antagonists for inhibition against recombinant *B. subtilis* 168

undecaprenyl-pyrophosphate synthase (UppS^{BS}). Using the coupled kinetic EnzCheck pyrophosphate detection assay (Life Technologies) described above the 35 priority antagonists were screened against the enzyme at 50 μ M, in duplicate. Compounds were pre-incubated with enzyme for 20 minutes and the reactions were initiated by the addition of substrate (FPP & IPP). Observed rates of pyrophosphate release were analyzed and compared to high and low controls. One-percent DMSO was used in both the high and low control reactions with and without substrate (IPP & FPP) respectively. Activity of the 35 priority antagonists was plotted as a percentage of the control reactions. Six compounds exhibited UppS inhibition, including MAC-0547630, using < 80% activity as a cut-off. Five of the six compounds were available for reorder and as such further study (Figure 3-2, Figure 3-8).

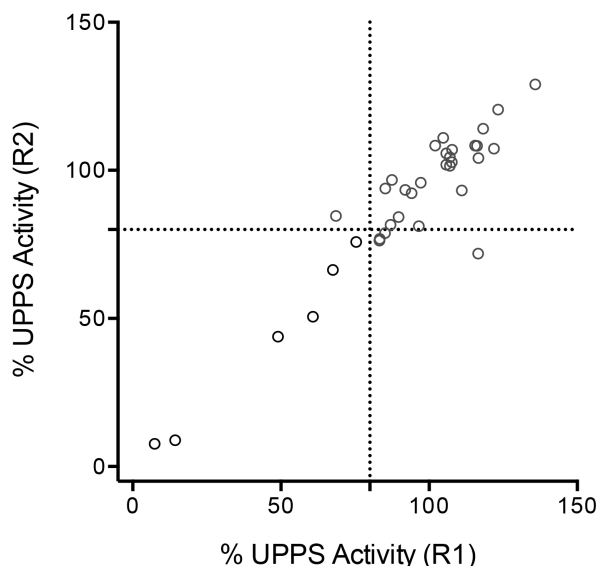


Figure 3-8: Replica plot depicting the results from the *in vitro* UppS screen of 35 priority antagonists. A Screen of the 35 priority antagonists was performed at 50 μ M in duplicate for *in*

in vitro inhibition of UppS. Compounds resulting in less than 80 % UppS activity in both replicates were deemed UppS inhibitors (black open circles) and the remainder were deemed inactive (open grey circles). 6 of the 35 priority antagonists tested showed perturbation of *in vitro* UppS function.

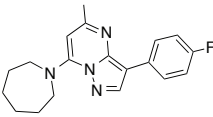
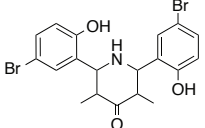
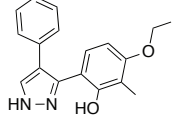
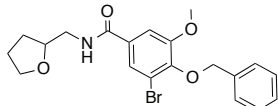
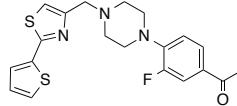
Dose dependent *in vitro* inhibition of UppS cloned from *B. subtilis* 168, *S. aureus*, and *E. coli*

As UppS is a conserved target amongst bacterial species, the spectrum of activity of these 5 inhibitors on recombinant UppS expressed from various bacterial species was of interest. Following optimization of over-expression conditions and purification, it was possible to obtain high-yields of homogeneous UppS from all three bacterial species. Appropriate kinetic parameters (K_m values) were determined for both substrates (IPP and FPP), for each of the three purified enzymes (Figure 3-7).

The 5 UppS^{BS} inhibitors were subsequently screened against the three recombinant UppS; *B. subtilis* 168 (UppS^{BS}), *S. aureus* (UppS^{SA}) and *E. coli* (UppS^{EC}). Dose dependent inhibition was established by calculation of IC₅₀ values using the same assay conditions as seen in the *in vitro* UppS^{BS} screen, with FPP and IPP at 1x and 5x K_m respectively. Interestingly the 5 inhibitors assayed had varied specificity for the three different UppS enzymes (Table 3-1, Supplemental Figure 3-1). For example, only MAC-0557874 had IC₅₀ values of less than 50 μ M for UppS from all three species while MAC-0547630 had strong

activity against the *B. subtilis* and *S. aureus* enzymes (0.05 and 1.6 μM , respectively).

Table 3-1: Assessment of *in vitro* inhibition of 5 novel inhibitors against recombinant UPPs from *B. subtilis*, *S. aureus*, and *E. coli*

Structure	MAC-ID ¹	UPPS ^{BS} IC ₅₀ ² (μM)	UPPS ^{SA} IC ₅₀ ³ (μM)	UPPS ^{EC} IC ₅₀ ⁴ (μM)
	MAC-0547630	0.05 \pm 0.007	1.60 \pm 0.24	NI *
	MAC-0557874	6.22 \pm 1.02	39.97 \pm 12.6	1.39 \pm 0.59
	MAC-0110792	> 340	> 340	11.66 \pm 2.03
	MAC-0588238	1.30 \pm 0.17	38.0 \pm 13.2	NI *
	MAC-0602693	42.9 \pm 4.0	NI *	NI *

1. MAC-ID are unique compound identifiers found within the 142,000 compound library
 2. UPPS^{BS} was cloned from *B. subtilis* 168. It was the enzyme used in the *in vitro* UPPS inhibition screen (Figure 2-6)
 3. UPPS^{EC} was cloned from *E. coli* BW25113.
 4. UPPS^{SA} was cloned from *S. aureus* (CA-MRSA USA300)
- * NI (non-inhibitory) – Compound shows no *in vitro* activity against the respective enzyme.

Growth inhibition studies against *B. subtilis* 168, *S. aureus* and *E. coli*

Following confirmation/investigation of UppS inhibitory activity, the susceptibility levels of all three bacterial species to these five inhibitors was assessed by dose

dependent growth inhibition studies. All five compounds showed clear growth inhibition against *B. subtilis* 168 with MIC values ranging from 0.1 to 12 $\mu\text{g/mL}$. Compounds MAC-0547630 and MAC-0588238 showed the most profound growth inhibition with MICs of 0.1 and 1.25 $\mu\text{g/mL}$, respectively. Interestingly, *S. aureus* was not as susceptible to these two inhibitors, with only ~ 50% reduction in growth observed. None of inhibitors showed any activity against the Gram-negative organism *E. coli* (Figure 3-9).

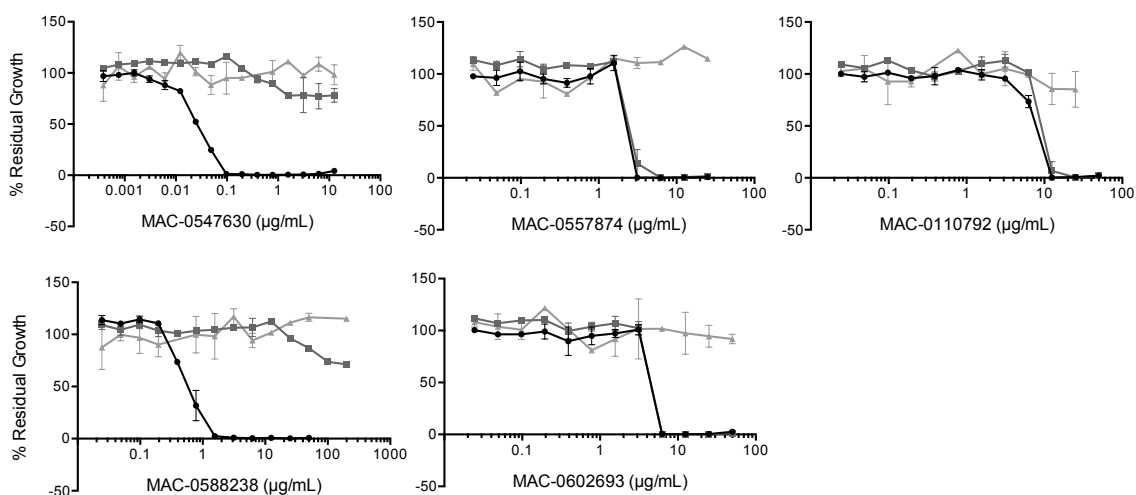


Figure 3-9. Dose dependent inhibition of *B. subtilis* 168, *S. aureus*, and *E. coli*. Dose dependent growth inhibition in the presence of 5 UppS inhibitors was assessed using *B. subtilis* 168 (black), *S. aureus* (dark grey) and *E. coli* (light grey). Residual growth is plotted on the y-axis as a percentage of the high (solvent) control. Growth is plotted as a function of inhibitor concentration (x-axis).

Generation of mutants against MAC-0547630 & MAC-0588238 reveal binding sites in UppS

To confirm that UppS was the target of these compounds in cells and to probe the binding sites of our UppS inhibitors, spontaneous mutants in *B. subtilis* were generated. *B. subtilis* was plated at 6×10^7 CFUs on solid LB media containing 4x, 8x, and 16x the MIC of each of the 5 inhibitors. Plates were incubated for 72 – 96 hours (until colonies appeared) and colonies were then picked & characterized. Only MAC-0547630 and MAC-0588238 generated resistant colonies and susceptibility testing on the emergent clones confirmed the generation of stable mutants with a shift in MIC > 4-fold. To assess whether the mutations responsible for resistance were located in *uppS*; targeted sequencing was performed of the gene. Six mutants resistant to MAC-0547630 and five mutants for MAC-0588238 were identified that contained single nucleotide polymorphisms (Figure 3-10A). To obtain a spatial sense of inhibitor binding within UppS, the mutations generated against MAC-0547630 and MAC-0588238 were mapped on the previously solved structure of UPPs^{SA} (PDB: 4H8E) (Figure 3-10B, Figure 3-10C). Previous studies of UppS inhibition have focused on 4 binding sites in the enzyme, sites 1,2 and 3 situated at the top of the catalytic tunnel and site 4 located near the bottom (Zhu et al., 2013). Both MAC-0547630 and MAC-0588238 generated mutations overlapping with site 3; which interfaces with α -helix 3 and 4 of the enzyme. A single mutant Thr₁₄₅Lys generated in the presence of MAC-0588238 is proximal to binding site 4 (bottom of the tunnel) and

as such may point to the orientation of MAC-0588238. Inhibitors overlapping with binding site 3 are intriguing as their presence may not only sterically interfere with substrates and or product intermediates but also interfere with the movement of α -helix 3 during changes in conformational states (Liang et al., 2002).

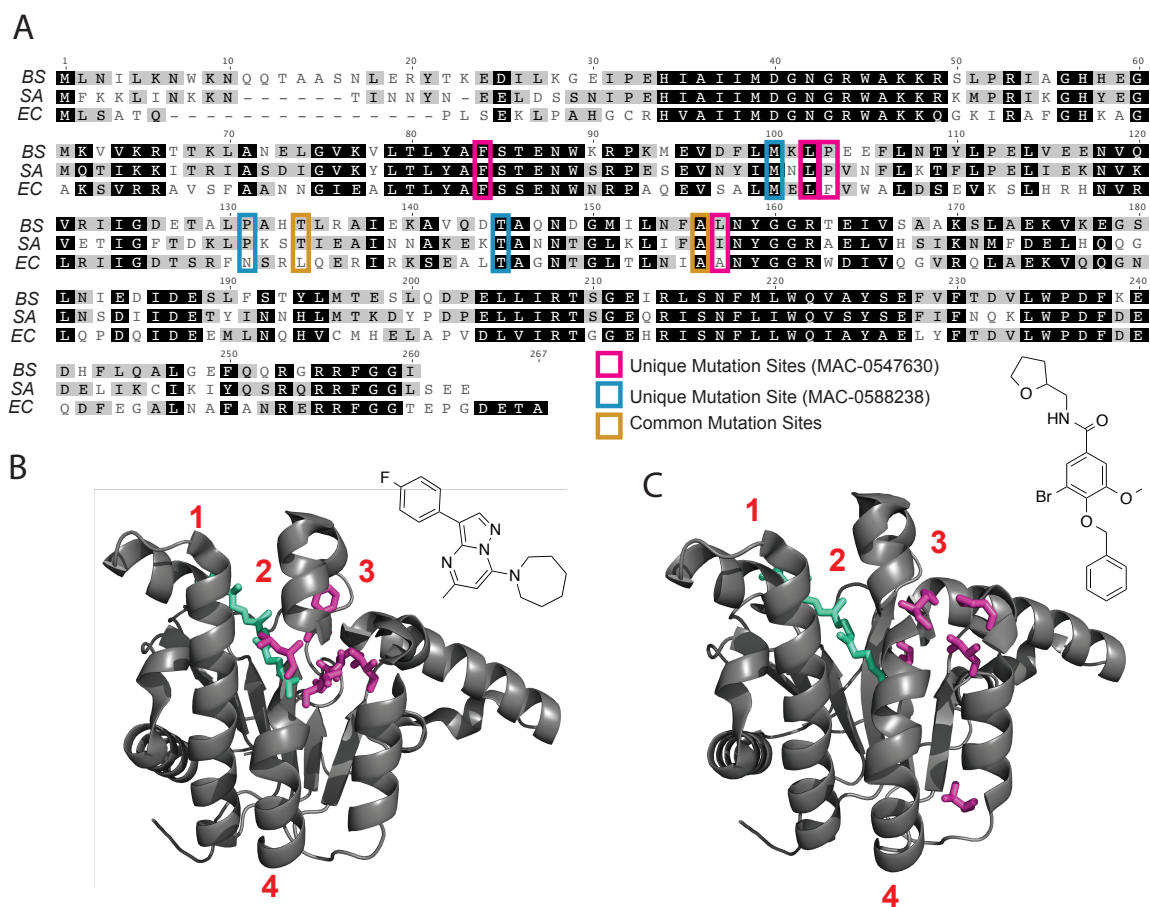


Figure 3-10: Mapping of spontaneously generated mutants developed in the presence of MAC-0547630 and MAC-0588238. (A) Aligned sequences of UppS from *B. subtilis* 168 (BS), *S. aureus* (SA), and *E. coli* (EC). Sites of substitution that lead to resistance to MAC-0547630 and MAC-0588238 are pictured in pink and blue boxes, respectively. Mutation sites common to the two inhibitors are in orange boxes. Sequences are also highlighted based on overall similarity between the three organisms: 100 % similar (black), > 60 % similar (grey), < 60 % similar (white). Amino acid numbering is in reference to the *B. subtilis* 168 sequence. (B) Sites of spontaneous mutations to produce resistance to the growth inhibitory action of MAC-0547630 are mapped to

the structure of UppS (PDB: 4H8E). Mutated amino acids are highlighted in pink and farnesyl pyrophosphate, present in the crystal structure, is depicted in green. Previously described binding sites of inhibitors in UppS (1 - 4) are depicted in red (Zhu et al., 2013). (C) Sites of spontaneous mutation to produce resistance to the growth inhibitory action of MAC-0588238 are mapped to the structure of UppS (PDB: 4H8E). Mutated amino acids are highlighted in pink and farnesyl pyrophosphate, present in the crystal structure, is depicted in green. Previously described binding sites of inhibitors in UppS (1 - 4) are depicted in red (Zhu et al., 2013).

Assessing cross resistance of MAC-0547630 and MAC-0588238 mutants

All 11 mutant strains generated to MAC-0547630 and MAC-0588238 were tested for resistance to the 5 novel inhibitors discovered along with the previously characterized UPPs inhibitor clomiphene (Table 3-2). Interestingly, the only cross-resistance observed was between mutant strains generated with MAC-0547630 and compound MAC-0588238. Similarly, mutants generated with MAC-0588238 only showed cross resistance with MAC-0547630 (Table 3-2).

Table 3-2. Resistance profile of mutants generated using MAC-0547630 and MAC-0588238.

Background	MIC of Inhibitor ($\mu\text{g/mL}$)					Clomiphene
	MAC-0547630	MAC-0557874	MAC-0110792	MAC-0588238	MAC-0602693	
Wild-type <i>B. subtilis</i> 168	0.10	3.13	6.25	1.56	6.25	6.25
MAC-0547630 Mutants						
1,721,465 T->A TTT TAT Phe ₈₄ Tyr	> 100	3.13	6.25	> 100	6.25	6.25
1,721,683 T->A CTT CAT Leu ₁₅₇ His	> 100	3.13	6.25	> 100	6.25	6.25
1,721,518 T->A CTT CAT Leu ₁₀₂ His	> 100	3.13	6.25	> 100	6.25	6.25
1,721,614 C->T ACA ATA Thr ₁₃₄ Ile	0.78	3.13	6.25	> 100	6.25	6.25
1,721,520 C->A CCG ACG Pro ₁₀₃ Thr	> 100	3.13	6.25	> 100	6.25	6.25
1,721,679 G->A GCT ACT Ala ₁₅₆ Thr	> 100	3.13	6.25	> 100	6.25	6.25
MAC-0588238 Mutants						
1,721,513 G->T ATG ATI Met ₁₀₀ Ile	1.56	3.13	6.25	> 100	6.25	6.25
1,721,680 C->T GGT GIT Ala ₁₅₆ Val	3.13	3.13	6.25	> 100	6.25	6.25
1,721,605 C->T CCG CIG Pro ₁₃₁ Leu	0.39	3.13	6.25	12.50	6.25	6.25
1,721,647 C->A ACG AAG Thr ₁₄₅ Lys	0.78	3.13	6.25	12.50	6.25	6.25
1,721,613 A->G ACA GCA Thr ₁₃₄ Ala	0.39	3.13	6.25	6.25	6.25	6.25

Evaluating the affects of the 5 novel UppS inhibitors on membrane potential

A recent study with various inhibitors of UppS has shown that they typically demonstrate off target affects on membrane potential due to their physical chemical properties (Feng et al., 2015). To determine whether the 5 UppS inhibitors identified in this study also exhibit pleotropic membrane effects, a membrane potential dose dependent assay, using the membrane potential-sensitive cyanine dye DiSC₃(5) was utilized. In this assay, compounds that affect membrane potential lead to changes in the steady state fluorescence, through perturbation of the proton motive force (PMF) (Farha et al., 2013b). Four of the compounds showed dose dependent increases in fluorescence when exposed to

dye loaded cells. However, MAC-0547630 demonstrated no affect on membrane potential (Figure 3-11).

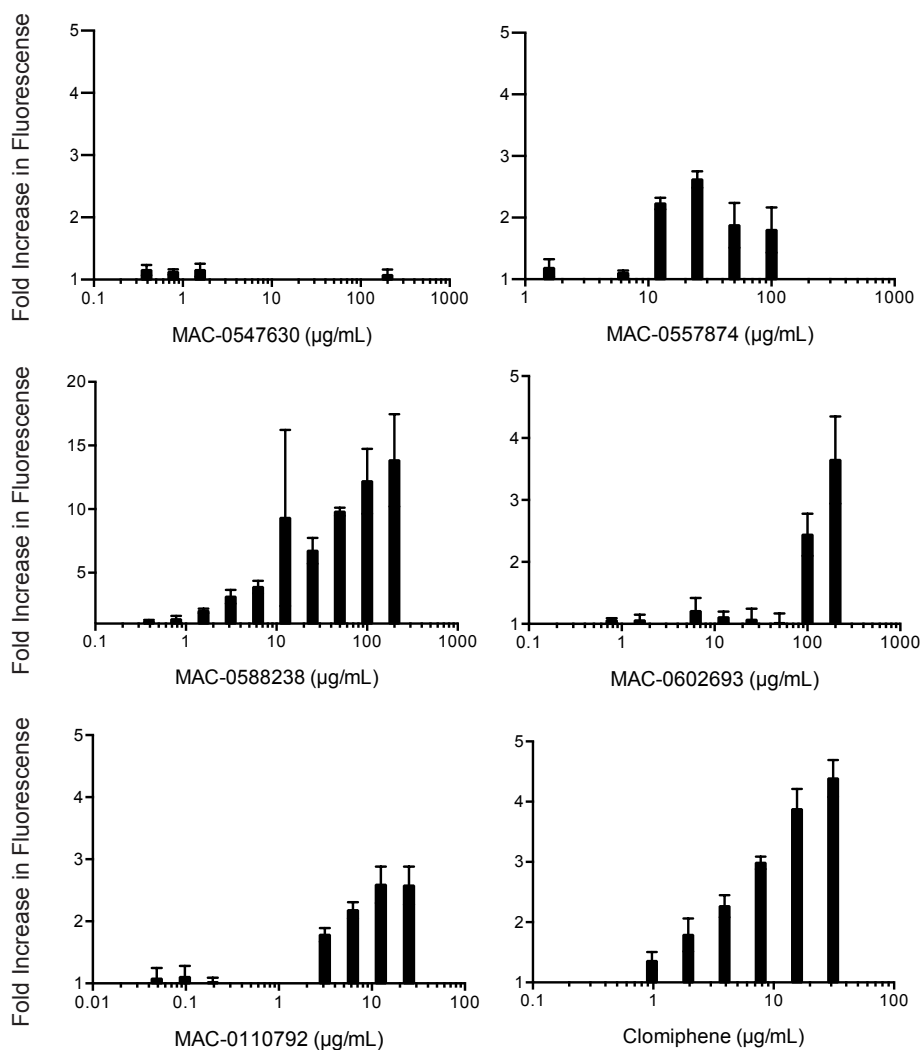


Figure 3-11: Assessment of the affects of UppS inhibitors on membrane potential. Each of the novel 5 characterized UppS inhibitors and clomiphene were assessed for dose dependent affects on membrane potential using the membrane-potential-sensitive cyanine dye DiSC₃(5). Data were normalized for background using solvent (DMSO) controls. Data are presented as a fold increase over the solvent control.

Evaluation of 5 novel UppS inhibitors as potential adjuvants of cefuroxime in CA-MRSA USA300

Previous work has demonstrated a strong interaction between β -lactam sensitization and inhibition of UppS (Farha et al., 2015; Lee et al., 2011). Thus inhibitors of UppS have strong potential as adjuvants of β -lactams in resistant pathogens. Using the micro broth dilution checkerboard method, the ability of the 5 UppS inhibitors to potentiate cefuroxime against MRSA (USA-300) was assessed. Of the 5 inhibitors tested MAC-0547630 and MAC-0588238 showed the strongest synergistic profiles when combined with cefuroxime (Figure 3-12), effectively reducing the MIC of cefuroxime in the previously resistant strain.

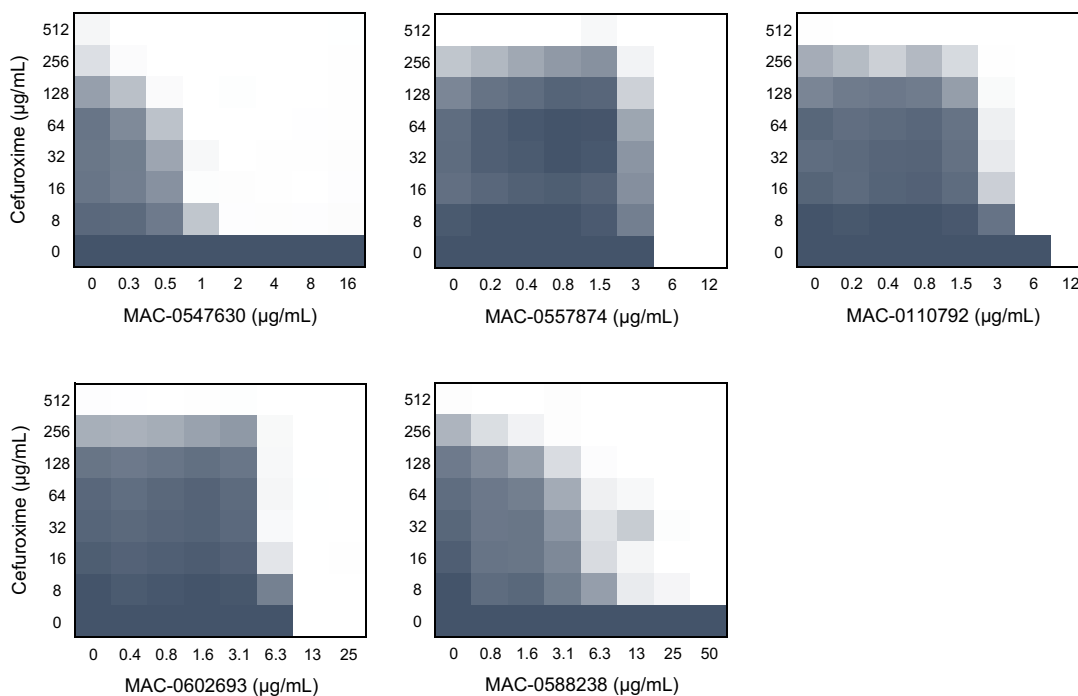


Figure 3-12. Interaction of 5 novel UppS inhibitors with cefuroxime in in methicillin resistant *S. aureus* (MRSA). Microdilution checkerboard analysis of the 5 characterized inhibitors of UppS using cefuroxime in CA-MRSA USA300.

DISCUSSION

UppS inactivation shows great promise as a route for new antibacterial drug discovery due to its conserved and indispensable role in the early steps of cell wall synthesis (Guo et al., 2007). To date, discovery campaigns for inhibitors of UppS have largely been limited to *in silico* approaches due to a lack of feasible high throughput methods (Durrant et al., 2011; Kuo et al., 2008; Sinko et al., 2014; Zhu et al., 2013). Though efforts have resulted in various interesting leads including bisphosphonates, tetramic acids, and metal chelators, none have been validated as potential antibiotics due to either unfavorable pharmacokinetics and or off-target toxicity (Athanasellis et al., 2010). In the work presented here, a streamlined approach has been developed for the discovery of whole cell active inhibitors of UppS, by exploiting complex gene dispensability found within the WTA biosynthetic pathway. Such phenotypic screening methods are key to increasing our arsenal of whole cell active and drug like inhibitors of UppS.

A focused, *B. subtilis* 168 active, chemical collection was collated by whole-cell growth inhibition screening of 142,000 small molecules. *B. subtilis* 168 was chosen for its amenability to high-throughput screening and its unique sensitivity to early step WTA inhibition. Such efforts led to a cherry-picked collection of 3,705 small molecules. To enrich for inhibitors of early step, and substrate producing WTA enzymes; a powerful targocil antagonistic screen was performed in *S. aureus*, followed by stringent potency analysis. The result was a collection

of 35 priority antagonists believed to be highly enriched for inhibitors targeting enzymes of interest. MAC-0547630 was selected for further study due to its exquisite potency. A spontaneous mutant in *B. subtilis* 168 to MAC-0547630 was generated and characterized using next generation whole genome sequencing. Such efforts resulted in the discovery of a SNP in *uppS*. Upon screening of the 35 priority antagonists in a UppS coupled *in vitro* pyrophosphate release assay, we identified that 6 of the 35 priority antagonists demonstrated UppS inhibition including MAC-0547630. Of the 6 inhibitors, 5 were available for resupply and were explored further. Such an enrichment strategy provides a concrete way forward in the discovery of new leads targeting UppS.

Since UppS is well conserved amongst bacterial species, we assessed whole cell activity of these inhibitors against *B. subtilis* 168, *S. aureus*, and *E. coli*. Interestingly the most potent inhibitors of *B. subtilis* 168, MAC-0547630 and MAC-0588238 with MIC values of 0.1 and 1.5 µg/mL respectively, had only modest growth inhibitory effects against *S. aureus*. None of the 5 inhibitors showed any growth inhibition against *E. coli*. To determine whether the differences in activity were due to varying whole cell permeability or target specificity, dose dependent *in vitro* activity of the 5 inhibitors was assessed against recombinant UppS from *B. subtilis* 168, *E. coli* and *S. aureus*. Activity of the 5 inhibitors varied greatly against UppS purified from the three organisms. Such variation and species selectivity has been previously demonstrated (Kuo et

al., 2008). Indeed, MAC-0547630 and MAC-0588238 that showed the strongest activity against UppS^{BS} (IC₅₀ values of 50 nM and 1.3 μM respectively) were only able to inhibit staphylococcal UppS^{SA} by 50 %. Such results correlate well with whole cell inhibition. As species selective antibiotics are gaining traction, inhibition of UppS could be a way forward.

UppS is a dimer of an identical subunit containing 260, 256, and 252 amino acids in *B. subtilis*, *S. aureus* and *E. coli* respectively. UppS^{BS}, UppS^{SA}, UppS^{EC} share modest sequence identity -- between 39 and 53 %. Previous structural studies uncovered that the active site of UppS resembles an elongated 'tunnel-shaped' conformation formed by β-strands and α-helix 2 and 3 (Guo et al., 2005; Liang et al., 2002). Previous work suggests that FPP and IPP are located at the top of the tunnel and the prenyl moiety is orientated toward the bottom of the tunnel, during consecutive condensations of IPP. To determine how the inhibitors interact with UppS, spontaneous mutants were generated at high concentrations of each inhibitor. Successful mutants were only obtained for MAC-0547630 and MAC-0588238. Previous studies searching for inhibitors of UppS via *in silico* screening reveal 4 inhibitor binding sites within UppS. Sites 1,2 and 3 are situated at the top of the catalytic tunnel and site 4 is located at the bottom (Zhu et al., 2013). Interestingly exposure to high concentrations of both MAC-0547630 and MAC-0588238 result in mutations overlapping with site 3; which interfaces with α-helix 3 and 4. A single mutant (Thr₁₄₅Lys) generated in the presence of

MAC-0588238 is proximal to binding site 4 (bottom of the tunnel) and as such may point to the orientation of MAC-0588238 within the UppS active site.

Inhibitors overlapping with binding site 3 are intriguing as their presence may not only sterically interfere with substrates and or product intermediates, but may also interfere with the movement of α -helix 3 during changes conformational states important for product release (Liang et al., 2002). Cross resistance studies of the spontaneous mutants, to all 5 inhibitors and the previously characterized clomiphene, revealed cross resistance only between MAC-0547630 and MAC-0588238.

Recent work by Feng X., *et al*, demonstrated that due to the hydrophobic nature of UppS inhibitors they are prone to affecting membrane potential in bacteria as a secondary target (Feng et al., 2015). Intriguingly of the 5 inhibitors tested, all affected membrane potential at some level, except for MAC-0547630. This finding reveals that MAC-0547630 is one of the few truly selective UppS inhibitors. Indeed, the levels of membrane depolarization exhibited by the remaining inhibitors may underlie why it was not possible to generate stable spontaneous mutants and additionally why cross resistance was only seen between MAC-0547630 and MAC-0588238. Since MAC-0547630 is a promising lead compound with selective inhibition of UppS, the activity of 13 analogs was investigated, to gain insight into SAR, and to determine if it is possible to broaden

species specificity. Unfortunately none of the analogs were as potent as MAC-0547630 (Supplemental Table 1).

With antibacterial resistance on the rise, adjuvants of previously established antibiotics are gaining traction as a way forward in the treatment of infections (Cottarel and Wierzbowski, 2007). Due to the involvement of UppS in the earliest stages of cell wall synthesis, inhibitors of UppS are strong candidates as adjuvants of late acting cell wall antibiotics, such as β -lactams (Farha et al., 2015; Zhu et al., 2013). Inhibition of UppS leads to lower pools of undecaprenyl phosphate, which results in lower levels of the peptidoglycan intermediate Lipid II. With lipid II being the substrate of PBPs, the targets of β -lactams, co-administration of UppS inhibitors and β -lactams has efficacious clinical potential. Indeed, all 5 inhibitors showed some synergistic phenotypes when combined with cefuroxime against MRSA.

Summation of the work presented here outlines a novel high-throughput method for the enrichment and discovery of whole cell active inhibitors of UppS by combining whole cell, phenotypic and *in vitro* screening techniques. Such a workflow is a powerful way forward for the discovery of novel UppS inhibitors. This approach led to the successful discovery and characterization of 5 inhibitors of UppS; of which MAC-0547630 has proven to be a uniquely selective. With no

observable effects on membrane depolarization this molecule has potential as a powerful probe of bacterial systems.

METHODS

Growth inhibition screen of *B. subtilis* 168

Screening for *B. subtilis* 168 growth inhibition was performed in 96-well microtiter plates (Catalog no. 3370, Corning) in duplicate using a standalone BiomekFX liquid handler (Beckman Coulter, Brea CA). The evening before screening a single colony of *B. subtilis* 168 (EB6) was grown in 5 mL of Luria-Bertani (LB) broth. On the day of screening a 1/100 subculture of the overnight was grown to an OD₆₀₀ of ~ 0.35 in LB broth. Cells were then diluted into fresh LB broth to a final OD₆₀₀ of 0.001. To each well 2 µL of the 142,000 compound small molecule library (1 mM dissolved in 100 % DMSO) was systematically dispensed in duplicate on separate plates. The BiomekFX liquid handler was then used to dispense 198 µL of culture (*B. subtilis* 168 OD₆₀₀ 0.001) into each well containing compound giving a final screening concentration of 10 µM. Outer columns were used for controls where in lieu of the library; 1 % DMSO and 10 µM Penicillin-G were used as high and low controls respectively. Upon completion a pre-incubation read of optical density at 600 nm was taken using an EnVision plate reader (Perkin Elmer). Plates were then incubated at 30 °C in HiGrow microtiter plate shaking incubator (DigiLab, Marlborough MA) at 550 rpm for 8 hours. A post read was taken at OD₆₀₀, again using an EnVision plate reader (Perkin Elmer).

Data obtained was analyzed by first by subtracting the pre-read from the post-read data for each well as a way of background subtraction. The background subtracted data was then normalized to take into account both plate and well positional effects as previously described (“Rank Ordering Plate Data Facilitates Data Visualization and Normalization in High-Throughput Screening.,” 2014). A statistical cut-off of 70 % (2 standard deviations below the mean of the data set) was established.

Screening for antagonism of targocil

Screening for antagonism of targocil was performed in 384-well microtiter plates (catalogue no. 3701, Corning) using a *S. aureus* Newman background in duplicate. All dispensing into microtiter plates was performed using a BiomekFX liquid handler (Beckman Coulter, Brea CA). The evening before screening a single colony of *S. aureus* Newman (EBII-61) was picked and grown overnight in cation adjusted Muller Hinton Broth (MHB) at 37 °C and 250 rpm. The morning of screening a 1/100 sub-culture was made of the overnight in MHB and grown under the same conditions to an OD₆₀₀ ~ 0.35. Cells were then diluted into fresh media to a final OD₆₀₀ of 0.001. The BiomekFX liquid handler was used to dispense 1 µL of targocil (0.8 mg/mL 100 % DMSO) into dry plates followed by the systematic addition of 1 µL of the 3,705 *B. subtilis* 168 active compounds (1 mM, 100% DMSO). The liquid handler was then subsequently used to dispense 48 µL of culture (*S. aureus* Newman OD₆₀₀ of 0.001) for a final screening

concentration of 20 μM of the *B. subtilis* 168 actives subset and 16 $\mu\text{g}/\text{mL}$ targocil. In lieu of targocil and *B. subtilis* 168 active compound the two outermost columns were used for high and low growth controls. Erythromycin at 16 $\mu\text{g}/\text{mL}$ was used as a low control and 4 % DMSO was used as a high (growth) control. Screening plates were grown at 37 °C shaking at 250 rpm for 12 hours. Absorbance was read at 600 nm using an EnVision plate reader (Perkin Elmer).

Data was normalized as a percentage of rescue for each well using the following: $(\text{Sample OD}_{600} - \text{IQ mean}) / (\text{mean high control} - \text{IQ mean}) * 100$; where IQ mean is the mean of the middle 50 % of the ordered raw data on the corresponding plate (“Rank Ordering Plate Data Facilitates Data Visualization and Normalization in High-Throughput Screening.,” 2014). Zero % represents no rescue and 100 % represents full rescue of targocil’s antibacterial activity.

Potency analysis on solid-media

Potency analysis of the 181 targocil antagonists against *B. subtilis* 168 was systematically performed on solid LB media at a single concentration of 125 μM . To generate plugs containing each compound 25 mL of 2 % agarose was poured into dry uni-well PlusPlates (Singer Instruments, UK). After allowing to solidify 12 circular plugs were removed per plate with a diameter of 1.5 cm leaving 12 wells for LB agar plugs containing compound. LB agar (1.5 %) containing each small molecule at 125 μM was then added into each well. Once solidified the 2 %

agarose cast was removed leaving 12 LB agar plugs containing small molecules on each plate. Plates were pinned with *B. subtilis* 168 using a Singer Rotor Instrument (Singer Instruments, UK) at 6,144 density. Once pinned plates were incubated for 16 hours overnight at 30 °C and growth inhibition was visually assessed for each agar plug. Compounds found in plugs which showed no colony formation were deemed growth inhibitory and priority antagonists. (French, *et al.* In Press - Molecular Biology of the Cell).

Cloning, Overexpression and Purification of UPPS^{BS}, UPPS^{SA}, and UPPS^{EC}

The gene *uppS* was cloned into a pET-19b vector (Novagene) modified to encode an engineered Tobacco Etch Virus (TEV) protease cleavage site. The *uppS* gene from *B. subtilis* 168 was generated using the primers below whereas *uppS* from *S. aureus* and *E. coli* was cloned using the gBlocks (Integrated DNA Technologies, Iowa, USA) listed below. UPPS cloned from each of the three bacterial strains was over-expressed in *E. coli* BL21 (Rosetta) using auto-induction (Studier, 2005). Cells were harvested by centrifugation at 6000 x g for 25 min at 4 °C. Cells were resuspended in buffer containing 50 mM NaH₂PO₄ (pH 8.0), 300 mM NaCl, 10 mM imidazole, 250 KU Lysozyme (Novagen) and an EDTA-free protease inhibitor tablet (Roche Diagnostics). Lysis of cell was performed using a cell disrupter (Constant Systems Limited, Daventry, UK). Lysates were cleared by centrifugation t 30,0000 × g for 35 minutes at 4 °C. UPPS was purified from lysate using a 30 mL free-flow gravity column and 5 mL

on Ni-NTA agarose (Sigma). Once loaded the column was washed with 10x volume 50 mM NaH₂PO₄ (PH 8.0), 300 mM NaCl, 20 mM imidazole. His-tagged UPPS was then eluted in buffer containing 50 mM NaH₂PO₄ (PH 8.0), 300 mM NaCl, 250 mM imidazole. Eluted fractions were subsequently dialyzed over night against 20 mM Tris · HCl (pH 8.0), 300 mM NaCl, and 1 mM DTT. Upon completion of dialysis eluted fractions were concentrated using Amicon Ultra centrifugation filters (10kDa cut-off) and quantified using a NanoDrop (Thermo Scientific).

Primers for *uppS*^{BS} construct (GeneBank sequence NC_000964.3)

uppS^{BS}-fwd: CTAGCATATG CTCAACATACTCAAAAATTG
uppS^{BS}-rev: CTAGCTACGAG CTAATTCCGCCAAA.

gBlock for *uppS*^{SA} construct (GeneBank sequence AP009351.1)

```
TGGCCACGTGGCCTATGCGCATATGTTTAAAAAGCTAATAAATAAAAAGAACACTATAAATAA
TTATAATGAAGAATTAGACTCGTCTAATATACCTGAACATATCGCTATTATTATGGATGGTAAT
GGGCGATGGGCTAAGAAGCGAAAAATGCCTAGAATTAAGGTCATTACGAAGGTATGCAAA
CAATAAAAAAATTACTAGGGTAGCTAGTGATATTGGTGTAAAGTACTTAACTTTATACGCCTT
TTCCACTGAAAATTGGTCAAGACCTGAAAGTGAAGTAAATTATATTATGAATTTGCCTGTCAAT
TTCTTAAAGACATTCTTACCGGAACCTAATTGAAAAAATGTCAAAGTTGAAACAATTGGATTTA
CTGATAAGTTGCCAAAATCAACGATAGAAGCAATTAATAATGCTAAAGAAAAGACAGCTAATA
ATACCGGCTTAAAATTAATATTTGCAATTAATTATGGTGGCAGAGCAGAAGTGTTCATAGTAT
TAAAAATATGTTTGACGAGCTTCATCAACAAGGTTTAAATAGTGATATCATAGATGAAACATAT
ATAACAATCATTTAATGACAAAAGACTATCCTGATCCAGAGTTGTTAATTCGTAATTCAGGA
GAACAAAGAATAAGTAATTTCTTGATTTGGCAAGTTTCGTATAGTGAATTTATCTTTAATCAAA
AATTATGGCCTGACTTTGACGAAGATGAATTAATTAATGTATAAAAAATTTATCAGTCACGTCA
AAGACGCTTTGGCGGATTGAGTGAGGAGTAGCTCGAGCTGGTCC
```

gBlock for *uppS*^{EC} construct (GeneBank sequence CP012868.1)

```
CTAGTAGCATATGATGTTGTCTGCTACTCAACCACTTAGCGAAAAATTGCCAGCGCATGGCT
GCCGTCATGTTGCGATCATTATGGACGGCAATGGCCGCTGGGCAAAAAGCAAGGGAAGAT
TCGTGCCTTTGGGCATAAAGCCGGGGCAAAATCCGTCCGCCGGGCTGTCTTTTTGCGGCC
AACACGGTATTGAGGCGTTAACGCTGTATGCCTTTAGTAGTAAAACTGGAACCGACCAGC
```

```
GCAGGAAGTCAGTGCCTAATGGAAGTGTGGTGGGCGCTCGATAGCGAAGTAAAAAGT
CTGCACCGACATAACGTGCGTCTGCGTATTATTGGCGATACCAGTCGCTTTAACTCGCGTTT
GCAAGAACGTATTCGTAAATCTGAAGCGCTAACAGCCGGGAATACCGGTCTGACGCTGAAT
ATTGCGGGCGAACTACGGTGGACGTTGGGATATAGTCCAGGGAGTCAGGCAACTGGCTGAAA
AGGTGCAGCAAGGAAACCTGCAACCAGATCAGATAGATGAAGAGATGCTAAACCAGCATGT
CTGTATGCATGAACTGGCCCTGTAGATTTAGTAATTAGGACTGGGGGGGAGCATCGCATT
GTAACTTTTTGCTTTGGCAAATTGCCTATGCCGAACCTTTACTTTACAGATGTTCTCTGGCCCG
ATTTTCGATGAACAAGACTTTGAAGGGGCGTTAAATGCCTTTGCTAATCGAGAGCGTCGTTTC
GGCGGCACCGAGCCCGGTGATGAAACAGCCTGACTCGAGCTAGTAG
```

Primers used for Sequencing *uppS* Mutants:

Sanger sequencing was performed of mutant UppS PCR products using the following primers.

Upstream-*uppS*-Fwd: AAAGACAAAGAAAAAGAAAT

Internal-*uppS*-Fwd: ATGCATTTTCAACAGAA

Internal-*uppS*-Rev: GTACATTTTCTCAACAAG

Downstream-*uppS*-Rev: CCCATAGCATAAATTAATAT

Screen for *in vitro* UppS inhibition

The screen for *in vitro* UppS inhibition was conducted in 96-well microtiter plates (Catalog no. 3370, Corning) using a kinetic EnzCheck pyrophosphate release assay (Life Technologies). 1 μ L of each priority antagonist was systematically added to dry plates (5 mM 100 % DMSO) with subsequent addition of 89 μ L of master mix. Final concentrations of master mix components in each reaction were as follows: 0.2 mM 2-amino-6-mercapto-7-methyl-purine ribonucleoside (MESG), 0.625 U of purine ribonucleoside phosphorylase (PNP), 0.2 U of

inorganic pyrophosphatase (PyroP), 0.125 µg of purified UppS^{BS} enzyme.

Reactions were allowed to pre-incubate for 20 minutes shaking at 25 °C. Upon completion of the pre-incubation reactions were initiated with 10 µL of UppS substrates. The final substrate concentrations for each reaction were 0.82 µM farnesyl pyrophosphate (FPP) (1xKM) and 65 µM isopentenyl pyrophosphate (IPP) (5xKM). High and low controls containing 1 % DMSO with and without substrate were used to normalize the data. 0 % activity represents full inactivation of the enzyme and 100 % activity represents no inhibition. See supplemental methods for overexpression and purification of UppS^{BS}.

Dose assessment of *in vitro* UppS activity

Dose assessment of inhibition against UppS expressed from three organisms (*B. subtilis* 168, *E. coli*, and *S. aureus*) was performed in accordance with methods found in the section above (Screen for *in vitro* UppS inhibition). Details on purification and assessment of KM parameters for each overexpressed enzyme can be found in supplemental methods. Substrate concentrations of 1xKM and 5xKM were used for FPP and IPP respectively (Supplementary Figure 1). Data was fitted using GraFit V5 (Erithacus Software) using a 4 parameter fit.

Determination of minimal inhibitory concentrations (MIC)

The minimal inhibitory concentration (MIC) defines the lowest concentration of a compound required to inhibit growth of a particular strain by more than 90 %. For all strains assessed, a single colony was picked and grown overnight in 5 mL of rich LB (*B. subtilis* 168/ *E. coli*) or MHB (*S. aureus*) media at 30 °C (*B. subtilis* 168) or 37 °C (*E. coli*/ *S. aureus*) shaking at 250 rpm. The overnight culture was subsequently diluted 100-fold into fresh rich media and grown under the same conditions to an OD₆₀₀ of ~ 0.35. Cells were then diluted to a final OD₆₀₀ of 0.001 in the same media and used to assess inhibition. The MICs were determined in 96-well microtiter plates (catalogue no. 3370, Corning) by adding 2 µL of inhibitor dissolved in 100 % DMSO to 198 µL culture. Inhibitors were then serially diluted in media in half-fold increments. Final volume for all wells was 100 µL. Plates were incubated at appropriate temperatures depicted above for 16 hours using Multitron microtiter shakers at 600 rpm (Infors HT, Switzerland). Upon incubation OD₆₀₀ was measured as a final readout using a Spectra-max Plus instrument (Molecular Devices).

DISC₃(5) membrane permeability assay

Cytoplasmic membrane permeabilization was determined by using the membrane-potential-sensitive cyanine dye DiSC₃(5) (Sims et al., 1974). Strain EB6 was grown at 30 °C with shaking to mid-logarithmic phase (OD₆₀₀ = 0.5 - 0.6). Cells were harvested by centrifugation at 4,000 rpm, and washed twice and

resuspended in buffer containing: Potassium Phosphate Monobasic (10mM), MgSO₄ (5mM), and Sucrose (250mM), to an OD₆₀₀ of 0.085. A 195 µL cell suspension was placed in each well of a black 96-well microtitre plate (Corning). The cell suspension was incubated with 0.2 µM DiSC₃(5) for 10 minutes to allow for uptake. The desired concentration of test compound (5µL volume) was subsequently added and the fluorescence reading was monitored using a Synergy HT multi-mode microplate reader (Biotek) at an excitation wavelength of 622 nm and an emission wavelength of 670 nm. DMSO controls were used as a background control and to normalize the dose dependent data.

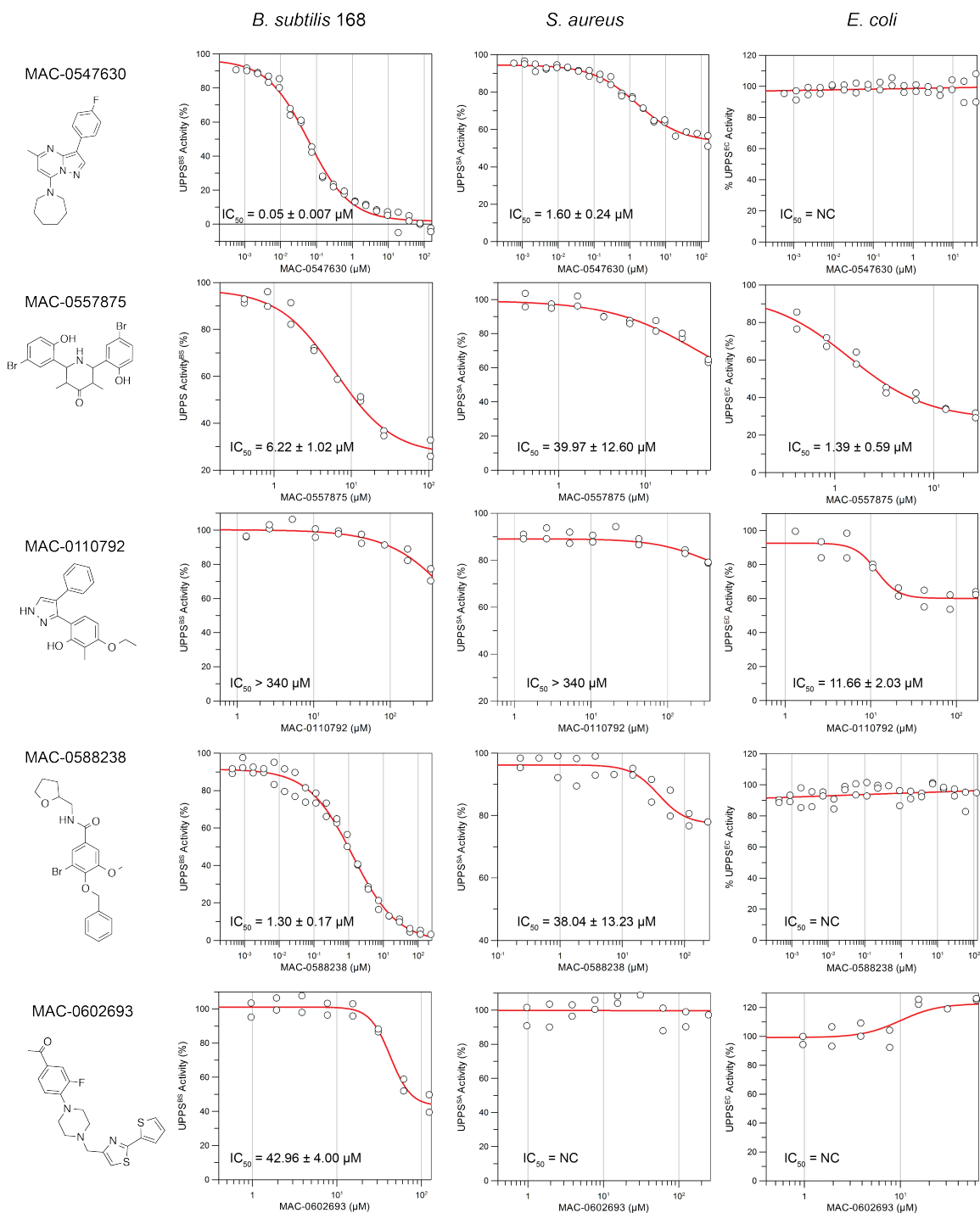
Isolation of spontaneously resistant mutants.

Mutants were generated by plating *B. subtilis* 168 (6×10^7 CFU) onto LB agar containing inhibitors at 4x and 8x above their MIC. Plates were incubated for 72 hours at 30 °C. Upon incubation visible colonies were picked from each plate and MICs were determined as described above to the respective compound. Mutants which showed greater than a 4-fold shift in MIC above WT *B. subtilis* 168 were characterized. Genomic DNA preps of resistant mutants were performed using Purgene Yeast/Bact. Kit (Catalogue No. 158567, Qiagen). PCR amplification of UPPS was subsequently performed (see supplemental methods for details) and sent for targeted (Sanger) sequencing (MOBIX Lab, McMaster University Canada). Sequencing results were analyzed and compared to the WT *B. subtilis* 168 sequence using Geneious R7 (Biomatters Limited, New Zealand).

Checkerboard Analysis

Interactions between inhibitors and Cefuroxime was established using a standard checkerboard broth dilution assay in 96-well microtiter plates (Catalog no. 3370, Corning). Colonies of *S. aureus* CA-MRSA USA300 were picked from a plate and suspended in 0.8 % NaCl aqueous solution to an OD₆₀₀ of 0.1. Cells were subsequently diluted 1/200 into fresh MHB media. 100 µL of culture was subsequently added to plates containing specified concentrations of the two inhibitors resulting in overall DMSO content of 2 %. Plates were incubated for 18 hours at 37 °C in Multitron microtiter shakers at 600 rpm (Infors HT, Switzerland). Upon incubation OD₆₀₀ was measured as a final readout using a Spectra-max Plus instrument (Molecular Devices).

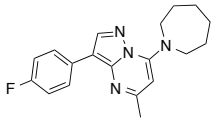
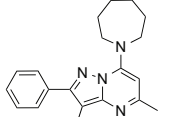
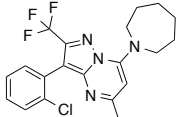
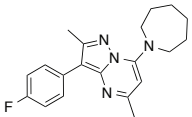
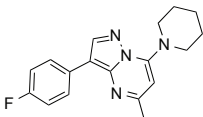
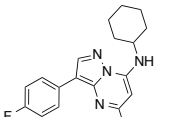
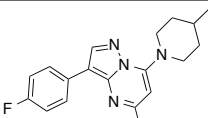
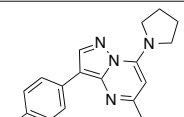
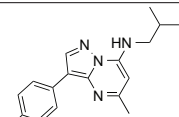
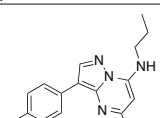
SUPPLEMENTAL DATA

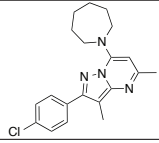
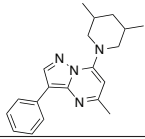
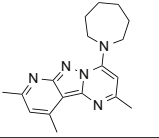
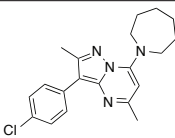


Supplemental Figure 3-2: Assessing *in vitro* inhibition of 5 novel inhibitors against UPPS isolated from *B. subtilis*, *S. aureus* and *E. coli*. Five novel UPPS inhibitors were evaluated in a dose dependent manner *in vitro* against UPPS cloned from *B. subtilis* 168 (UPPS^{BS}), *S. aureus*

(UPPS^{SA}), and *E. coli* (UPPS^{EC}). Activity is reported as a % of uninhibited activity and plotted as a function of inhibitor concentration. IC₅₀ values were determined using a 4-parameter fit GraFit (Erithacus Software, UK). Compounds which showed no activity against the tested enzyme were labeled as non-calculable (NC).

Supplemental Table 1: MIC determination of MAC-0547630 analogs against *B. subtilis* 168, *E. coli*, and *S. aureus*.

Structure	MAC-ID	<i>B. subtilis</i> 168 MIC (µg/mL)	<i>S. aureus</i> MIC (µg/mL)	<i>E. coli</i> MIC (µg/mL)
	MAC-0547630	0.10	> 100	--
	MAC-0547630.1	1.00	> 100	--
	MAC-0547630.2	--	--	--
	MAC-0547630.3	1.0	--	--
	MAC-0547630.4	0.5	--	--
	MAC-0547630.5	--	--	--
	MAC-0547630.6	> 100	> 100	> 100
	MAC-0547630.7	> 100	--	--
	MAC-0547630.8	--	--	--
	MAC-0547630.9	--	--	--

	MAC-0547630.10	--	--	--
	MAC-0547630.11	--	--	--
	MAC-0547630.12	32	>100	32
	MAC-0547630.13	16	--	--

REFERENCES

- Athanasellis, G., Igglessi-Markopoulou, O., Markopoulos, J., 2010. Tetramic and tetrionic acids as scaffolds in bioinorganic and bioorganic chemistry. *Bioinorg Chem Appl* 2010, 315056. doi:10.1155/2010/315056
- Atilano, M.L., Pereira, P.M., Yates, J., Reed, P., Veiga, H., Pinho, M.G., Filipe, S.R., 2010. Teichoic acids are temporal and spatial regulators of peptidoglycan cross-linking in *Staphylococcus aureus*. *Proc. Natl. Acad. Sci. U.S.A.* 107, 18991–18996. doi:10.1073/pnas.1004304107
- Bhavsar, A.P., Brown, E.D., 2006. Cell wall assembly in *Bacillus subtilis*: how spirals and spaces challenge paradigms. *Molecular Microbiology* 60, 1077–1090. doi:10.1111/j.1365-2958.2006.05169.x
- Brown, E.D., Wright, G.D., 2016. Antibacterial drug discovery in the resistance era. *Nature* 529, 336–343. doi:10.1038/nature17042
- Brown, E.D., Wright, G.D., 2005. New targets and screening approaches in antimicrobial drug discovery. *Chem. Rev.* 105, 759–774. doi:10.1021/cr030116o
- Bugg, T.D.H., Braddick, D., Dowson, C.G., Roper, D.I., 2011. Bacterial cell wall assembly: still an attractive antibacterial target. *Trends Biotechnol.* 29, 167–173. doi:10.1016/j.tibtech.2010.12.006
- Campbell, J., Singh, A.K., Santa Maria, J.P., Kim, Y., Brown, S., Swoboda, J.G., Mylonakis, E., Wilkinson, B.J., Walker, S., 2011. Synthetic lethal compound combinations reveal a fundamental connection between wall teichoic acid and peptidoglycan biosyntheses in *Staphylococcus aureus*. 6, 106–116. doi:10.1021/cb100269f
- Cottarel, G., Wierzbowski, J., 2007. Combination drugs, an emerging option for antibacterial therapy. *Trends Biotechnol.* 25, 547–555. doi:10.1016/j.tibtech.2007.09.004
- D'Elia, M.A., Millar, K.E., Beveridge, T.J., Brown, E.D., 2006a. Wall teichoic acid polymers are dispensable for cell viability in *Bacillus subtilis*. *J. Bacteriol.* 188, 8313–8316. doi:10.1128/JB.01336-06
- D'Elia, M.A., Pereira, M.P., Chung, Y.S., Zhao, W., Chau, A., Kenney, T.J., Sulavik, M.C., Black, T.A., Brown, E.D., 2006b. Lesions in teichoic acid biosynthesis in *Staphylococcus aureus* lead to a lethal gain of function in the otherwise dispensable pathway. 188, 4183–4189. doi:10.1128/JB.00197-06
- Durrant, J.D., Cao, R., Gorfe, A.A., Zhu, W., Li, J., Sankovsky, A., Oldfield, E., McCammon, J.A., 2011. Non-Bisphosphonate Inhibitors of Isoprenoid

Biosynthesis Identified via Computer-Aided Drug Design. *Chemical Biology & Drug Design* 78, 323–332. doi:10.1111/j.1747-0285.2011.01164.x

Falconer, S.B., Brown, E.D., 2009. New screens and targets in antibacterial drug discovery. *Current Opinion in Microbiology* 12, 497–504. doi:10.1016/j.mib.2009.07.001

Farha, M.A., Brown, E.D., 2015. Unconventional screening approaches for antibiotic discovery. *Ann. N. Y. Acad. Sci.* 1354, 54–66. doi:10.1111/nyas.12803

Farha, M.A., Czarny, T.L., Myers, C.L., Worrall, L.J., French, S., Conrady, D.G., Wang, Y., Oldfield, E., Strynadka, N.C.J., Brown, E.D., 2015. Antagonism screen for inhibitors of bacterial cell wall biogenesis uncovers an inhibitor of undecaprenyl diphosphate synthase. *Proc. Natl. Acad. Sci. U.S.A.* 201511751. doi:10.1073/pnas.1511751112

Farha, M.A., Leung, A., Sewell, E.W., D'Elia, M.A., Allison, S.E., Ejim, L., Pereira, P.M., Pinho, M.G., Wright, G.D., Brown, E.D., 2013a. Inhibition of WTA Synthesis Blocks the Cooperative Action of PBPs and Sensitizes MRSA to β -Lactams 8, 226–233. doi:10.1021/cb300413m

Farha, M.A., Verschoor, C.P., Bowdish, D., Brown, E.D., 2013b. Collapsing the proton motive force to identify synergistic combinations against *Staphylococcus aureus*. *Chem. Biol.* 20, 1168–1178. doi:10.1016/j.chembiol.2013.07.006

Feng, X., Zhu, W., Schurig-Briccio, L.A., Lindert, S., Shoen, C., Hitchings, R., Li, J., Wang, Y., Baig, N., Zhou, T., Kim, B.K., Crick, D.C., Cynamon, M., McCammon, J.A., Gennis, R.B., Oldfield, E., 2015. Antiinfectives targeting enzymes and the proton motive force. *Proc. Natl. Acad. Sci. U.S.A.* 112, E7073–E7082. doi:10.1073/pnas.1521988112

French, S., Mangat, C., Bharat, A., Côté, J.-P., Mori, H., Brown, E.D., 2016. A robust platform for chemical genomics in bacterial systems. *Mol. Biol. Cell mbc.* E15–08–0573. doi:10.1091/mbc.E15-08-0573

Guo, R.-T., Cao, R., Liang, P.-H., Ko, T.-P., Chang, T.-H., Hudock, M.P., Jeng, W.-Y., Chen, C.K.-M., Zhang, Y., Song, Y., Kuo, C.-J., Yin, F., Oldfield, E., Wang, A.H.-J., 2007. Bisphosphonates target multiple sites in both cis- and trans-prenyltransferases. *Proc. Natl. Acad. Sci. U.S.A.* 104, 10022–10027. doi:10.1073/pnas.0702254104

Guo, R.-T., Ko, T.-P., Chen, A.P.-C., Kuo, C.-J., Wang, A.H.-J., Liang, P.-H., 2005. Crystal structures of undecaprenyl pyrophosphate synthase in complex with magnesium, isopentenyl pyrophosphate, and farnesyl thiopyrophosphate: roles of the metal ion and conserved residues in catalysis. *J. Biol. Chem.* 280, 20762–20774. doi:10.1074/jbc.M502121200

- Holland, L.M., Conlon, B., O'Gara, J.P., 2011. Mutation of tagO reveals an essential role for wall teichoic acids in *Staphylococcus epidermidis* biofilm development. *Microbiology (Reading, Engl.)* 157, 408–418. doi:10.1099/mic.0.042234-0
- Kuo, C.-J., Guo, R.-T., Lu, I.-L., Liu, H.-G., Wu, S.-Y., Ko, T.-P., Wang, A.H.-J., Liang, P.-H., 2008. Structure-based inhibitors exhibit differential activities against *Helicobacter pylori* and *Escherichia coli* undecaprenyl pyrophosphate synthases. *J. Biomed. Biotechnol.* 2008, 841312–6. doi:10.1155/2008/841312
- Langmead, B., Trapnell, C., Pop, M., Salzberg, S.L., 2009. Ultrafast and memory-efficient alignment of short DNA sequences to the human genome. *Genome Biol* 10, R25. doi:10.1186/gb-2009-10-3-r25
- Lee, S.H., Jarantow, L.W., Wang, H., Sillaots, S., Cheng, H., Meredith, T.C., Thompson, J., Roemer, T., 2011. Antagonism of chemical genetic interaction networks resensitize MRSA to β -lactam antibiotics. *Chem. Biol.* 18, 1379–1389. doi:10.1016/j.chembiol.2011.08.015
- Liang, P.-H., Ko, T.-P., Wang, A.H.-J., 2002. Structure, mechanism and function of prenyltransferases. *Eur. J. Biochem.* 269, 3339–3354.
- Mangat, C.S., Bharat, A., Gehrke, S.S., Brown, E.D., 2014. Rank Ordering Plate Data Facilitates Data Visualization and Normalization in High-Throughput Screening. *J Biomol Screen* 1087057114534298. doi:10.1177/1087057114534298
- Ogura, K., Koyama, T., 1998. Enzymatic Aspects of Isoprenoid Chain Elongation. *Chem. Rev.* 98, 1263–1276. doi:10.1021/cr9600464
- Rank Ordering Plate Data Facilitates Data Visualization and Normalization in High-Throughput Screening, 2014. Rank Ordering Plate Data Facilitates Data Visualization and Normalization in High-Throughput Screening. 1087057114534298. doi:10.1177/1087057114534298
- Sewell, E.W., Brown, E.D., 2013. Taking aim at wall teichoic acid synthesis: new biology and new leads for antibiotics. *J. Antibiot.* doi:10.1038/ja.2013.100
- Sims, P.J., Waggoner, A.S., Wang, C.H., Hoffman, J.F., 1974. Studies on the mechanism by which cyanine dyes measure membrane potential in red blood cells and phosphatidylcholine vesicles. *Biochemistry* 13, 3315–3330.
- Sinko, W., Wang, Y., Zhu, W., Zhang, Y., Feixas, F., Cox, C.L., Mitchell, D.A., Oldfield, E., McCammon, J.A., 2014. Undecaprenyl diphosphate synthase inhibitors: antibacterial drug leads. *J. Med. Chem.* 57, 5693–5701. doi:10.1021/jm5004649

- Swoboda, J.G., Meredith, T.C., Campbell, J., Brown, S., Suzuki, T., Bollenbach, T., Malhowski, A.J., Kishony, R., Gilmore, M.S., Walker, S., 2009. Discovery of a small molecule that blocks wall teichoic acid biosynthesis in *Staphylococcus aureus*. 4, 875–883. doi:10.1021/cb900151k
- van Heijenoort, J., 2007. Lipid intermediates in the biosynthesis of bacterial peptidoglycan. *Microbiol. Mol. Biol. Rev.* 71, 620–635. doi:10.1128/MMBR.00016-07
- Wang, H., Gill, C.J., Lee, S.H., Mann, P., Zuck, P., Meredith, T.C., Murgolo, N., She, X., Kales, S., Liang, L., Liu, J., Wu, J., Santa Maria, J., Su, J., Pan, J., Hailey, J., McGuinness, D., Tan, C.M., Flattery, A., Walker, S., Black, T., Roemer, T., 2013. Discovery of wall teichoic acid inhibitors as potential anti-MRSA β -lactam combination agents. *Chem. Biol.* 20, 272–284. doi:10.1016/j.chembiol.2012.11.013
- Weidenmaier, C., Kokai-Kun, J.F., Kristian, S.A., Chanturiya, T., Kalbacher, H., Gross, M., Nicholson, G., Neumeister, B., Mond, J.J., Peschel, A., 2004. Role of teichoic acids in *Staphylococcus aureus* nasal colonization, a major risk factor in nosocomial infections. *Nature Medicine* 10, 243–245. doi:doi:10.1038/nm991
- Winstel, V., Kühner, P., Salomon, F., Larsen, J., Skov, R., Hoffmann, W., Peschel, A., Weidenmaier, C., 2015. Wall Teichoic Acid Glycosylation Governs *Staphylococcus aureus* Nasal Colonization. *MBio* 6, e00632. doi:10.1128/mBio.00632-15
- Zhu, W., Zhang, Y., Sinko, W., Hensler, M.E., Olson, J., Molohon, K.J., Lindert, S., Cao, R., Li, K., Wang, K., Wang, Y., Liu, Y.-L., Sankovsky, A., de Oliveira, C.A.F., Mitchell, D.A., Nizet, V., McCammon, J.A., Oldfield, E., 2013. Antibacterial drug leads targeting isoprenoid biosynthesis. *Proc. Natl. Acad. Sci. U.S.A.* 110, 123–128. doi:10.1073/pnas.1219899110

CHAPTER FOUR – Exploring the antagonism of bepridil with targocil.

PREFACE

The screen of 1,600 previous approved drugs for targocil antagonism was previously published in the following paper:

Farha, M.A., Czarny, T.L., Myers, C.L., Worrall, L.J., French, S., Conrady, D.G., Wang, Y., Oldfield, E., Strynadka, N.C.J, Brown, E.D. (2015). Antagonism screen for inhibitors of bacterial cell wall biogenesis uncovers an inhibitor of undecaprenyl diphosphate synthase. Proceedings of the National Academy of Science of the United States of America, September 2015 vol. 112 no. 35 11048-11053.

I performed all experiments presented in this chapter with the exception of:

- (1) Physical binding assay between Und-P - bepridil that was conducted by Robert Gale.
- (2) Imaging of prepared samples containing bepridil treated *B. subtilis* 168 were collected by Dr. Shawn French.

SUMMARY

As described in chapter 3, screening for targocil antagonists is a powerful method to enrich for inhibitors of UppS. Herein, we explore other potential targets in this screen through the study of bepridil. Bepridil is a previously approved calcium channel blocker, once used to treat angina, which demonstrates strong antagonistic interactions with targocil but does not inhibit UppS *in vitro*. We explore its mechanism using chemical-genetic approaches along with various phenotypic assays. Though the target of this compound remains unknown, the work presented here points strongly towards the lipid-linked steps of cell-wall synthesis.

INTRODUCTION

The complex gene dispensability phenotypes observed within the wall teichoic acid biosynthetic pathway have been well utilized for drug discovery. In addition to numerous screens for late stage inhibitors (Swoboda et al., 2009; Wang et al., 2013), it has now been demonstrated that this unique dispensability pattern can be harnessed to enrich for inhibitors of UppS (see chapter 3). With the mechanistic connection between UppS inhibition and antagonism of targocil mostly, if not solely, relying on undecaprenyl phosphate levels; it seems likely that blockages of other parts of cell wall biosynthesis that perturb Und-P pools, may too show interactions with targocil. To test this hypothesis, a focus was put on elucidating the mode of action (MOA) of bepridil -- a previously approved calcium channel blocker (Yatani et al., 1986). Bepridil is antagonistic with targocil but shows no inhibition of UppS.

Bepridil was selected for study from 1,600 previously approved drugs that were screened for antagonism with targocil in *S. aureus* (Farha et al., 2015). Of interest were antagonists that possessed antibacterial activity against *S. aureus*. Twelve such compounds, including bepridil were elucidated. Bepridil was chosen for further study due to its strong antagonistic profile with targocil and synergistic interactions with β -lactams; many techniques were employed including chemical genetic and phenotypic assays to explore its potential target.

RESULTS

A screen of 1,600 previously approved drugs for targocil antagonism coupled with *S. aureus* growth inhibition led to 12 priority active molecules

A screen for targocil antagonists was performed in *S. aureus* using a library of 1,600 previously approved drugs (MicroSource). The 1,600 molecules were systematically screened at 20 μM for antagonism at 8x the MIC of targocil (16 $\mu\text{g}/\text{mL}$) (see chapter 3 for screen optimization). Data were analyzed using the middle two quartiles of the data as a baseline and the high controls as a theoretical ceiling for rescue (Mangat et al., 2014). Compounds that restored growth by >5 % were classified as primary hits. Such a cut-off led to 68 primary hits (Figure 4-1A). Dose confirmation of targocil antagonism was subsequently performed on the 68 primary hits. Compounds that showed dose dependent rescue of targocil at 8x the MIC were deemed confirmed actives; 62 compounds showed such profiles. Dose dependent growth inhibition studies were performed on the 62 confirmed actives in *S. aureus*, which allowed for prioritization of compounds that inhibit essential cellular targets. Overall, 12 priority actives were identified, one of which was bepridil.

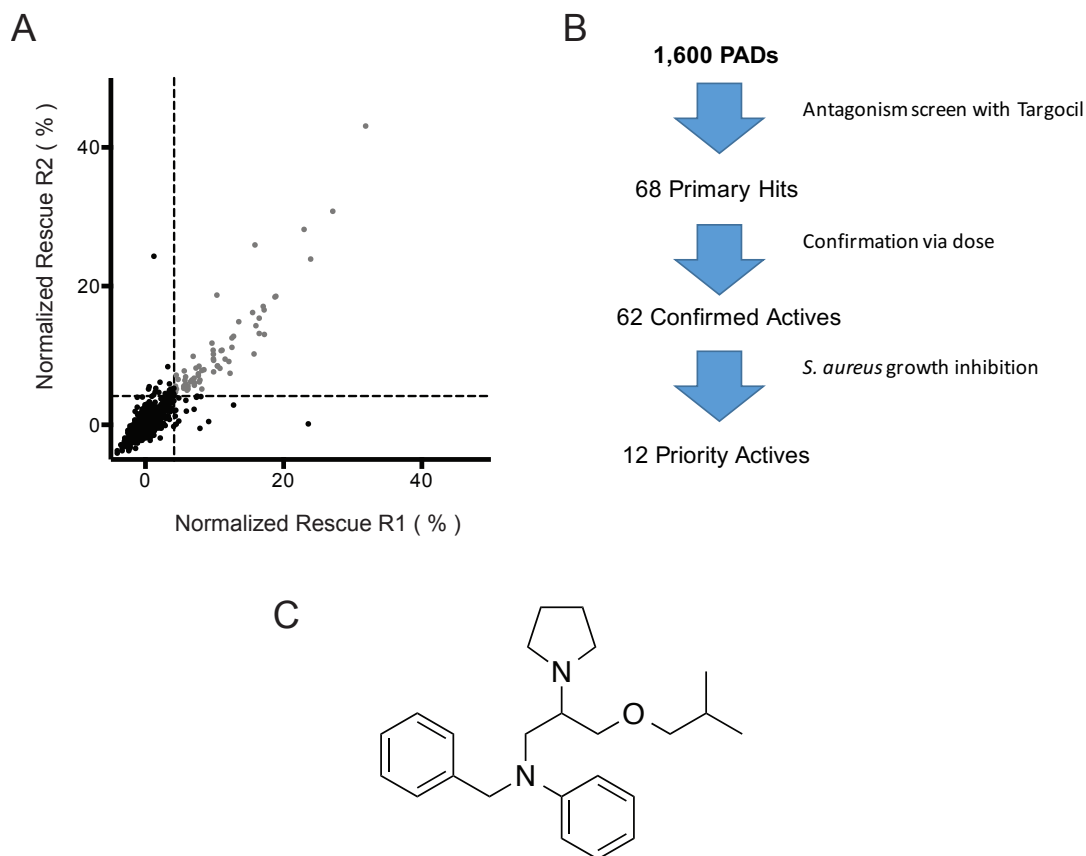


Figure 4-1: Screen for targocil antagonists and growth inhibition led to the study of bepridil. (A) 1,600 previously approved drugs (PADs) were systematically screened for antagonism with targocil at 8x its MIC in *S. aureus*. Normalized rescue for replicate 1 and 2 is plotted on the x and y axis respectively. PADs that produced a rescue value >5 % were deemed primary hits. **(B)** The workflow started with 1,600 PADs screened for antagonism, which resulted in 68 primary hits that were confirmed in dose, resulting in 62 confirmed actives. As targets of interest were essential in nature, a counter screen for growth inhibition against *S. aureus* was conducted resulting in the shortlisting of 12 priority actives. **(C)** Chemical structure of bepridil (one of the 12 priority actives chosen for study).

Bepridil shows strong antagonistic and synergistic interactions with targocil and β -lactams respectively

To comprehensively assess the interaction between bepridil and targocil, a standard micro-broth dilution checkerboard assay was performed. As anticipated, bepridil antagonised the activity of targocil (Figure 4-2A). Previous work in our lab and others has demonstrated that the inhibition of undecaprenyl phosphate synthesis and early steps in WTA synthesis could be synergistic with the action of β -lactam antibiotics against MRSA. Thus a micro-broth dilution checkerboard assay was used to assess the interaction between bepridil and cefuroxime, and established that bepridil was synergistic with β -lactams in MRSA (Figure 4-2B).

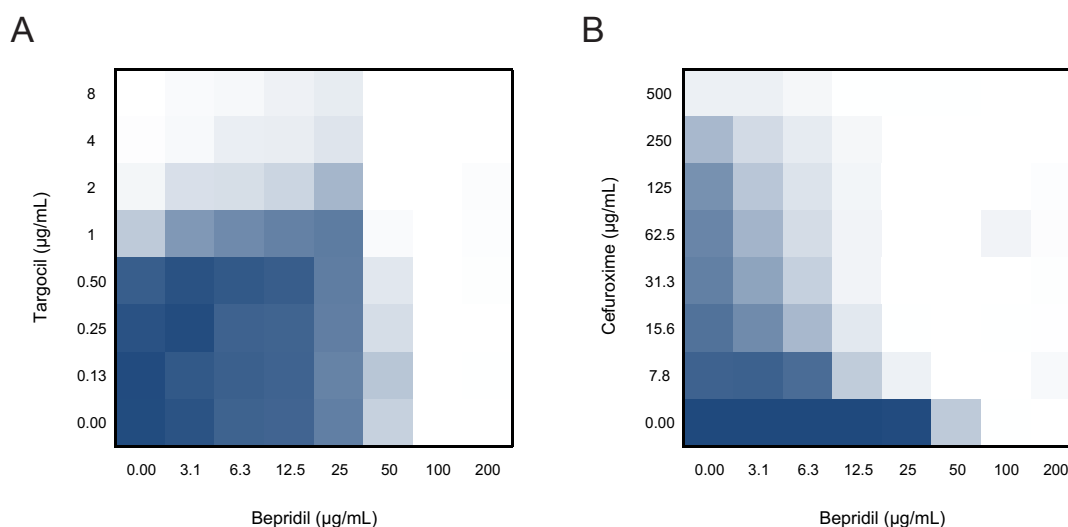


Figure 4-2: Assessment of bepridil's interaction with targocil and cefuroxime in *S. aureus* CA-MRSA USA300. (A) Using a standard broth dilution checkerboard the antagonistic interaction between bepridil (x-axis) and targocil (y-axis) was assessed. **(B)** Using a standard broth dilution checkerboard the synergistic interaction between bepridil (x-axis) and cefuroxime (y-axis) was assessed. For both **(A)** and **(B)** growth is represented by a blue gradient. Dark blue represents growth and white represents no growth.

Bepridil has no activity on UppS *in vitro*

To test whether bepridil was an inhibitor of UppS, the compound was subjected to a dose dependent *in vitro* evaluation against recombinant UppS from *B. subtilis* 168. Using the EnzCheck pyrophosphate release assay (Invitrogen) described in chapter 2 & 3, UppS activity was assessed by monitoring MESG degradation at 360 nm. No effects on UppS activity were observed at any of the concentrations tested (Figure 4-3).

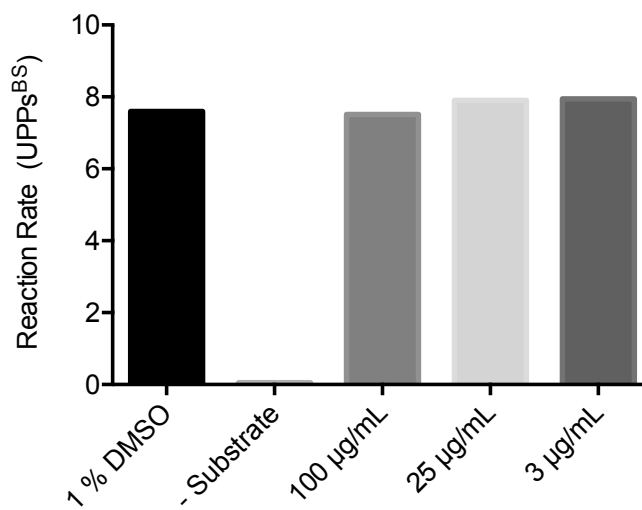


Figure 4-3: Bepridil does not inhibit UppS^{BS} activity *in vitro*. Bepridil was tested for *in vitro* activity against UppS^{BS} using the EnzCheck pyrophosphate release assay. Breakdown of MESG was monitored kinetically by measurement of absorbance at 360 nm. Reaction rates are plotted on the y-axis for: 1 % (v/v) DMSO (high control), - substrate (low control), Bepridil at 100, 25 and 3 µg/mL.

Sensitization of *B. subtilis* 168 CRISPRi essential knockdown library to the presence of bepridil at sub-MIC

To generate hypotheses regarding the target of bepridil, a library of precise essential gene knock-downs generated using the CRISPRi method in *B. subtilis* 168 was employed. Such a library can be used to screen for colonies sensitized to the exposure of bepridil at sub-MIC concentrations (see chapter 2 for details regarding the CRISPRi library). To determine appropriate screening conditions, the activity of bepridil against WT *B. subtilis* was first assessed on solid media using an automated colony pinning device (Singer Rotor) to inoculate colonies as previously described (French et al., 2016). An MIC of 100 µg/mL was determined for these growth conditions (Figure 4-4A).

Subsequent sensitization screens were performed at 1/2, 1/4, and 1/8th the MIC. The CRISPRi library was pinned in quadruplicate onto LB agar containing bepridil at a density of 1,536 colonies per plate (Figure 4-4B). Following incubation, these plates were scanned and analyzed using computer software to determine colony volume (integrated density) (French et al., 2016). Bepridil screened at 1/4 its MIC (25 µg/mL) gave the greatest resolution in the experiment. Upon analysis, gene knockdowns of *ftsZ* and *ftsA* show clear sensitization (Figure 4-4C).

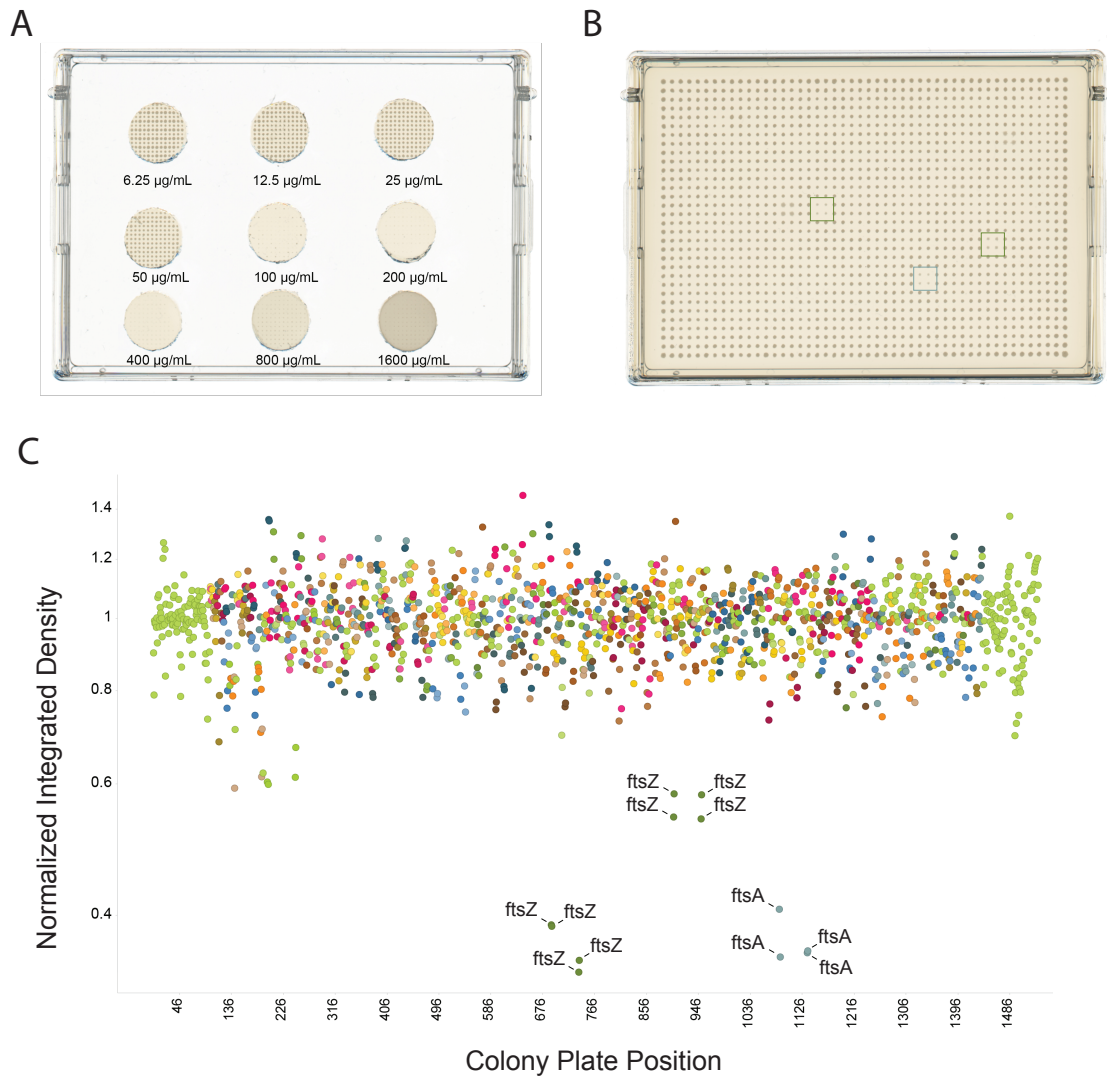


Figure 4-4: Sensitization of *B. subtilis* 168 CRISPRi knockdowns to bepridil. (A) The solid MIC of bepridil was determined by pinning WT *B. subtilis* 168 using a Singer Rotor at 6,144 density onto LB agar plugs containing bepridil at various concentrations. **(B)** CRISPRi *B. subtilis* 168 essential knockdown collection was pinned onto bepridil at 25 µg/mL in quadruplicate (1,536 density). Green boxes highlight colonies with knockdowns in *ftsZ* while the grey box highlights a knockdown of *ftsA*. **(C)** Integrated density analysis was computationally performed to quantify colony volume at each position of the pinned plate containing bepridil at 25 µg/mL. Normalized integrated density is plotted on the y-axis as a function of colony plate position (x-axis). Each color represents a different knockdown target and the most sensitized clones are highlighted.

Attempts in generating spontaneous mutants to bepridil

In a parallel approach to generate hypotheses regarding the target of bepridil, attempts were made to generate spontaneous mutants in *B. subtilis* 168. First attempts to generate spontaneous mutants were executed by plating *B. subtilis* 168 (6×10^9 , 6×10^8 , 6×10^7 CFU) on plates containing 8x, 4x, and 2x MIC of bepridil. Plates were incubated for 20 days and checked daily for spontaneous mutants. No observable mutations were detected under any of the tested conditions. Following this, efforts were made involving passage at sub-inhibitory concentrations of the drug, to determine whether such selective pressure could induce spontaneous mutations. Liquid cultures of *B. subtilis* 168 were grown in the presence of bepridil at 1/2 MIC to saturation. Upon saturation, 6×10^8 CFUs were plated on 4x MIC. Additionally the saturated culture was passaged 1/1000 and cultured again in the presence of bepridil at 1/2 MIC to saturation. This cycle was repeated 25 times. All passages were incubated for a minimum of 20 days and checked regularly for mutants. No spontaneous mutants were observed.

Assessing bepridil's affect on membrane potential

With an inability to generate spontaneous mutants in the presence of bepridil, it seems possible that the compound may have affects on the bacterial membrane. To determine bepridil's affect on the membrane a dose dependent study using the membrane potential sensitive dye DISC₃(5) was performed. Compounds that elicit an effect on the $\Delta\Psi$ component of PMF result in increases in fluorescence

(Farha et al., 2013b). Indeed, it was observed that exposure of *B. subtilis* 168 to bepridil results in a dose dependent increase in fluorescence (Figure 4-5A). To ensure that bepridil does not have auto-fluorescent properties, the compound was assayed in the absence of *B. subtilis* 168. No dose dependent increase in fluorescence was seen under these conditions (Figure 4-5B)

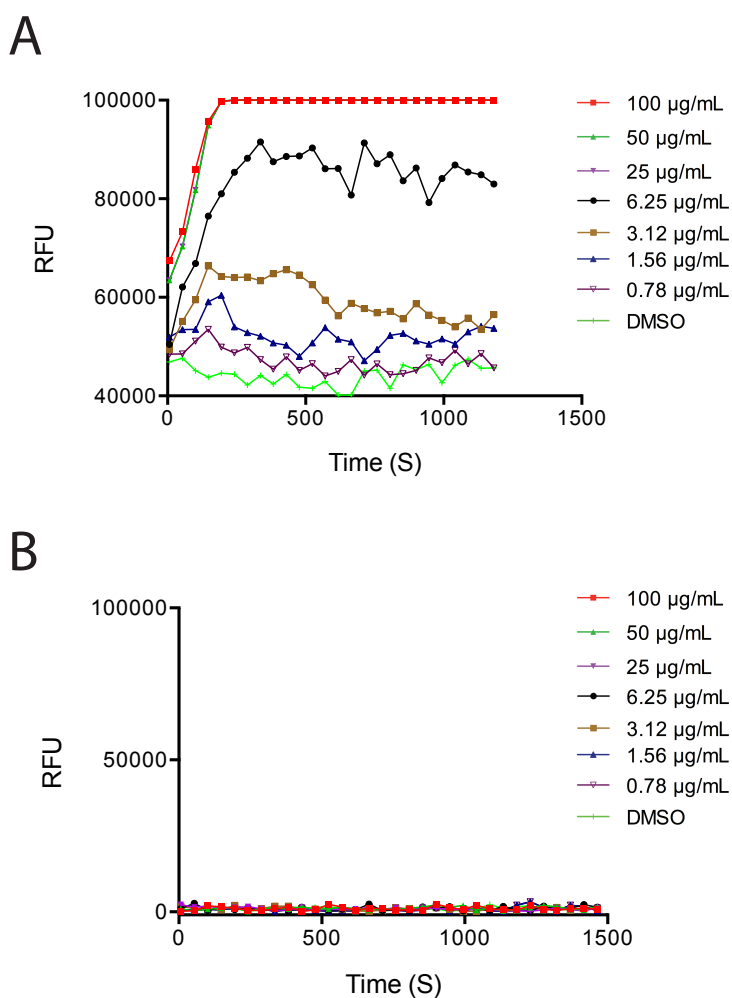


Figure 4-5: Dose dependent assessment of bepridil's effect on the proton motive force. (A) Dose dependent affect of bepridil on the membrane were measured kinetically by monitoring relative fluorescence (RFU) of the membrane-potential-sensitive cyanine dye DISC₃(5). **(B)**

Assessment of bepridil's auto-fluorescent properties in identical assay conditions without *B. subtilis* 168. Relative fluorescence was again measured kinetically for all concentrations tested.

Inhibitors of membrane potential do not have antagonistic interactions with targocil

Having determined that that bepridil was membrane-active, we sought to determine if other such compounds demonstrated antagonistic growth inhibition phenotypes with targocil. To assess this hypothesis, microtiter broth dilution checkerboards were performed with targocil and 3 compounds previously shown to affect PMF in *S. aureus* (Farha et al., 2013b). I1 and I2 increase DISC₃(5) fluorescence and as such target the $\Delta\Psi$ component of proton motive force. As a comparator, D2 was tested in addition to I1 and I2; D2 decreases DISC₃(5) fluorescence and therefore dissipates the ΔpH component of the proton motive force. Overall, no interactions were observed between any of the three membrane-active compounds and targocil (Figure 4-6)

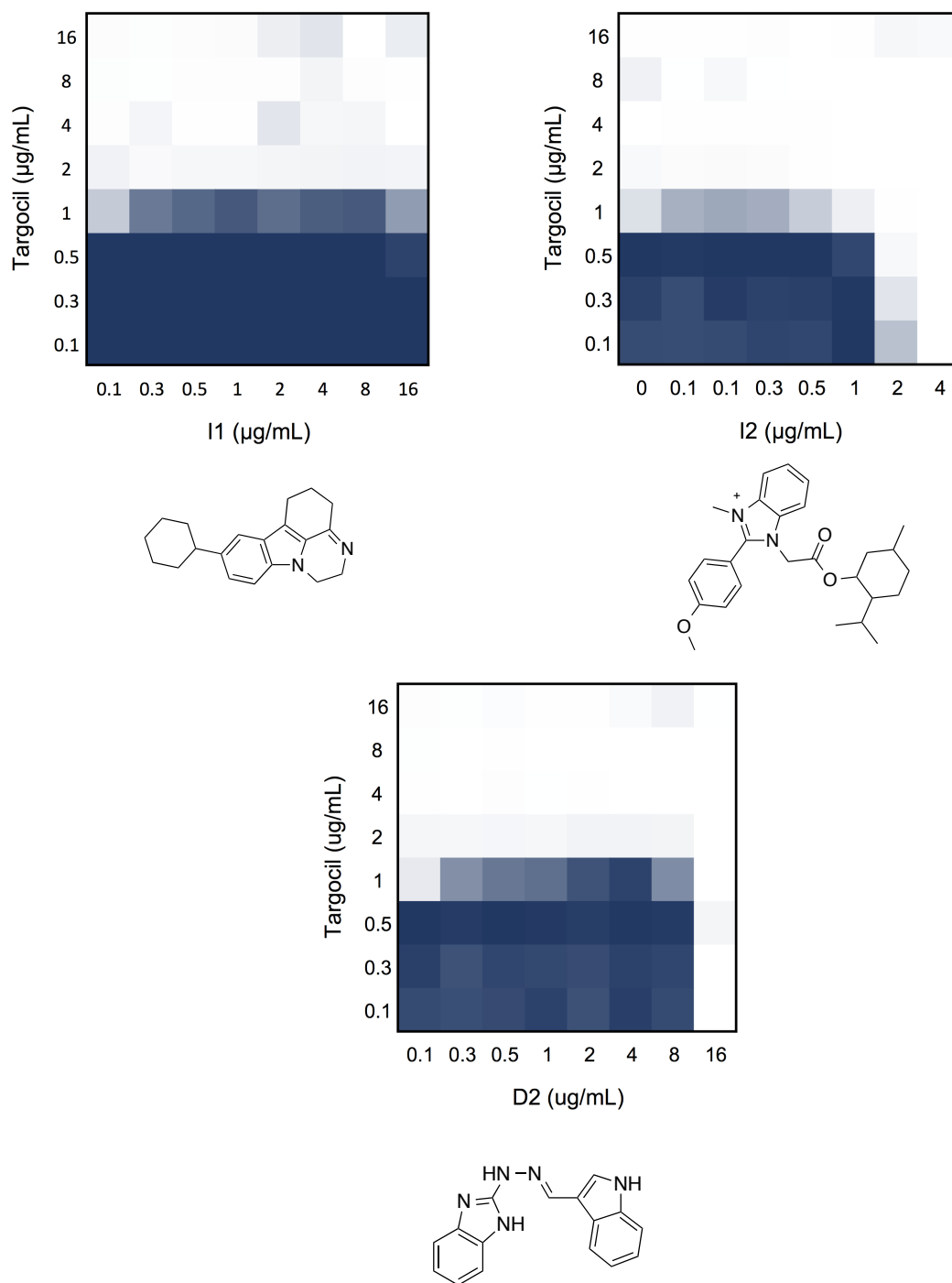


Figure 4-6: General PMF perturbing compounds do not interact with targocil in *S. aureus* CA-MRAS USA300. Using standard broth dilution checkerboards, the interactions between 3 compounds inhibiting PMF (x-axis) and targocil (y-axis) were determined. Growth is represented

by a blue gradient. Dark blue represents growth and white represents no growth. Chemical structures of I1, I2 and D2 are displayed under their corresponding checkerboard.

Assessing the bepridil spectrum of activity

Dose dependent growth inhibition was assessed against a variety of bacterial species to determine the spectrum of bepridil activity, and potentially also shed light on the MOA. This included the ESKAPE pathogens (Boucher et al., 2009), wild-type and hyper-permeable & efflux deficient strains of *E. coli* ($\Delta bamB$, $\Delta tolC$), along with a $\Delta tarO$ *S. aureus* strain (Figure 4-7). Though the antibacterial activity of bepridil against the ESKAPE pathogens was limited to *S. aureus* (MIC of 50 $\mu\text{g}/\text{mL}$), it is interesting that this activity was obviated in the $\Delta tarO$ *S. aureus* background. Additionally, bepridil had no activity against wild-type *E. coli* BW25113, but it did inhibit the growth of a hyperpermeable and efflux deficient counterpart, with an MIC of 10 $\mu\text{g}/\text{mL}$.

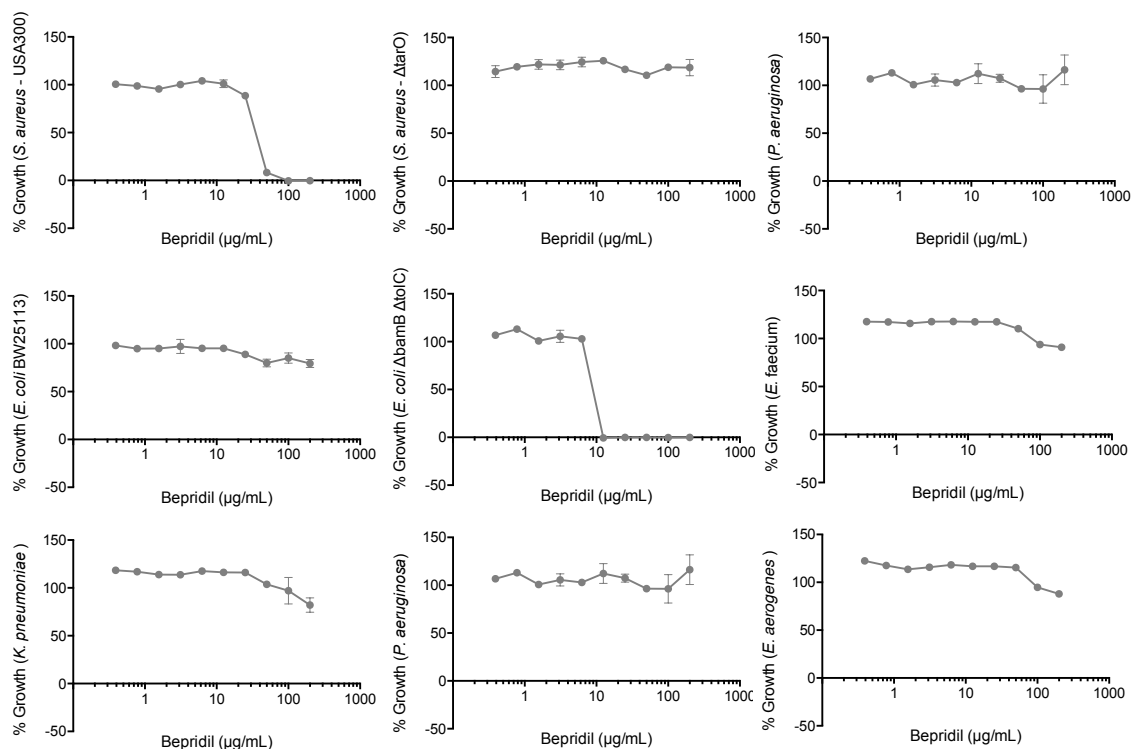


Figure 4-7: Bepridil antibacterial spectrum. The antibacterial activity of bepridil was assessed in a dose dependent manner against the ESKAPE pathogens along with wild-type *E. coli* BW25113, hyper-permeable *E. coli* BW25113 ($\Delta bamB$, $\Delta tolC$), and *S. aureus* ($\Delta tarO$). Growth in response to various concentrations is depicted as a percentage of the solvent control for each corresponding strain (y-axis).

Bepridil interacts with the first lipid-linked steps of peptidoglycan and wall teichoic acid synthesis

Since complete rescue of bepridil antibacterial activity was observed in the $\Delta tarO$ *S. aureus* background, it was of interest to determine whether or not it was possible to chemically phenocopy this result using ticlopidine -- a previously discovered inhibitor of TarO (Farha et al., 2013a). Indeed, checkerboard analysis revealed an antagonistic interaction between bepridil and ticlopidine (Figure 4-

8A). With a clear connection to the first lipid linked step of WTA synthesis we wondered if the inhibition of *MraY* function (the first lipid linked step of PG synthesis) would also interact with the action of bepridil. Microtiter broth dilution checkerboards with tunicamycin, a known natural product that inhibits *MraY*, showed clear synergy with bepridil in both *S. aureus* and *B. subtilis* 168 (Figure 4-8BC).

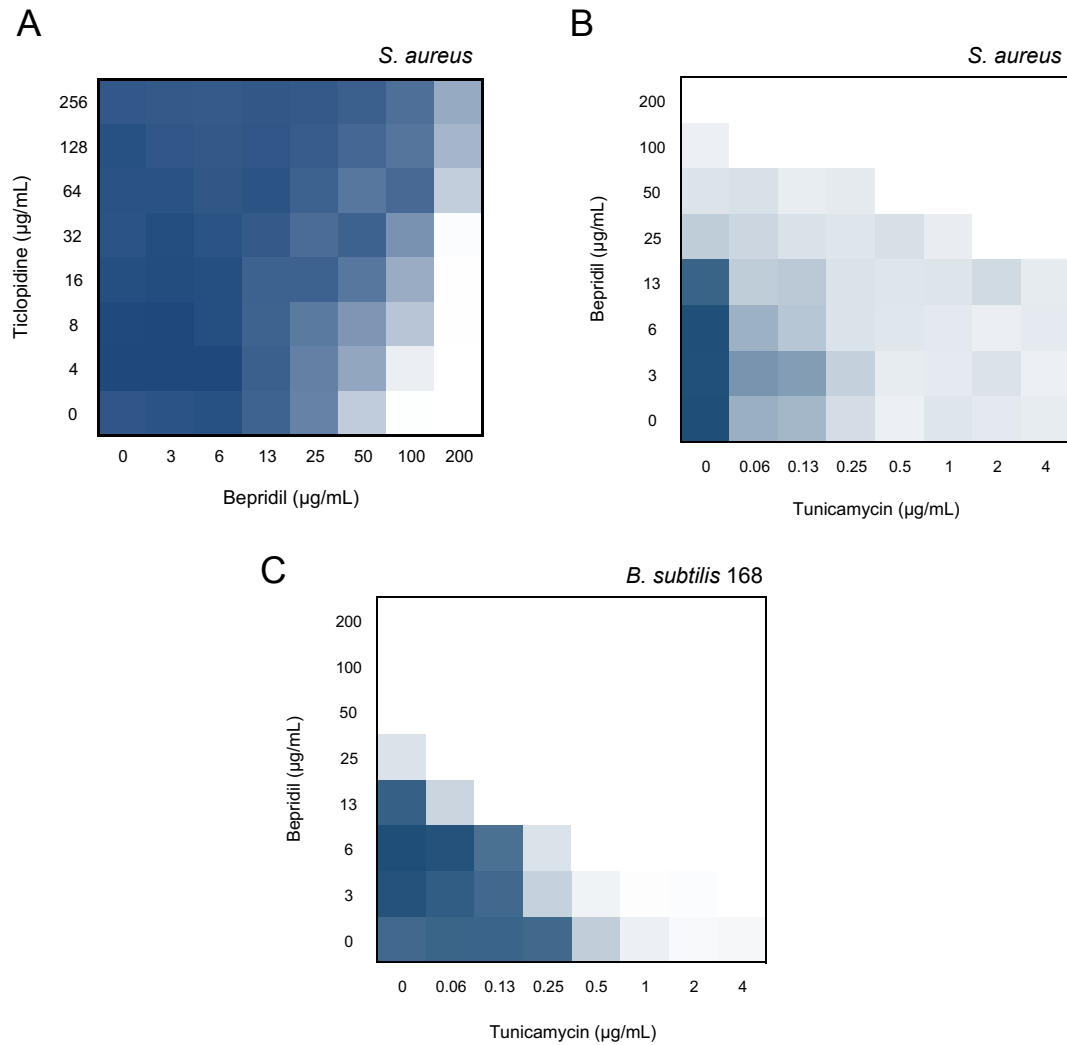


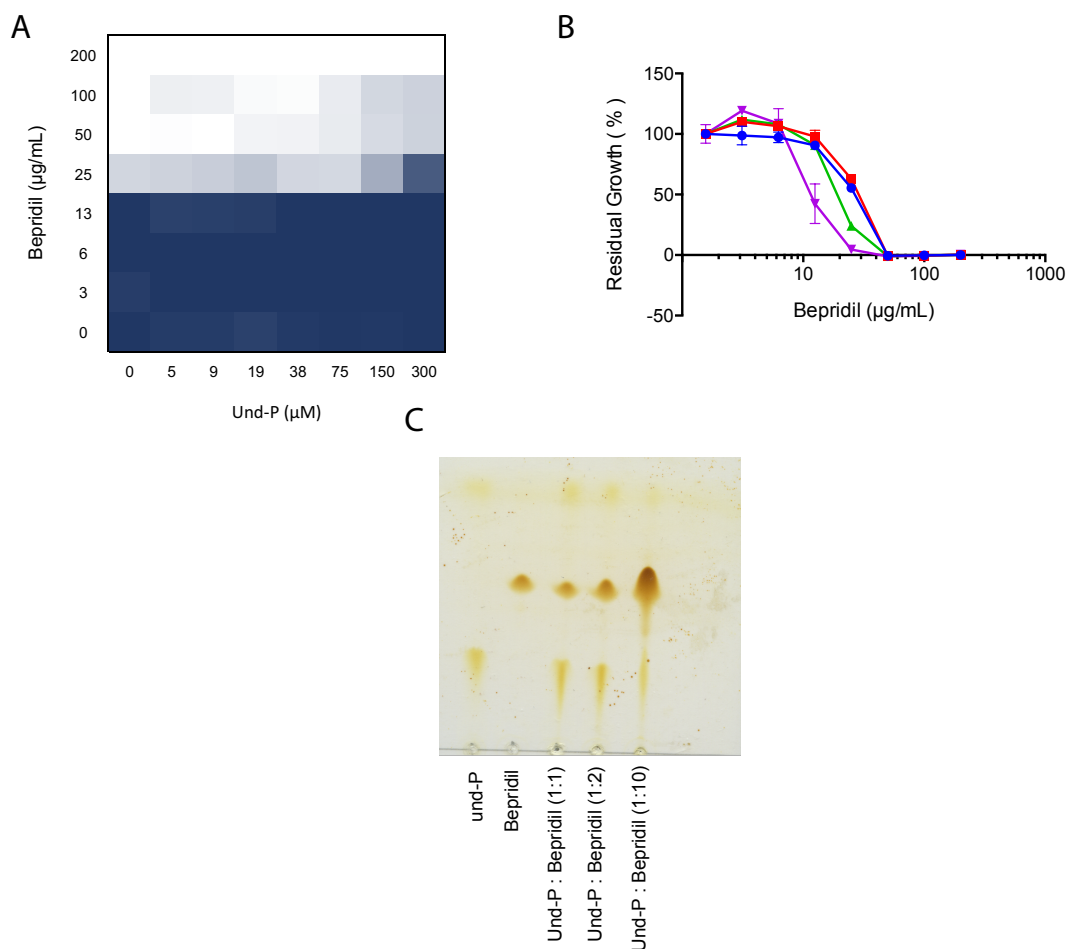
Figure 4-8: Bepridil displays interactions with the first lipid linked step of wall teichoic acid and peptidoglycan. Interactions of bepridil and the first lipid linked steps of PG and WTA

synthesis were established by performing standard broth dilution checkerboards with bepridil and ticolopidine (**A**), and with bepridil and tunicamycin (**B**) (**C**). Strains used in each checkerboard are depicted in the top left corner of the corresponding checkerboard. Growth is represented by a blue gradient. Dark blue represents growth and white represents no growth.

Interactions of bepridil with Und-P

Bepridil's ability to depolarize the membrane, along with its clear interactions with the first lipid linked steps of both WTA and PG synthesis, led to questioning whether it had the ability to physically sequester Und-P. To test this hypothesis, a first attempt involved a chemical suppression experiment with Und-P. A standard broth dilution checkerboard assay was performed with bepridil and exogenous Und-P to determine if exogenous Und-P could suppress the lethality of bepridil. Exogenous Und-P showed only a modest ability to antagonise the activity of bepridil at concentrations as high as 300 μ M (Figure 4-9A). It has been previously shown that exogenous Und-P can rescue the inhibition of UppS (Farha et al., 2015). A concern nevertheless, was whether exogenous Und-P could effectively suppress the action of a compound that sequesters Und-P. As an alternative approach, I investigated the impact of lowering UppS expression on using the *B. subtilis* 168 CRISPRi UppS knockdown strain. Knockdown of UppS would presumably lower the levels of Und-P and sensitize *B. subtilis* 168 to bepridil. While no suppression was observed in our genome-wide analysis (Figure 4.4), I endeavoured to test this with standard MIC methodology to be thorough. MICs were performed with bepridil against the knockdown strain,

which was induced to different levels. There were slight changes in the MIC curves, however it was concluded that there were no meaningful shifts in susceptibility levels (Figure 4-9B). To determine whether bepridil forms complexes with Und-P *in vitro*, a physical binding assay was performed involving thin layer chromatography as described by Ling, Schneider, et al. (ref). Bepridil was co-incubated with Und-P at various stoichiometries and separated on TLC. No binding interactions were observed (Figure 4-9C).

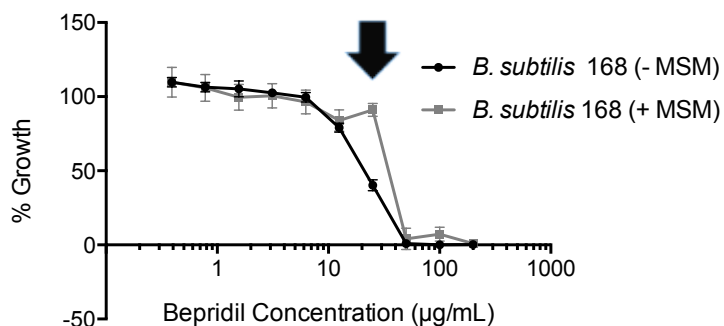


Newman background by ways of a standard broth dilution checkerboard. **(B)** Sensitization of *B. subtilis* 168 CRISPRi UppS knockdown strain to bepridil at increasing levels of inducer (xylose). Data corresponding to 0, 0.01, 0.05, and 0.1 % xylose are depicted in red, blue green and purple respectively. **(C)** Physical binding of bepridil to Und-P was assessed by thin layer chromatography. Und-P and bepridil were co incubated for 1 hour at various ratios followed by separation using TLC in 65:25:4 chloroform/methanol/water.

Affects of osmo-protectants on bepridil in *B. subtilis* 168

To assess whether the antibacterial activity of bepridil could be rescued with osmo-protectants (Czarny et al., 2014; Leaver et al., 2009), dose dependent growth inhibition studies of *B. subtilis* 168 in the presence and absence of MSM (20 mM MgCl₂, 0.5 M Sucrose, 20 mM Maleic acid) were performed. Slight rescue was observed at sub-MIC concentration (25 µg/mL) (Figure 4-10A). However, there were striking differences in the morphological phenotypes of *B. subtilis* 168 exposed to 25 µg/mL bepridil (+/- MSM). In the absence of MSM, when *B. subtilis* 168 is exposed to bepridil, the cells become 'puffy' prior to lysis. However, in the presence of osmo-protectants, *B. subtilis* 168 resembles early stage L-forms of *B. subtilis* 168 (Leaver et al., 2009) (Figure 4-10B).

A



B

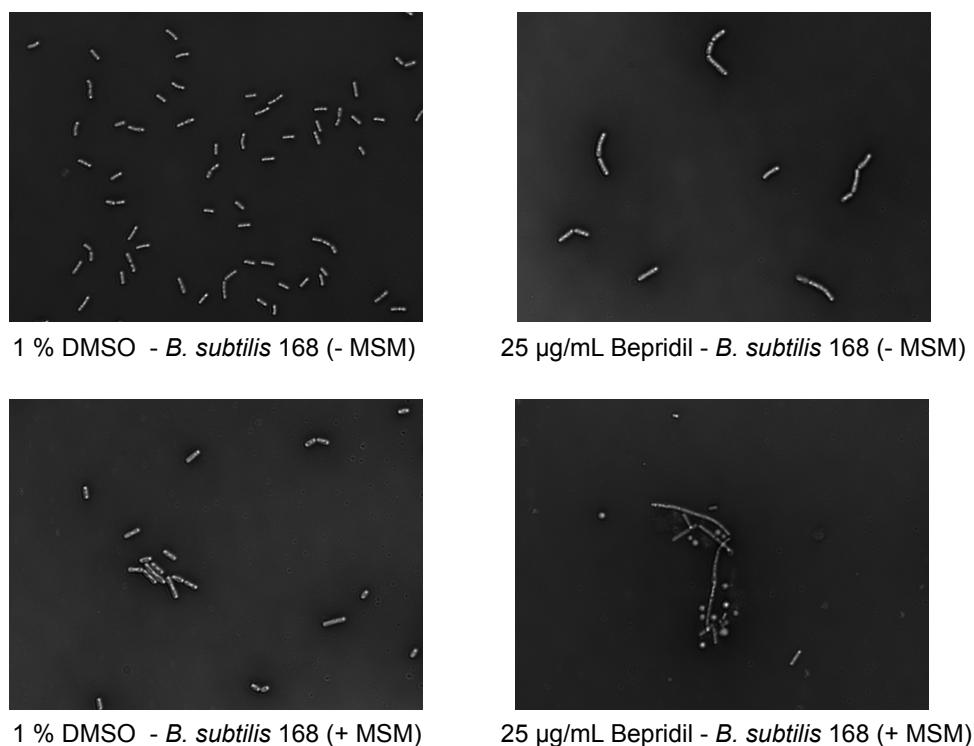


Figure 4-10: Affects of osmo-protectants on Bepridil's activity in *B. subtilis* 168. (A) Dose dependent activity of bepridil was assessed on *B. subtilis* 168 in the presence and absence of osmo-protectants (MSM). % Growth is depicted on the y-axis and is a function of solvent controls for the corresponding condition. (B) Imaging of *B. subtilis* 168 (+/- MSM) exposed to 1 % DMSO (solvent control) and a sub-MIC concentration of bepridil (25 µg/mL).

DISCUSSION

As described in chapter 3, cell wall biosynthesis is inherently complex. It involves many biosynthetic pathways that are both temporally and spatially regulated. One such complexity, the idiosyncratic dispensability pattern of WTA biosynthetic genes, has been successfully exploited in the discovery of late stage WTA inhibitors (refs). As demonstrated in chapter 3 we can also harness the complex genetics of WTA biosynthesis to enrich for and discover inhibitors of UppS. What is unknown however is whether there are additional interactions with this pathway that include targets further afield than, for example, UppS. Though incompletely characterized at this time, the discovery and action of bepridil suggests that additional target-inhibitor pairs can also be captured with this platform.

Screening 1,600 previously approved drugs (PADs) for targocil antagonism led to 68 primary hits. Upon dose-dependent confirmation of antagonism, 62 hits were confirmed. With a predominant interest in inhibitors of essential processes (not early steps of WTA), growth inhibition studies in *S. aureus* were performed. This shortlisted the confirmed actives to 12 priority actives, one of which was bepridil. Bepridil had strong antagonistic interactions with targocil. It is believed that there is a strong connection between processes that affect Und-P pools and antagonism of late stage WTA synthesis; as such, bepridil's synergistic interaction with β -lactams was of interest. However, synergy with β -lactams in MRSA can be a consequence of inhibiting many targets including isoprenoid,

PG, WTA synthesis etc. (Farha et al., 2015; 2013a; Lee et al., 2011; Swoboda et al., 2009). UppS was ruled out as the target using an *in vitro* UppS inhibition assay. As the MOA of bepridil remained unknown, a genome wide chemical-genetic approach was taken to identify the target. Using the *B. subtilis* 168 CRISPRi essential knockdown library (described in chapter 2) was screened for sensitization at sub-MIC concentrations of bepridil. Intriguingly, knockdowns in cell division machinery (*ftsZ* and *ftsA*) showed the greatest sensitization when exposed to bepridil at sub-MIC concentrations. FtsZ is a self-assembling GTPase that directs ring formation at future septa of bacterial division. Assembling into tubulin-like protofilaments, FtsZ is anchored to the inner-membrane by FtsA, which is also responsible for the recruitment of downstream cell division proteins (Adams and Errington, 2009). Interestingly, a knockdown strain of *ftsZ* has previously been shown to sensitize MRSA to β -lactams (Lee et al., 2011). To investigate cell division as a potential target, attempts were made to generate spontaneous mutants. However, no spontaneous mutants were observed using two distinct methods, even following 20 days of serial passage at sub-inhibitory concentrations.

Previous studies demonstrate that many inhibitors of bacterial tubulin (FtsZ) work indirectly by disrupting its localization, which is achieved through targeting of the $\Delta\Psi$ component of the proton motive force (PMF) (Foss et al., 2013). With an inability to generate spontaneous mutants to bepridil, it was postulated that

bepridil may have affects on membrane potential. Upon performing dose dependent studies of membrane potential using the cyanine dye DISC₃(5), bepridil resulted in perturbations of the $\Delta\Psi$ component of the PMF. The targocil antagonism screen has thus far led to higher hit-rates than expected; which may be due to non-specific inhibitors of the proton motive force. To investigate this phenomenon, established inhibitors of the PMF were utilized. Previous work identified inhibitors of both the $\Delta\Psi$ and ΔpH components of PMF (Farha et al., 2013b). In testing I1 and I2 ($\Delta\Psi$ inhibitors) and D2 (a ΔpH inhibitor) no interactions with targocil were observed. This finding suggested that bepridil may have an additional mode of action beyond its affects on the PMF. Additionally this gave some comfort in that the targocil antagonism screen was not specifically enriching for membrane-active compounds.

In testing for antibacterial susceptibility of the ESKAPE pathogens, *E. coli* (WT and hyper-permeable / efflux-deficient), and *S. aureus* (ΔtarO) an interesting pattern emerged. While, among the ESKAPE pathogens, bepridil only showed activity against *S. aureus*, its activity was lost in a *S. aureus* ΔtarO background. Additionally, activity against hyper-permeable and efflux deficient *E. coli* was evident. This narrowed potential targets. As wall teichoic acid is not found in *E. coli*, the entire WTA biosynthetic pathway was eliminated as a potential target for bepridil. Additionally, as *B. subtilis* 168 and *S. aureus* use fundamentally different pathways to generate isoprenoids, they too were eliminated (Wanke et al., 2001).

Since suppression of activity was observed in the $\Delta tarO$ *S. aureus* background we wondered whether we could phenocopy this suppression using ticlopidine – a known TarO inhibitor (Farha et al., 2013a). Indeed, this was the case. With TarO being the first lipid-linked biosynthetic step of wall teichoic acid synthesis, it was next investigated whether bepridil would also interact with the first lipid-linked step of peptidoglycan synthesis catalyzed by MraY. Tunicamycin, a nucleoside natural product and a known inhibitor of MraY (Bugg et al., 2011), was tested for interactions with bepridil. Synergy was observed leaving us with the sense that the target of bepridil would be central to the two enzymes. Thus we investigated whether bepridil was forming a complex with Und-P similar to that of antibiotics such as bacitracin (Economou et al., 2013), and teixobactin (Ling et al., 2015). Admittedly, both bacitracin and teixobactin are large natural products that make many interactions with Und-PP and we were skeptical that bepridil could achieve sequestration owing to its modest size. Nevertheless, we endeavored to examine this possibility with careful experimentation, first by chemical suppression with Und-P, secondly by knocking down Und-P production to look for sensitization, and finally by assessing physical binding between Und-P and Bepridil *in vitro*. None of these studies showed compelling interactions between Und-P and bepridil.

With an inability to pinpoint Und-P as the target; a more general approach to MOA was taken. In recent years, Leaver *et al*, have demonstrated that stable *B.*

subtilis 168 L-forms, lacking a cell wall, could be propagated in the presence of cell wall antibiotics when cultured in rich hyperosmotic media (Leaver et al., 2009). It was next assessed whether or not a change in susceptibility levels could be observed in the presence of osmo-protectants that would be indicative of a target in cell wall biogenesis. Slight rescue was observed at sub-MIC concentrations of bepridil but no shift in MIC was observed. However, when examined using bright-field microscopy the morphologies of *B. subtilis* 168 at sub-MIC concentrations looked drastically different with and without osmo-protectants. In the presence of osmo-protectants, *B. subtilis* 168 presented with morphological phenotypes resembling early-stage L-forms (Leaver et al., 2009). Pointing us, once again, to cell-wall as the target. Though the exact mode of action of bepridil remains unknown, results thus far point to early lipid linked steps of PG synthesis. Additionally, it is evident that bepridil has secondary pleotropic effects on membrane potential. Further studies eliminating targets one-by-one using *in vitro* enzyme based assays may shed additional light on the exact mechanism of bepridil action.

METHODS

Screen of 1,600 previously approved drugs (PADs) for targocil antagonism in *S. aureus*

Screening for antagonism of targocil was performed in 384-well microtiter plates (catalogue no. 3701, Corning) using a *S. aureus* Newman background in duplicate. All dispensing into microtiter plates was performed using a BiomekFX liquid handler (Beckman Coulter, Brea CA). The evening before screening a single colony of *S. aureus* Newman (EBII-61) was picked and grown overnight in cation adjusted Muller Hinton Broth (MHB) at 37 °C and 250 rpm. The morning of screening a 1/100 sub-culture was made of the overnight in MHB and grown under the same conditions to an OD_{600nm} ~0.35. Cells were then diluted into fresh media to a final OD_{600nm} of 0.001. The BiomekFX liquid handler was used to dispense 1 µL of targocil (0.8 mg/mL 100 % DMSO) into dry plates followed by the systematic addition of 1 µL of the 1,600 previously approved drugs (PADs) (1 mM, 100% DMSO). The liquid handler was then subsequently used to dispense 48 µL of culture (*S. aureus* Newman OD_{600nm} of 0.001) for a final screening concentration of 20 µM of the PADs subset and 16 µg/mL targocil. In lieu of targocil and PADs the two outermost columns were used for high and low growth controls. Erythromycin at 16 µg/mL was used as a low control and 4 % DMSO was used as a high (growth) control. Screening plates were grown at 37 °C shaking at 250 rpm for 12 hours. Absorbance was read at 600 nm using an EnVision plate reader (Perkin Elmer).

Data was normalized as a percentage of rescue for each well using the following: $(\text{Sample OD}_{600} - \text{IQ mean}) / (\text{mean high control} - \text{IQ mean}) * 100$; where IQ mean is the mean of the middle 50 % of the ordered raw data on the corresponding plate (“Rank Ordering Plate Data Facilitates Data Visualization and Normalization in High-Throughput Screening,” 2014). Zero % represents no rescue and 100 % represents full rescue of Targocil’s antibacterial activity.

Determination of minimal inhibitory concentrations (MIC)

The minimal inhibitory concentration (MIC) defines the lowest concentration of a compound required to inhibit growth of a particular strain by more than 90 %. For all strains assessed, a single colony was picked and grown overnight in 5 mL of rich LB (*B. subtilis* 168/ *E. coli*) or MHB (ESKAPE pathogens, *S. aureus* $\Delta tarO$) media at 30 °C (*B. subtilis* 168) or 37 °C (ESKAPE/ *S. aureus* $\Delta tarO$, *E. coli*) shaking at 250 rpm. The overnight culture was subsequently diluted 100-fold into fresh rich media and grown under the same conditions to an OD_{600} of ~ 0.35. Cells were then diluted to a final $\text{OD}_{600\text{nm}}$ of 0.001 in the same media and used to assess inhibition. The MICs were determined in 96-well microtiter plates (catalogue no. 3370, Corning) by adding 2 μL of inhibitor dissolved in 100 % DMSO to 198 μL culture. Inhibitors were then serially diluted in media in half-fold increments. Final volume for all wells was 100 μL . Plates were incubated at appropriate temperatures depicted above for 16 hours using Multitron microtiter shakers at 600 rpm (Infors HT, Switzerland). Upon incubation OD_{600} was

measured as a final readout using a Spectra-max Plus instrument (Molecular Devices).

Standard broth dilution checkerboards

Interactions between bepridil and various compounds were assessed by a standard checkerboard broth dilution assay in 96-well microtiter plates (Catalog no. 3370, Corning). Colonies of *S. aureus* or *B. subtilis* 168 were picked from a plate and suspended in 0.8 % NaCl aqueous solution to an OD_{600nm} of 0.1. Cells were subsequently diluted 1/200 into fresh media (*B. subtilis* 168 – LB, *S. aureus* – MHB). 100 µL of culture was subsequently added to plates containing specified concentrations of the two inhibitors resulting in overall DMSO content of 2 %. Plates were incubated for 18 hours at a temperature of 37 °C (*S. aureus*) or 30 °C (*B. subtilis* 168) in Multitron microtiter shakers at 600 rpm (Infors HT, Switzerland). Upon incubation OD_{600nm} was measured as a final readout using a Spectra-max Plus instrument (Molecular Devices).

***In vitro* UppS EnzCheck pyrophosphate release assay**

A Kinetic EnzCheck pyrophosphate assay (Life Technologies) was used to assess inhibition of bepridil *in vitro* with accordance to the manufacturers suggested guidelines. Reactions were setup in 100 µL volumes using a flat bottom 96-well plate (Costar 3370) in duplicate. Reactions with 100, 25, and 3.5 µg/mL Bepridil were conducted with a final concentration of 1 % DMSO in the

presence of: 0.2 mM 2-amino-6-mercapto-7-methyl- purine ribonucleoside (MESG), 0.625 U of purine ribonucleoside phosphorylase (PNP), 0.2 U of inorganic pyrophosphatase (PyroP), 0.125 µg of purified UPPS enzyme, 0.82 µM farnesyl pyrophosphate (FPP) (1xKM) and 65 µM isopentenyl pyrophosphate (IPP) (5x KM). Data was fit using GraFit V5 software (Erithacus Software).

Solid MIC determination of bepridil

MIC analysis of bepridil was performed against *B. subtilis* 168 on solid LB media. To generate plugs containing each compound 25 mL of 2 % agarose was poured into dry uni-well PlusPlates (Singer Instruments, UK). After allowing to solidify 12 circular plugs were removed per plate with a diameter of 1.5 cm leaving 12 wells for LB agar plugs containing compound. LB agar (1.5 %) containing bepridil at the desired concentrations (half fold dilutions starting at 1,600 µg/mL) was added into each well. Once solidified the 2 % agarose cast was removed leaving 12 LB agar plugs containing Bepridil at desired concentrations. Plates were pinned with *B. subtilis* 168 using a Singer Rotor Instrument (Singer Instruments, UK) at 6,144 density. Once pinned plates were incubated for 16 hours overnight at 30 °C and growth inhibition was visually assessed (French et al., 2016).

Profiling of bepridil using the *B. subtilis* 168 CRISPRi library

Glycerol stocks of the library (in 96-well format, 4 plates total) were pinned onto PLUSPLATES (Cat. PLU-001, Singer Instruments, UK) containing LB Agar and

incubated at 30 °C overnight. Once grown the library was up-scaled to 384 format using a Singer Rotor (Singer Instruments, UK) on PLUSPLATES containing LB Agar. Plates were incubated at 30 °C overnight. The library was up-scaled again the next day to 1536 format using the same method. The 1536 density *B. subtilis* CRISPRi library was pinned onto PLUSPLATES containing LB agar supplemented with sub-MIC ($1/2$ $1/4$ and $1/8^{\text{th}}$ MIC) concentrations of bepridil. Plates were grown overnight at 30 °C and scanned using a transmissive scanner (Epson Perfection V700, Epson USA). Images were analyzed using FIJI and R as previously described (French et al., 2016). Data was visualized using Spotfire (Tibco Software Inc., USA).

Assessing bepridils affects on membrane potential using DiSC₃(5)

Cytoplasmic membrane permeabilization was determined by using the membrane-potential-sensitive cyanine dye DiSC₃(5)(Sims et al., 1974). Strain EB6 was grown at 30 °C with shaking to mid-logarithmic phase ($OD_{600} = 0.5 - 0.6$). Cells were harvested by centrifugation at 16,000 x g, washed once with buffer (150 mM Tris-HCl, pH 7.2), and re-suspended in assay buffer (10 mM Tris-HCl, pH 7.2) to an OD_{600} of 0.04. A 100 μ L cell suspension was placed in each well of a clear 96-well microtitre plate (catalog no. 3370, Corning Costar). The cell suspension was incubated with 0.4 μ M DiSC₃(5) until DiSC₃(5) uptake was maximal (as indicated by a stable reduction in fluorescence due to fluorescence quenching as the dye became concentrated in the cell by the membrane

potential). The desired concentration of bepridil was subsequently added and the fluorescence reading was monitored using a Synergy HT multi-mode microplate reader (Biotek) at an excitation wavelength of 622 nm and an emission wavelength of 670 nm. The maximal fluorescence increase due to the disruption of the cytoplasmic membrane was recorded. A blank with only cells and the dye was used to subtract the background. To assess whether or not bepridil had auto-fluorescent properties the DiSC₃(5) assay was performed as above with the omission of *B. subtilis* 168 cells.

Bepridil-Und-P complex formation assay

Complex formation between Bepridil and Und-P was assessed by TLC. 2 nmol purified Und-P was incubated in 10mM Tri-HCL for 30 min at room temperature, with molar ratios (und-P to Bepridil) of 1:1, 1:2, 1:10. Mixtures along with Und-P and Bepridil were analyzed by TLC using chloroform/methanol/water (65:25:4). Protocol adapted from (Münch et al., 2014).

REFERENCES

- Adams, D.W., Errington, J., 2009. Bacterial cell division: assembly, maintenance and disassembly of the Z ring. *Nat. Rev. Microbiol.* 7, 642–653. doi:10.1038/nrmicro2198
- Boucher, H.W., Talbot, G.H., Bradley, J.S., Edwards, J.E., Gilbert, D., Rice, L.B., Scheld, M., Spellberg, B., Bartlett, J., 2009. Bad bugs, no drugs: no ESKAPE! An update from the Infectious Diseases Society of America. *Clin. Infect. Dis.* 48, 1–12. doi:10.1086/595011
- Bugg, T.D.H., Braddick, D., Dowson, C.G., Roper, D.I., 2011. Bacterial cell wall assembly: still an attractive antibacterial target. *Trends Biotechnol.* 29, 167–173. doi:10.1016/j.tibtech.2010.12.006
- Czarny, T.L., Perri, A.L., French, S., Brown, E.D., 2014. Discovery of Novel Cell Wall-Active Compounds Using PywaC, a Sensitive Reporter of Cell Wall Stress, in the Model Gram-Positive Bacterium *Bacillus subtilis*. *Antimicrob. Agents Chemother.* 58, 3261–3269. doi:10.1128/AAC.02352-14
- Economou, N.J., Cocklin, S., Loll, P.J., 2013. High-resolution crystal structure reveals molecular details of target recognition by bacitracin. *Proc. Natl. Acad. Sci. U.S.A.* 110, 14207–14212. doi:10.1073/pnas.1308268110
- Farha, M.A., Czarny, T.L., Myers, C.L., Worrall, L.J., French, S., Conrady, D.G., Wang, Y., Oldfield, E., Strynadka, N.C.J., Brown, E.D., 2015. Antagonism screen for inhibitors of bacterial cell wall biogenesis uncovers an inhibitor of undecaprenyl diphosphate synthase. *Proc. Natl. Acad. Sci. U.S.A.* 201511751. doi:10.1073/pnas.1511751112
- Farha, M.A., Leung, A., Sewell, E.W., D'Elia, M.A., Allison, S.E., Ejim, L., Pereira, P.M., Pinho, M.G., Wright, G.D., Brown, E.D., 2013a. Inhibition of WTA Synthesis Blocks the Cooperative Action of PBPs and Sensitizes MRSA to β -Lactams 8, 226–233. doi:10.1021/cb300413m
- Farha, M.A., Verschoor, C.P., Bowdish, D., Brown, E.D., 2013b. Collapsing the proton motive force to identify synergistic combinations against *Staphylococcus aureus*. *Chem. Biol.* 20, 1168–1178. doi:10.1016/j.chembiol.2013.07.006
- Foss, M.H., Eun, Y.-J., Grove, C.I., Pauw, D.A., Sorto, N.A., Rensvold, J.W., Pagliarini, D.J., Shaw, J.T., Weibel, D.B., 2013. Inhibitors of bacterial tubulin target bacterial membranes in vivo. *Medchemcomm* 4, 112–119. doi:10.1039/C2MD20127E
- French, S., Mangat, C., Bharat, A., Côté, J.-P., Mori, H., Brown, E.D., 2016. A robust platform for chemical genomics in bacterial systems. *Mol. Biol. Cell* mbc.E15-08-0573. doi:10.1091/mbc.E15-08-0573
- Leaver, M., Domínguez-Cuevas, P., Coxhead, J.M., Daniel, R.A., Errington, J., 2009. Life without a wall or division machine in *Bacillus subtilis*. *Nature* 457, 849–853.

doi:10.1038/nature07742

- Lee, S.H., Jarantow, L.W., Wang, H., Sillaots, S., Cheng, H., Meredith, T.C., Thompson, J., Roemer, T., 2011. Antagonism of chemical genetic interaction networks resensitize MRSA to β -lactam antibiotics. *Chem. Biol.* 18, 1379–1389. doi:10.1016/j.chembiol.2011.08.015
- Ling, L.L., Schneider, T., Peoples, A.J., Spoering, A.L., Engels, I., Conlon, B.P., Mueller, A., Schäberle, T.F., Hughes, D.E., Epstein, S., Jones, M., Lazarides, L., Steadman, V.A., Cohen, D.R., Felix, C.R., Fetterman, K.A., Millett, W.P., Nitti, A.G., Zullo, A.M., Chen, C., Lewis, K., 2015. A new antibiotic kills pathogens without detectable resistance. *Nature* 517, 455–459. doi:10.1038/nature14098
- Mangat, C.S., Bharat, A., Gehrke, S.S., Brown, E.D., 2014. Rank Ordering Plate Data Facilitates Data Visualization and Normalization in High-Throughput Screening. *J Biomol Screen* 1087057114534298. doi:10.1177/1087057114534298
- Münch, D., Müller, A., Schneider, T., Kohl, B., Wenzel, M., Bandow, J.E., Maffioli, S., Sosio, M., Donadio, S., Wimmer, R., Sahl, H.-G., 2014. The Lantibiotic NAI-107 Binds to Bactoprenol-bound Cell Wall Precursors and Impairs Membrane Functions. *J. Biol. Chem.* 289, 12063–12076. doi:10.1074/jbc.M113.537449
- Sims, P.J., Waggoner, A.S., Wang, C.H., Hoffman, J.F., 1974. Studies on the mechanism by which cyanine dyes measure membrane potential in red blood cells and phosphatidylcholine vesicles. *Biochemistry* 13, 3315–3330.
- Swoboda, J.G., Meredith, T.C., Campbell, J., Brown, S., Suzuki, T., Bollenbach, T., Malhowski, A.J., Kishony, R., Gilmore, M.S., Walker, S., 2009. Discovery of a small molecule that blocks wall teichoic acid biosynthesis in *Staphylococcus aureus*. 4, 875–883. doi:10.1021/cb900151k
- Wang, H., Gill, C.J., Lee, S.H., Mann, P., Zuck, P., Meredith, T.C., Murgolo, N., She, X., Kales, S., Liang, L., Liu, J., Wu, J., Santa Maria, J., Su, J., Pan, J., Hailey, J., Mcguinness, D., Tan, C.M., Flattery, A., Walker, S., Black, T., Roemer, T., 2013. Discovery of Wall Teichoic Acid Inhibitors as Potential Anti-MRSA β -Lactam Combination Agents. *Chem. Biol.* 20, 272–284. doi:10.1016/j.chembiol.2012.11.013
- Wanke, M., Skorupinska-Tudek, K., Swiezewska, E., 2001. Isoprenoid biosynthesis via 1-deoxy-D-xylulose 5-phosphate/2-C-methyl-D-erythritol 4-phosphate (DOXP/MEP) pathway. *Acta Biochim. Pol.* 48, 663–672
- Yatani, A., Brown, A.M., Schwartz, A., 1986. Bepridil block of cardiac calcium and sodium channels. *J. Pharmacol. Exp. Ther.* 237, 9–17.

CHAPTER FIVE – Future Directions

A brief summary and look into the future

As our knowledge of the intricate links between pathways and various physiological states grows; our ability to develop novel and unique screening platforms grows with it. This thesis is built upon harnessing discoveries in the field of bacterial chemical-genetics in unique ways which bridge whole-cell and target based drug discovery.

Chapter 2 explores how the power of the P_{ywaC} promoter-reporter system can be exploited in the discovery of cell wall synthesis inhibitors as a whole (Czarny et al., 2014). Chapter 3 and 4 are built upon years of research into WTA dispensability (D'Elia et al., 2006) and focus on harnessing the idiosyncratic pattern in a way not utilized before in drug discovery. In the introduction of the thesis it is mentioned that the overarching goal is to prove the utility of such approaches through the discovery and characterization of new classes of inhibitors. Both the P_{ywaC} promoter-reporter system and antagonism screening approach have proven their utility in spades not only by identifying general cell wall actives but a plethora of new classes of UppS inhibitors.

What is intriguing is that almost all of the UppS inhibitors discovered in previous chapters show at least some level of species selectivity. Species selectivity is typically attributed to one of three causes: species-specific targets, species-

specific permeability / efflux, or differences in the sequence of conserved enzymes (Lewis, 2013). In the case of UppS; both *in vitro* and *in vivo* data demonstrate that UppS can be harnessed as a selective target due to differences in sequence identity among bacterial species. Indeed, finding species selective inhibitors through HTS campaigns has historically been easier than finding broad-spectrum inhibitors (Lewis, 2013). In the past species-selective inhibitors would be discarded during the drug discovery process as the gold standard was broad-spectrum. However, we are becoming progressively aware and sensitive to the advantages of species-selective compounds. Indeed, this may begin a paradigm shift in antibacterial drug discovery.

We are becoming conscious of the potential adverse effects of wiping out our microbiota through the use of broad-spectrum antibiotics. The delicate composition of the microbiome appears to have an effect on everything from drug effectiveness, obesity and immunity to gastrointestinal disease (Kau et al., 2011; Larsen et al., 2010; Turnbaugh et al., 2009). Additionally, narrow spectrum / species specific inhibitors remove much of the obstacles surrounding toxicity as they are less likely to have off-target effects in mammals. Finally, and maybe one of the most compelling reasons for species selective drug discovery, is the implication for bacterial resistance. Resistance to broad-spectrum compounds often emerges in commensal bacteria and then moves into pathogens. The selective pressure / effectiveness of such an approach for inhibitors targeting

specific pathogenic species is severely diminished. Though the development of species-selective antibiotics shows many advantageous affects; such a paradigm shift in antibiotic drug discovery must be accompanied by better diagnostic tools for the rapid identification of disease-causing pathogen.

Though discovery of new antibiotics to treat infectious disease is the predominant goal in developing such discovery platforms; inhibitors that are discovered are not always suitable for further development as anti-infective therapies. Though unfavorable chemistry of pharmacokinetics can derail further development of leads, their value should not be underestimated. Selective inhibitors such as MAC-057630 discussed in chapter 3 have great potential as probes of biological complexity (Falconer et al., 2011). Unlike the use of genetic approaches, perturbation of a system using chemicals can be titrated and pulsed at any desired time point. Additionally, unlike genetic approaches, the use of chemicals does not generate pleotropic effects on neighbouring gene products. Indeed, targocil, which has little potential as an anti-infective therapy (due to high frequency of resistance) has demonstrated great potential as a probe of biology in chapters 3 and 4.

Built upon years of research into WTA dispensability; chapter 3 and 4 harness antagonism of late step lesions to screen for early step and WTA substrate producing inhibitors. Not only did the antagonism platform developed enrich for

UppS inhibition but it has left questions with regards to what other targets are being enriched.

Looking to the future, it is obvious that a clearer understanding of what targets are being enriched for is required. Indeed, chapter 4 tries to address this issue by elucidating the mode of action of bepridil; however, this 'hunt and peck' method is unsustainable. With *S. aureus* essential gene knockdown libraries and non-essential transposon libraries readily available; a chemical-genetic approach is a tangible tack. This indeed is a step backwards; however, it will allow for a better understanding of what targets are truly antagonistic with lesions in late step WTA synthesis. Generating a list of antagonistic genes would not only shed light on complexities within cell wall biosynthesis but would also aid in mode of action studies.

Overall this thesis outlines two effective and innovative approaches in identifying novel cell wall active compounds. Both of these approaches were tested and have proven their merits through interrogations of small molecule libraries. Both the 26,000 and 140,000 compound libraries are deemed 'drug like' by notions that they follow Christopher Lipinski's rule of 5 (Lipinski and Hopkins, 2004). These rules however focus on bioavailability rather than chemical properties which make for good antibiotic. Indeed, much of our antibiotic arsenal used today is sourced from soil dwelling bacteria which often produce potent antibacterial

agents which do not follow Lipinski's rules.

It is evident that the ever growing range of clever and effective whole-cell targeted screening approaches will not be the bottle neck in antibiotic drug discovery in the future. Rather, it will be the lack of relevant chemical matter to assess using these unique approaches. Gone is most, if not all, of the low hanging fruit in natural product drug discovery. As such the time is now to look for chemical matter from alternate sources such as marine microbial natural products or 'unculturable' soil dwelling bacteria (Ling et al., 2015; Wright, 2015). Indeed, without the development of 'relevant' chemical space; the unique approaches developed in this thesis may be limited to the discovery of chemical probes.

REFERENCES

- Czarny, T.L., Perri, A.L., French, S., Brown, E.D., 2014. Discovery of Novel Cell Wall-Active Compounds Using PywaC, a Sensitive Reporter of Cell Wall Stress, in the Model Gram-Positive Bacterium *Bacillus subtilis*. *Antimicrob. Agents Chemother.* 58, 3261–3269. doi:10.1128/AAC.02352-14
- D'Elia, M.A., Pereira, M.P., Chung, Y.S., Zhao, W., Chau, A., Kenney, T.J., Sulavik, M.C., Black, T.A., Brown, E.D., 2006. Lesions in teichoic acid biosynthesis in *Staphylococcus aureus* lead to a lethal gain of function in the otherwise dispensable pathway. 188, 4183–4189. doi:10.1128/JB.00197-06
- Falconer, S.B., Czarny, T.L., Brown, E.D., 2011. Antibiotics as probes of biological complexity. *Nat Chem Biol* 415–423. doi:10.1038/nchembio.590
- Kau, A.L., Ahern, P.P., Griffin, N.W., Goodman, A.L., Gordon, J.I., 2011. Human nutrition, the gut microbiome and the immune system. *Nature* 474, 327–336. doi:10.1038/nature10213
- Larsen, N., Vogensen, F.K., van den Berg, F.W.J., Nielsen, D.S., Andreassen, A.S., Pedersen, B.K., Al-Soud, W.A., Sørensen, S.J., Hansen, L.H., Jakobsen, M., 2010. Gut Microbiota in Human Adults with Type 2 Diabetes Differs from Non-Diabetic Adults. *PLoS ONE* 5, e9085. doi:10.1371/journal.pone.0009085
- Lewis, K., 2013. Platforms for antibiotic discovery. *Nat Rev Drug Discov* 12, 371–387. doi:10.1038/nrd3975
- Ling, L.L., Schneider, T., Peoples, A.J., Spoering, A.L., Engels, I., Conlon, B.P., Mueller, A., Schäberle, T.F., Hughes, D.E., Epstein, S., Jones, M., Lazarides, L., Steadman, V.A., Cohen, D.R., Felix, C.R., Fetterman, K.A., Millett, W.P., Nitti, A.G., Zullo, A.M., Chen, C., Lewis, K., 2015. A new antibiotic kills pathogens without detectable resistance. *Nature* 517, 455–459. doi:10.1038/nature14098
- Lipinski, C., Hopkins, A., 2004. Navigating chemical space for biology and medicine. *Nature* 432, 855–861. doi:10.1038/nature03193
- Turnbaugh, P.J., Hamady, M., Yatsunenko, T., Cantarel, B.L., Duncan, A., Ley, R.E., Sogin, M.L., Jones, W.J., Roe, B.A., Affourtit, J.P., Egholm, M., Henrissat, B., Heath, A.C., Knight, R., Gordon, J.I., 2009. A core gut microbiome in obese and lean twins. *Nature* 457, 480–484. doi:10.1038/nature07540
- Wright, G., 2015. Antibiotics: An irresistible newcomer. *Nature* 517, 442–444. doi:10.1038/nature14193